Proceedings of:

Metal Platings for Precision Finishing Operations

1991 Spring Topical Meeting

April 15-18, 1991

Westward Look Resort

Tucson, Arizona

The American Society for Precision Engineering (ASPE) is a multidisciplinary professional and technical society concerned with research and development, design, manufacture and measurement of high accuracy components and systems. ASPE activities encompass relevant aspects of mechanical, electronic, optical and production engineering, physics, chemistry, and computer and materials science. Membership is open to anyone interested in any aspect of precision engineering.

Founded in 1986, ASPE provides a new focus for a diverse but important community. Other professional organizations have covered aspects of precision engineering, always as a sideline to their principal goals. ASPE is based on the core of generic concepts necessary to achieve precision in any application; independent of discipline, ASPE intends to be the focus for precision technology — and to represent all facets from research to application.

ASPE — The American Society for Precision Engineering
401 Oberlin Road, Suite 108
P.O. Box 10826
Raleigh, NC 27605-0826
Phone (919) 839-8444 Fax (919) 839-8039

Preface

This book comprises the proceedings of the 1991 Spring Topical Meeting. The contributions reflect the authors' opinions and are published as presented to ASPE, without change. Their inclusion in this publication does not necessarily constitute endorsement by the ASPE, or its editorial staff.

Individual readers of this book and nonprofit libraries acting for them are permitted to make fair use of the material contained in this book to be used in teaching or research, provided they copy said paper in total, as written by the author. Permission is granted to quote excerpts from the scientific or technical works in this book with proper acknowledgement of the source to include: the author's name, the book name, and the ASPE tag line. Reproduction of figures and tables is likewise permitted from the contents of this book, provided that the same acknowledgement of the same source and content is printed.

Any other type reproduction, systematic copying or multiple reproduction of any material in this book is expressly prohibited except with the written permission of the ASPE editorial staff, addressed to the Society's headquarters.

ISBN 1-887706-05-4

1991 Spring Topical Meeting

Organizing Committee

Co-Chairs:

Chris Evans, National Institute of Standards and Technology
John Taylor, Lawrence Livermore National Laboratory

Members:

William Bryan, 3M Company
John Dini, Lawrence Livermore National Laboratory
David Lunt, Tucson Optical Research Corporation
Andrea Plain, Fresnel Optics, Inc.
Robert Parks, University of Arizona

Cooperating Sponsors

SPIE (The International Society for Optical Engineering)
Optical Society of America

1991 Spring Topical Meeting

Contents

Preface — Organizing Committee ii

Contents iii

Program iv

Technical Paper Index ..... v-vi

Foreword vii

Technical Papers 3-147

Author Index 148

1991 Spring Topical Meeting

Program

Conference Schedule

	Monday, April 15		Tuesday, April 16	Wednesday, April 17	Thursday, April 18
8:00					
	INTRODUCTION	7:30	CONTINENTAL BREAKFAST		
8:10-9:45	MINI-TUTORIAL 1	8:30		TECHNICAL SESSIONS	
		10:00			
			COFFEE BREAK		
10:15-11:45	MINI-TUTORIAL 2	10:30		TECHNICAL SESSIONS	
		12:00			
			LUNCH		
1:00-2:45	MINI-TUTORIAL 3	1:30	TECHNICAL	SESSIONS	
		3:00			
			BREAK		
3:15-4:45	MINI-TUTORIAL 4	3:30	TECHNICAL	SESSIONS	TECHNICAL VISITS
		5:00			
6:00	OPENING TECHNICAL SESSION		DINNER (6:00-8:00)		
7:00	ASPE Spring Topical Meeting Reception with Tucson Companies		EXPERIENCES/OPEN FORUM	COMMERCIAL SESSION/ DISCUSSION	

Technical Paper Index

1. ***The fabricator-plater relationship: An architecture for meeting customer's specifications***
   K. L. Blaedel and J. S. Taylor (Lawrence Livermore National Lab); C. J. Evans (Nat'l Institute of Standards & Technology) ..... *page 3*
2. ***Invited Paper — Experiences with polishing electroless nickel****
   N. J. Brown, J. S. Taylor and B. A. Fuchs (Lawrence Livermore National Lab)
3. ***Invited Paper — Selecting the correct work piece material: An overview of issues concerning the fabricator and plater***
   W. J. Bryan (3M Company) ..... *page 10*
4. ***Invited Paper — Hard copper plating****
   S. B. Collins, H. L. Krinke and F. J. Rouser (3M Company)
5. ***Smooth nonmagnetic electroless nickel deposition for the computer memory disk***
   D. Crotty (Allied Kelite, Division of Witco Corporation) ..... *page 14*
6. ***Niklad 797 — Hardness and wear resistance of boron electroless nickel for the price of phosphorus electroless nickel***
   D. Crotty (Allied Kelite, Division of Witco Corporation) ..... *page 15*
7. ***Invited Paper — Perspective on plating for precision finishing***
   J. W. Dini (Lawrence Livermore National Lab) ..... *page 17*
8. ***Machining forces in diamond turning of plated copper and unplated substrates***
   J. D. Drescher and T. A. Dow (NC State University) ..... *page 44*
9. ***Sputtered beryllium coatings for the precision fabrication of optical components***
   C. M. Egert and J. B. Arnold (Optics MODIL, Oak Ridge National Lab) ..... *page 54*
10. ***Focal plane array testing support****
    D. Engelhaupt (Center for Applied Optics, Univ. of Alabama/Huntsville)
11. ***Laser gold plating: for developing an NBS (NIST) standard and a coating for the Keck Telescope secondary mirror***
    D. Epner (Epner Technology) ..... *page 66*
12. ***Thick deposits with electroless nickel***
    G. H. Graham (Process Engineering Section, Oklahoma City Air Logistics Center) ..... *page 70*
13. ***Invited Paper — Metallurgy of nickel phosphorus alloys***
    D. S. Lashmore (Electrodeposition Group, Nat'l Institute of Standards & Technology) ..... *page 77*
14. ***Electroless nickel coatings for x-ray synchrotron optics****
    D. Lunt (Tucson Optical Research Corporation)
15. ***Electroforming complex internal surfaces in high power components***
    G. Malone (Electroformed Nickel) ..... *page 81*
16. ***Electrodeposited coatings for diamond turning applications***
    A. Mayer, R. D. Bramlett and R. D. Day (Los Alamos National Lab); C. J. Evans and R. S. Polvani (Nat'l Institute of Standards & Technology) ..... *page 84*
17. ***Optics for synchrotron radiation: A user's perspective***
    W. R. McKinney (Lawrence Berkeley Laboratory) ..... *page 90*
18. ***Thick gold plating for optical surfaces***
    R. D. Mikkola, H. L. Gerth and R. C. Waldrop (Oak Ridge Y-12 Plant, Martin Marietta Energy Systems, Inc.) ..... *page 91*
19. ***Observations on polishing electroless nickel plated surfaces***
    R. E. Parks (University of Arizona/Tucson) and C. J. Evans (Nat'l Institute of Standards & Technology) ..... *page 95*

* *Paper not available at press time*

20. ***Electroless nickel plating for enhanced gold coating: A lesson in bimetallics***
S. Scott (Diamond Point Machining Group, Texas Instruments Inc.) ..... *page 99*

21. ***Invited Paper — Design of articles to be electroplated and electroformed***
R. Shneck and J. Margolin (Metal Surfaces, Inc.) ..... *page 106*

22. ***Invited Paper — Figure and finish characterization of high-performance metal mirrors***
P. Z. Takacs (Brookhaven National Lab, Instrumentation Division) and E. L. Church (US Army ARDEC) ..... *page 110*

23. ***Fabrication of a metal-plated mirror, beginning from a performance requirement***
J. S. Taylor (Lawrence Livermore National Lab) and C. J. Evans (Nat'l Institute of Standards & Technology) ..... *page 118*

24. ***Electroformed astronomical x-ray optics***
M. P. Ulmer, R. Haidle and R. Altkorn (Northwestern University, Basic Industry Research Labs) ..... *page 134*

25. ***On investigating material parameters influencing the diamond turning of electroless nickel plate*****
S. E. Becker (University of Tennessee, Knoxville) ..... *page 144*

*** Paper submitted but not orally presented*

Foreword

Precision engineering is, by definition, multi-disciplinary. This conference involved participants not just from a range of engineering disciplines, but from three distinct communities:

- *fabricators;*
- *platers; and*
- *users.*

The conference was born of frustration. Fabricators of plated optics and precision mechanical systems often blame platers for the inadequacies in the product they deliver. Platers, meanwhile, find some of their customers unreasonable, while the users are bemused by the angst that their simple requests sometimes provoke. Such technical bigotry might be mitigated, we felt, by dialogue and by improved understanding.

Precision finishing operations are performed on a wide variety of platings; results, and hence part performance, depend on many interacting facets of the overall production process. Both the commonality of problems, and the diversity of materials and applications were covered both in presentations and in lively discussion sessions. Inevitably, these proceedings cannot capture the full technical content of the meeting; we hope the record they provide will be a useful addition to the rather sparse published literature in this field.

The success of the conference was due, in large measure, to the efforts of the organizing committee. Our thanks go to Jack Dini, Bill Bryan, Dave Lunt, Bob Parks, Andrea Plain and, of course, ASPE Headquarters staff.

Chris Evans
John Taylor
Conference Chairmen

Technical Papers

The fabricator-plater relationship: an architecture for meeting the customer's specification.

K L Blaedel, J S Taylor
Lawrence Livermore National Laboratory

C J Evans
National Institute of Standards and Technology

Presented at
"Metal Platings for Precision Finishing Operations"
ASPE Spring Topical Meeting
Apr 91, Tucson, AZ

INTRODUCTION

The motivation for this topical meeting stems from the desire to successfully fabricate precision (reflective) optics and specifically the desire to help bring about successful plating of the substrate, something beneficial to both the fabricator and the plater. Borrowing the nomenclature from the introductory remarks to this meeting, the "customer" refers to the scientist who specifies and will use the plated (optical) surface. The "project engineer" has overall responsibility for making the surface to specification. He must translate the performance specifications (including the optical and mission requirements) into fabrication specifications. The consequence of an inappropriately plated surface is manifold beyond the loss of time and money on any particular job. For example, if a fabricator feels he has lost control over the plating process because he farms it out to the wrong plating shop and gets a poor coating, then he will be tempted to bring the plating in-house in order to regain control over the plating process. The loss to the plater is twofold; he lost future business and he also gained a competitor in the plating business.

The overriding conclusion to this conference in general was the need for communication. Many of the problems illustrated in the horror stories were attributed to lack of dialog between project engineer and plater. Further testimony in support of increased communication came from each of the attending platers. In summary, the personnel shown in Fig 1 are a team. The project engineer must live with the plating he receives; he cannot farm out responsibility to the plater. He therefore must assure himself that a successful plating will occur.

The goal of this session is to try to provide an architecture (for example, a specification) which addresses the comments made at this conference by the users and venders of platings which are a critical element of precision components. This can then be the basis for communication between fabricators and the plater when a coating is required for use as an optical surface. This goal will not be achieved here, but this conference will provide a good start. We will have pointed out some of the missing information required to communicate, but must also realize that plating for precision optical components continues to develop.

A VEHICLE FOR COMMUNICATION

Consider the paint on ship hulls or the anodization of an aluminum bracket. Porosity, pinholes, lack of adhesion, poor abrasion resistance, poor gloss all give rise to failure of the coating to perform its function. These are quite similar concerns to those for conventional metal coatings, but only the beginning for metal coatings for optical elements. A fundamental driver for metal coatings for optical components is that there are often machining operations like polishing or diamond

turning that go on after the coating is applied, that is, the coating is an intermediate process, not the final process in the fabrication sequence.

When, as a fabricator of optics, you can't get what you want from an outside source and failure to do so has extreme consequences, you are faced with choices of doing it yourself, designing your way around the problem or applying further pressure on the outside source to develop his process. The first step in applying the third approach is to understand the other person's process. In doing so, you figure out how to communicate what is possible and what is not. Ideally, this gives rise to the second step of developing a specification which documents what can be (routinely) done. This step may never materialize if a coating is used for many different purposes. Simultaneous with these steps is the development of technology to do what currently can't be done. The status of metal coatings for finishing operations lies still with trying to understand each others operations. Evidence to support this assessment lies in the plethora of horror stories chronicling the activities of fabricators and platers.

This meeting has aided in understanding each other's process and this session is an attempt to initiate the second step. We would like to develop a specification, but this implies that we completely define the characteristics of the plating process which are important, quantifiable, repeatable, and controllable. Further, the result must not be a response from the plater like, "Get the hell out of my shop!" Instead, we will begin with a check list of issues to negotiate between project engineer and plater before a contract is let.

We will attempt here to develop a check-list specifically for Electroless Nickel since it appears to be one of the more popular coatings, but with the hope that the list also largely applies to other coatings like Copper for example. We do not begin with Mil Spec C-26074D [1] because it controls electroless nickel plating for a very different purpose than that dealt with at this meeting and therefore addresses few of our concerns.

CONSIDERATIONS FOR ELECTROLESS NICKEL COATINGS FOR PRECISION FINISHING OPERATIONS

The substrate and its preparation by the fabricator(s) prior to plating is important to the success of the coating.

Exposure to fluids in the roughing stage can cause problems with cleaning the substrate prior to plating. An example of this is the use of silicones. This can be further compounded by challenging geometry, for example, cleaning a difficult fluid from a tapped, blind hole.

There are certain *geometries which do not lend themselves to high quality plating*. For example, deep, narrow grooves do not plate to the same thickness as a flat surface during electrolytic deposition. Chamfers represent similar challenges. Another consequence of this is that the thickness of a coating on a witness coupon (used to audit the thickness of the deposit) may be quite different from that on the actual workpiece. This effect is less pronounced in electroless deposition.

Isolated defects in the substrate can have a significant effect on the plating, even if the plating is quite thick. The defect can propagate through the plating.

Roughness of the substrate can affect the coating particularly its adhesion.

The effect of *"print-through"* of diamond turned tool marks is well documented [2]. Here, the roughness or waviness (documented for spatial wavelengths of about 30 μm) of the substrate replicates itself on the surface of the plating even after the plating has been machined. It is

speculated that the print-through effect is caused by an elastic deformation of the machine tool structural loop in response to the variations in cutting force associated with a varying depth of cut, due in turn to the initial surface waviness.

The *microstructure of the substrate* affects the quality of the plating and consequently, the ultimate surface finish that is achievable in post polishing. This is documented in the presentation of D. Lunt.

The substrate preparation by plater is critical to the quality of the plating.

The plater generally *cleans the substrate* for adhesion of the coating. Some techniques, particularly etching, radically alter the substrate surface. For example, etching a diamond turned surface will alter the contour as well as the microroughness of the substrate.

In some cases, *metalization* or a series of platings is laid down to facilitate adhesion of the final coating

The manufacture of optics sometimes requires that a datum surface be machined in the substrate and that that datum be preserved throughout the whole fabrication process. In this case, that surface may neither be etched nor plated. The techniques of *masking* such datum surfaces is quite varied depending on the coating to be applied and the geometry of the surface to be preserved. The masking also affects the quality of the plating adjacent to the mask.

The post plating and service environments of the part are of interest to the plater because the behavior of the plating may be sensitive to the environment. An example is the tendency of amorphous Ni-P to crystallize at elevated temperatures that one might see in a bake-out for use in a vacuum.

The thickness of the plating is a critical issue for most optics.

The *actual thickness* is important because it must be adequate to ensure that any post plating machining will not remove the whole thickness of the plating in areas and expose the substrate. Note that Mil Spec 26074 calls out specific thicknesses for the three different classes. None of these is necessarily appropriate for optical surfaces.

The *uniformity of the thickness* is important if the exact contour of the substrate were machined accurately before plating and expected to be preserved after plating. If the plating is thicker in areas, then the contour of the plated part is quite different from that which was machined. Also, the surface mechanical properties are certainly a function of the plating thickness and if these are critical, then so also is the uniformity of the thickness of the plating.

There are many methods for determining the thickness of the coating depending on the coating itself, the substrate and the accuracy to which the thickness must be ascertained [13-19].

Residual stress of the plating can be controlled when applying electroless Nickel and should be zero as stated in J Dini's presentation.

The first reason is that, as presented by J Taylor, a highly stressed layer will *deform a workpiece* if the substrate is thin, a condition which characterizes most optical elements. If the substrate was contoured prior to plating, then it will no longer maintain that contour with a highly stressed layer of Nickel after plating. If the coated substrate is to be contoured after plating by removing a portion of the plated layer, then the contour will continually change as material is removed. This makes the chore of arriving at a given contour that much more difficult.

The second reason for striving for low residual stress is that there is a *tendency to recrystallize* over time and temperature occurs as a function of residual stress for electrodeposited Nickel. The deleterious effects of the recrystallized Nickel coating grossly affect subsequent diamond turning or polishing. Also, a volume change accompanies the transformation from amorphous to crystalline structure and hence further dimensional change to the optic results. This transformation occurs particularly for high phosphorous Nickel and bright Copper.

Thirdly, high residual stress in the plating can cause *poor adherence* of subsequently applied dielectric films as mentioned in J Dini's presentation.

Residual stress can be measured by a number of methods. Deformation of a spiral strip can be measured and the residual stress inferred [11]. An instrument for real-time monitoring of the stress at which a plating is deposited also exists [12].

Adhesion of the plating is often addressed in conventional plating and hence a number of methods for testing adhesion have arisen. Each of these tests applies to a small range of plating thickness and because of its destructiveness, must be applied to a witness sample plated with the part rather than the part itself. The pressure tape adhesion test [20] uses "scotch tape" to peel off thin coatings of less than about 10 μm. The "Sebastian I" test [22] uses a stud which is bonded to the coating and the tensile force required to separate the plating from the substrate is indicative of adhesion. The "Ring Shear" test [21], not yet an ASTM standard, gives quantitative information about adherence of electroplated coatings.

The specification for a polished optic usually controls the final surface finish of the plated surface. Roughness of the plating sets the initial condition for polishing and hence greatly influences time to polish and the amount of material to be removed to arrive at the specified roughness.

The microstructure of the plating plays an important role in subsequent machining of the coating.

Electroless Nickel can be deposited as either *crystalline or amorphous* or both depending on phosphorous content and heat treatment [3]. The amorphous microstructure yields lower surface roughness and lower wear of a diamond tool during post plating machining. The mechanical properties are also influenced by the microstructure. For example, the thermal expansion of ENi plating is quite sensitive to the microstructure (phosphorous content). Further, as-deposited electroless nickel is metastable and undergoes a crystalline transition at moderate time and temperature as shown in the presentation of Meyer.

The *grain size* of the (crystalline) plating should be fine and should be stable over the time and temperature of the service environment of the workpiece.

Isolated inclusions in the plating fall into a number of categories, all of which potentially cause deleterious effects depending on the size and distribution of the inclusions. Among the consequences are local scattering of light and difficulties in machining the coating. Many of the defects can be mitigated by steadfast filtration of the plating bath.

The *composition* of the inclusion is of great concern because, if it is hard, it can cause tool wear if diamond turned or rip up the lap if polished. If the "inclusion" is gaseous, that is, a void, then it can in some cases of polishing, entrain polishing abrasives thereby resulting in a poor surface finish in the area immediately surrounding a void. These affects are chronicled here in the presentation of Brown.

The motivation to control porosity of the plating stems from a number of concerns. Firstly, the *corrosion resistance* is often sensitive to the size and distribution of the porosity. Secondly, porosity leads to *scattering of light* off reflective surfaces. Thirdly, porosity makes *cleaning* the surface more difficult because the pores tend to retain contaminants.

The corrosion resistance of the plated substrate is of interest in the link between the customer and plater and between the project engineer and the plater. The surface must be corrosion resistant in its service environment, but also, if machining fluids are to be used which cause corrosion (through porosity for example), then this is a topic to discuss between fabricator and plater. There are a number of tests for corrosion resistance [5,6,7].

Hardness and abrasion resistance is often a manifestation of the microstructure of the plating[2]. In addition to the comments listed under microstructure, which equally apply here, there is the issue of handling damage. For example, soft copper is a nuisance because it cannot drag wiped without scratching the surface. Various ways to measure (micro)hardness abound in the literature [8,9].

Quality assurance engulfs all of a plater's operation from how frequently he changes the filters on the plating bath to how well trained are his employees. Quality assurance as a whole may be difficult for a customer to assess, but at a minimum, inspection of a part must occur before and after plating. Inspection before plating ensures that ill conditions mentioned in the section on substrate preparation do not preclude a good plating. Inspection after plating often takes the form of (destructive) testing in a non-critical region of the actual part or of a witness sample, allowing an audit of the plating process as well as the substrate preparation. In the case of a witness coupon, the question arises whether it well represents the actual workpiece. Even if the coupons are processed simultaneously with the workpiece, the plating may fundamentally differ from the workpiece. For example, the surface of a flat witness coupon may be polished quite differently from that of the contoured workpiece and the quality of the plating is functionally dependent on the quality of the polished surface. Hence, testing the plating of the witness coupon may tell little about the plating of the actual workpiece.

Liability and terms & conditions should be clearly spelled as part of the contract negotiations. In many cases the substrate, as it is received by the plater, may have very high value and may be quite difficult to replace. The cost for the plater to take responsibility for the part may far outweigh the cost of the plating itself. These terms apply not only to the time the part is at the plater's shop but also extend to the packing and shipping of the part.

REFERENCES

[1] Mil Spec MIL-C-26074D "Requirements for Electroless Nickel Coatings".

[2] Husheng, G, Haicheng, G, and Huijiu, Z, "Sliding wear and fretting fatigue resistance of amorphous Ni-P coatings", WEAR, V 142, N 2, 1 Mar 91, pp 291-301.

[3] Taylor, J S, Syn, C K, Saito, T T, and Donaldson, R R, "Surface finish measurements of diamond-turned electroless-nickel-plated mirrors", OPTICAL ENGINEERING, V 25, N 9, Sep 86, pp 1013-20.

[4] Syn, C K, Taylor, J S, Donaldson, R R, "Diamond Tool Wear vs Cutting Distance on Electroless Nickel Mirrors", SPIE Annual Mtg, August 18-22, 1986, San Diego, CA

[5] ANSI/ASTM B 537- "Rating of Electroplated Panels Subjected to Atmospheric Exposure".

[6] ANSI/ASTM B 117- "Standard Method of Salt Spray (Fog) Testing".

[7] ANSI/ASTM B 287- "Acetic Acid-Salt Spray (Fog) Testing".

[8] ANSI/ASTM E 384- "Microhardness of Materials".

[9] ANSI/ASTM B 578- "Microhardness of Electroplated Coatings".

[10] ANSI/ASTM B 571- "Adhesion of Metallic Coatings".

[11] ANSI/ASTM B 636- "Internal Stress Measurement with the Spiral Contractometer".

[12] available from Dawn Electrochemical Engineering (Engelhaupt, D), 517 Nance Rd, Madison, AL 35758.

[13] ANSI/ASTM B 499- "Magnetic Thickness Measurement for Ductility of Electrodeposits".

[14] ANSI/ASTM B 504- "Thickness Measurement of Metals - Coulometric Method".

[15] ANSI/ASTM B 530- "Thickness Measurement Magnetic Nickel Mag/Nonmag Substrates".

[16] ANSI/ASTM B 567- "Thickness Measurement by the Beta Backscatter Method".

[17] ANSI/ASTM B 568- "Coating Thickness by X-Ray Spectrometry".

[18] ANSI/ASTM B 659- "Measuring Thickness of Electrodeposited and Related Coatings".

[19] GM4260P- "Measuring Thickness of Electrodeposits and Anodic Coatings" General Motors.

[20] Ott, J, "Semi-Quantitative Measurement of Pressure Tape Adhesion for Vacuum Metalizing", METAL FINISHING, p61, 1/78.

[21] Dini, J W, Kelley, W K and Johnson, H R, "Ring Shear Testing of Deposited Coatings", TESTING OF METALLIC AND INORGANIC COATINGS, ASTM STP 947, 1987, pp320-8.

[22] Available from Quad Group, The Quad Building, 2030 Alameda Padre Serra, Santa Barbara, CA 93103.

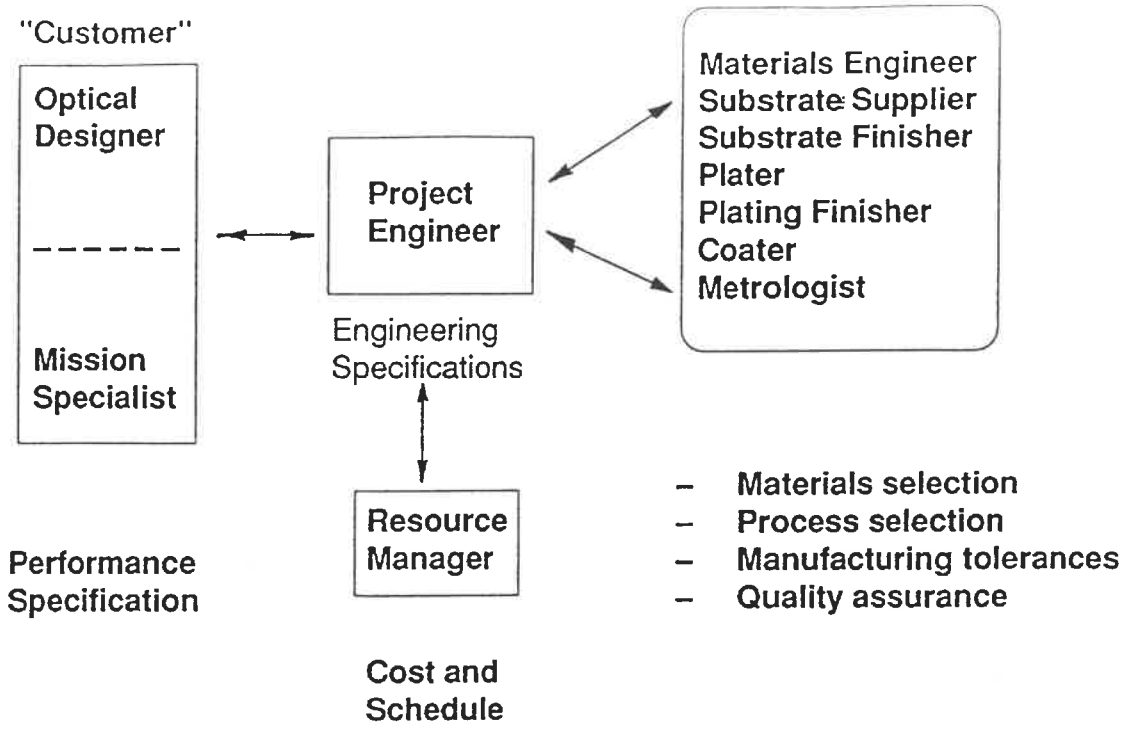

Figure 1. Fabricating a metal-plated mirror involves contributions from an interdisciplinary project team.

Selecting the Correct Work Piece Material:

An overview of Issues Concerning the Fabricator and Plater

William J. Bryan
3M Company
Optics Technology Center
Petaluma, California

April 1991

Introduction:

The fabrication of optical components utilizing the diamond turning process requires the highest quality materials. Selecting the right work piece material or substrate for a particular application can be a difficult task. When the wrong substrate is selected and the fabrication process begins, there is a strong likelihood the work piece will not meet the intended purpose. The designer may not have seriously reviewed the various choices of materials nor consulted the fabricator or plater. A review of the substrate selection process is described, as well as technical concerns of the fabricator and plater.

The designer usually analyzes the design function, creates a part drawing, then bases the substrate selection on material properties best suited to meet the design goal. Selecting a substrate for optical applications is a difficult job. A detailed analysis of the material properties of a candidate material is the first step. Solicitation of the manufacturing concerns of the fabricator and the plater should be the second step.

Material Selection:

In many situations, component design and fabrication methodology go hand in hand. The designer usually keeps in mind a general method of fabrication. Unfortunately, the electroplater is usually the last person to be consulted. Very often he is given little information about the job, but is then expected to produce flawless quality at minimum cost. An important criteria for a successful project is the need to bring the design engineer, fabricator, and if necessary, the electroplater together early in the process to critically review the material selection.

As the design function evolves, so must the material selection process. The designer must determine the physical and optical properties needed for the work piece and specify these in general terms. For metal optics, the most sought after quality is surface finish and form accuracy. These two requirements are dependent upon the substrate material. The designer must also consider other properties that may effect the work piece function. The following are several useful physical and optical properties which a designer should consider:

Physical Properties:

Density (weight)
Conductivity
Young's Modulus
Corrosion Resistance
Coefficient of Linear Expansion
Yield Strength
Fracture Toughness
Dimensional Stability
Hardness

Optical Properties:

Reflectivity
Wave Length of Radiation
Form Accuracy
Surface Roughness
Scatter

and above. For this application, the designer must know the coefficient of linear expansion and account for dimensional changes of the mold. For high power laser optics, the designer may need to actively cool the mirror. Data on thermal conductivity, density, and specific heat must be available to do a good job of analyzing these thermal problems. In selecting the best material for the application, a formal design review is a useful technique.

For optics where coatings are applied, the designer must be aware of surface chemistry especially prior to the coating operation. Cleaning of the substrate is especially important prior to plating. Some solvents may be chemically incompatible and stain the substrate prior to coating. In the case of vapor coating, the substrate should be checked for the possibility of "out gassing", which would interfere with the deposition process.

Fabrication and Plating Considerations:

Once a material category has been selected, the fabricator and plater must now consider all aspects of their process and determine whether the substrate will be suitable for the fabrication process. If wrought materials are selected, the fabricator must be concerned about the source. Most wrought materials are made in large quantities, in "dirty" environments, and specified to meet mechanical material specifications. Entrapped dirt in the wrought material can lead to poor surface finish and extensive tool wear. A memorable example of "entrapped dirt" was the case of two steel screws rolled directly into a brass sheet delivered from the factory for our "optical" use.

Residual stresses are inevitably present if cold working is used to achieve appropriate levels of grain size, strength and hardness. Dimensional instability can then become a problem. In flat stock for instance, the rolling direction causes non-uniform stress. It is our experience that diamond turning an optical flat from cold rolled, round bar stock can be very difficult. Residual stress at the circumference can continue to affect the flatness of the surface after several roughing passes have been made.

There is a temptation to simply anneal wrought material in an attempt to avoid the residual stress problem. Annealing may have the side effect of making the material too soft. Wrought material in the copper and brass family have demonstrated improved diamond turnability after having been cold worked to a size reduction of 25 to 50%. Cold working increases the hardness and reduces ductility below 25% elongation.

In diamond turning, the quality of the machine tool is the key variable in improving surface finish. However, when surface roughness values approach 25 nm Ra and below, material properties play an ever more important role.

The following table outlines various concerns of the fabricator and plater:

Fabrication Concerns:	**Plating Concerns:**
Residual Stress in Blank	Adhesion
Grain Size	Plating Stress
Material Voids & Entrapped Dirt	Pits
Heat Treatment	Masking
Tool Wear	Bath Chemistry
Compatibility with Coolant	Cleaning
Availability and Cost	Current Density
Part Distortion	Electroless vs. Electro
	Coating Thickness

Grain size is an important factor when considering wrought materials. Grains are formed during solidification from a liquid, and their crystal orientation becomes random. Grain stiffness can vary by a factor of five to one depending upon crystal orientation. As the diamond tool traverses through an individual grain, cutting forces deflect the grain prior to cleaving. The resultant topography resembles an "orange peel" appearance which contributes to light scattering. Surface measurements on grainy materials show height changes of 25-50nm from grain to grain. For this reason, amorphous materials are preferred, such as electroless nickel.

Diamond Turned Brass Sample
50X

Etched Brass Sample
80X (30μm grain size)

If plating is necessary, the fabrication process becomes more complex. The designer, fabricator and plater must work together to select a viable fabrication process. A general specification for the plated coating is required. At a minimum, the coating type is required, as well as average thickness, variation of thickness, areas to be masked, and hardness. Other parameters such as the size and number of permissible pits, adhesion of the plating, levels of residual stress, and surface uniformity must be carefully specified.

When specifying electroless nickel, it is prudent to define the minimum and maximum levels of phosphorus. Phosphorus content can dramatically affect tool wear in the diamond turning process. The following graph illustrates the effect of phosphorus content on tensile strength:

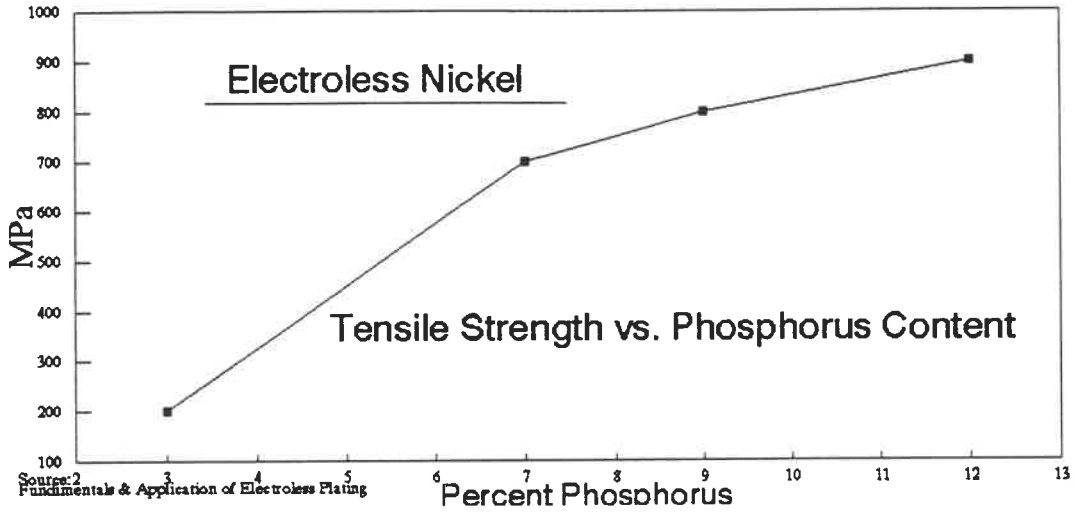

If the material on which the coating is to be applied can be arbitrarily selected, then it's important to involve the plater as soon as possible. Many platers prefer to apply coatings on specific alloys for processing purposes, such as adhesion strength.

Surface texture of the substrate is also a platers concern. Substrate surface texture can directly influence the topography of the coating. A smooth and clean surface is needed. If the substrate is diamond turnable, a preferred processing method is to diamond turn the rough shape and leave the cutting oil on the work piece. This predetermines the surface chemistry of the substrate, which is advantageous to the plater.

The designer should be aware of bimetallic work pieces. This can happen when the substrate is of a different material than the plated material. If there's a difference in work piece temperature at the time of machining, versus the parts "ultimate use" temperature, the possibility of part distortion is very real.

Work pieces that require plating present added problems to the fabricator. These parts require that the machining process must happen twice. Rough machining is required to prepare the work piece for plating. This usually requires a separate NC data file. For concave parts, the radius of curvature becomes larger prior to plating. For convex work pieces, the radius becomes smaller to allow for the plating thickness. Mistakes can easily be made in allowing for plating thickness of complex shapes. The overall cost of the work piece can easily double if plating is required, and failures are common even for the most seasoned project engineer.

The choice of materials that are suitable for diamond turning is somewhat limited because of tool wear. The fabricator must keep tool wear to a manageable level. Materials that are diamond turnable usually have face-centered-cubic structures. Aluminum is the most common diamond turned material. Infrared mirrors, computer discs, VCR's and copier scanners all utilize aluminum. Polymers, such as PMMA are commonly used in the ophthalmic industry.

Electroless nickel and electro plated copper are favored for precision optical fabrication by many vendors. Electroless nickel is a relatively hard surface and lends itself to post polishing. Tool wear in electroless nickel is high, although manageable for small parts. Electro plated copper offers the fabricator a number of advantages. Benefits include: very fine grain size, low tool wear, and low ductility. Diamond wear of 0.25μm has been measured on tools with travel lengths of 160 kilometers. Disadvantages can include: non-uniform plating stresses, self annealing if plated hard, and a surface prone to corrosion. The following table gives several material properties for common diamond turnable materials.

Materials	Young's Modulus (GPa)	Tensile Strength (MPa)	Percent Elongation (%)	Hardness (Vickers)	Grain Size (Micrometers)
Alum.–6061–T6	71	310	12	91	–
Copper–Annealed	119	206	45	96	200
Brass (70–30) 1/2Hd.	106	427	25	150	30
Brass (micrograin) Anl.	106	509	36	140	1–2
Electro Plated Cu.	119	620	7	200	0.1
Electroless Nickel(8% P)	55	750	4	500	–
PMMA	3	65	4	23	–

Conclusion:

This paper addresses several important issues for the selection of materials used in the diamond turning process. Review of material properties as they relate to the fabrication process, plating process, and functional use of the work piece is required to properly select a substrate. A team approach is desirable in the selection process and shall include the designer, fabricator and plater. Specifications should be provided for each process as well as information regarding part history. This is especially important for the plater.

The quality of a process can be measured in how well the customers expectations are met. Expectations are usually conveyed in a set of specifications and process requirements. If the requirements are not listed, are poorly communicated or simply not understood, the likelihood for a high quality work piece is poor. The best recommendation for selecting a substrate is to effectively communicate the application to those involved and develop a set of realistic specifications.

Acknowledgements:

The author wishes to thank William M. Shubin of 3M, for his contribution and comments regarding electroless nickel plating.

References:

1) Brooks, C. R. "*Nonferrous Alloys*", American Society of Metals, Metals Park, Ohio

2) Field, J. E. (edited) "*The Properties of Diamond*", Academic Press, San Diego, Ca. 1979

3) Mallory, Glynn O., Hajdu, Juan B., "*Electroless Plating: Fundamentals and Applications*", American Electroplaters and Surface Finishers Society, Orlando, Florida 1990

4) Stadler, H. J., Freisleben, B., Heubeck, C. "Response of Metallic Material to Micromachining", Forth International Precision Engineering Seminar, 1987

Smooth Nonmagnetic Electroless Nickel Deposition For the Computer Memory Disk

David Crotty, Ph.D.
Allied Kelite Company
Division of Witco Corporation
29111 Milford Road
New Hudson, Michigan 48165

The most popular computer data storage media has long been the aluminum disk plated with electroless nickel and topped with a memory media of plated or sputtered cobalt. This media seems likely to remain an attractive choice despite competition from several emerging technologies. The competition does put pressure on the disk drive manufacturers to reduce costs and, at the same time, improve data density and access times. The plater must respond to these pressures by obtaining improved aluminum substrate and improved processing.

The ultimate goal of our research in this area has been two-fold: first, provide a plating cycle that gives a smooth surface that requires a minimum of final finishing; and second, provide an electroless nickel deposit that remains nonmagnetic at the higher sputtering temperatures required to obtain the higher coercivity media.

Plating Cycles

The substrates used for the computer memory disk vary widely in alloy and surface finish. Pretreatment cycles must be tailored carefully to suit the substrates. Each substrate type responds differently to the pretreatment conditions.

The cycles usually include an alkaline and an acid cleaner. Several processes in the Niklad Alprep line have been developed to suit the various substrates.

A zinc immersion layer is critical to the initiation of the electroless nickel and to adhesion. The most common zinc immersion is the alkaline type ARP 302ZN or ARP 303ZN. Recently, an acid zinc immersion process, ARP 350, has been developed to provide a smoother underlayer for the electroless nickel.

Several cycles consisting of these processes have been developed to provide the best pretreatment for the substrates being used by the industry.

Electroless Nickel

Electroless nickel processes currently in use include Niklad 719. This workhorse process has long been the standard of the industry. However, the deposit is more nodular than is desired and the deposit becomes magnetic at the higher temperatures required for the new media topcoats.

A novel process has been developed to fill the need for a smoother deposit with higher temperature magnetic stability. This process, Niklad 725, has been integrated into the pretreatment cycles developed for the various substrates.

Future Work

While the processes described are an improvement over current technology, they can only be considered an evolutionary step in the overall research scheme. Development continues with an eye on improving pretreatment and electroless nickel.

Niklad 797
Hardness and Wear Resistance of Boron Electroless Nickel For the Price of Phosphorus Electroless Nickel

David Crotty, Ph.D.
Allied Kelite Company
Division of Witco Corporation
29111 Milford Road
New Hudson, Michigan 48165

In the past, when a parts designer needed a hard wear resistant surface there were few choices, with hard chrome or boron electroless nickel being the main alternatives. Hard chrome does not provide a uniform surface due to the variation of thickness with current density, and boron electroless nickel is very expensive.

The other types of electroless nickel have been useful in a wide range of applications, but never came close to the wear resistance and hardness required for some applications without heat treatment. A new type of electroless nickel is now available that provides an "as plated" hardness like that of boron electroless nickel and a heat treated hardness that is almost as hard as hard chrome. Niklad 797 belongs to this class of electroless nickel. Besides the desirable deposit properties, Niklad 797 also has exceptional processing characteristics that allows parts to be plated quickly and more easily than is typical for electroless nickel processes.

Hardness

Hardness is measured at a specific load according to the ASTM B578 method. The average "as plated" hardness, expressed as Knoop hardness at 100 gram load, obtained for the various classes of electroless nickel are listed in Table 1. Clearly, the lower phosphorus deposit provides the best hardness of the phosphorus alloy electroless nickels and rivals the properties provided by the boron alloys.

Wear Resistance

Abrasive wear resistance is determined using the Taber wear index (TWI) using CS-10 abrasive wheels and a 1000 gram load. The weight loss on a rotating panel is stated as milligrams/1000 revolutions. Wear resistance does not always follow with hardness. Table 1 lists data for Taber wear tests for various deposits. Again, the low phosphorus Niklad 797 as plated deposit performs as well as the best boron deposit.

Internal Stress

Internal stress is sometimes a consideration in determining the suitability of a deposit for an application. Stress is measured using the Spiral Contractometer using the ASTM B636 method. Niklad 797 deposits exhibit very low tensile stress, and contrary to the behavior of other processes, the stress decreases slightly with the age of the plating bath. Table 2 illustrates the internal stress measured for deposits obtained from a Niklad 797 bath as it is used. The deposits obtained from this process are consistent from fresh makeup to the end of the bath's life.

Processing Considerations

Considerations that are important to the plater include ease of control, bath life and plating rate. Niklad 797 is packaged as a self controlled process. Addition of the components according to a simple analysis maintains bath chemistry and pH automatically. The bath is stable and deposits are consistent through at least 10 metal regenerations, which is considered excellent.

Finally, the plating rate is fast, often at 1 mil/hour, through the bath life. In fact, a good plating rate may be obtained at as low as 170°F. This may be used to the plater's advantage to save some heating costs, or may be useful for some parts that are sensitive to higher temperatures.

Table 1
Knoop Hardness and Taber Wear of Nickel Deposits

Process Name	Alloy	Hardness HK100		Taber Wear Index mg/1000 rev	
		As Plated	Heated	As Plated	Heated
Niklad 797	3-5% P	655-735	960-990	9.9-11.8	
Niklad 794	6-9% P	500-600	800-900	18.8-20.0	10.2-11.9
Niklad 1000	10-13% P	450-500	800-900	24.0-24.5	10.6-14.2
Niklad 752	0.1-1.0% B	750	600	8.0-8.6	7.5-9.4
Niklad 740	2-3 % B	700	900	22.3-23.5	12.1-13.5

Table 2
Spiral Contractometer Stress
0.9 mil deposit Niklad 797

Bath Age Metal Regenerations	Stress PSI
0	2350 tensile
1	2180 tensile
9	361 tensile

PERSPECTIVE ON PLATING FOR PRECISION FINISHING

J. W. DINI
Lawrence Livermore National Laboratory*
P. O. Box 808, L-332
Livermore, CA 94550

Invited paper for ASPE Spring Topical Meeting on Metal Platings for Precision Finishing Operations
Tucson, Arizona
April 15-18, 1991

Introduction

This paper is intended as an overview on platings for precision finishing operations. After a brief review of the two processes (polishing and precision machining) by which a coating on a part can be converted to a precision surface, the coatings which work successfully in these applications will be discussed. Then adhesion and stress aspects of deposits will be covered. Electroless nickel, which is a particularly attractive coating for precision finishing applications, will be discussed in some detail, from its early years as the "Kanigen" process to the present. Since microstructural changes in deposits are important for precision parts, this aspect will be covered for electroless nickel, copper and silver deposits. Lastly, some words will be directed at potential future electrodeposited coatings including nickel-phosphorus alloys, and various silver alloys.

Precision Finishing

There are two processes by which a coating on a part can be converted into an optical surface. These are conventional grinding and polishing and precision machining. While these processes are quite different the result of their application is the removal of physical irregularities on the coated surface, the generation of specific shape required, and the improvement of finish (reduction of surface roughness) to a level where any resultant scattered radiation is within tolerable limits.

Polishing

The removal of any material by polishing, be it glass or metal, is roughly a process of wear(1). Here a polishing or grinding lap base is coated with a deformable material (these vary greatly in compliance, viscosity and other

* Work performed under the auspices of the U.S. Department of Energy by the Lawrence Livermore National Laboratory under contract No. W-705-ENG-48.

material properties depending on the application). This lap is placed against the surface to be worked and continuously fed with a polishing compound, usually a fine, less than 3 μm diameter particle size metal oxide powder. The lap and workpiece are moved with respect to one another in a series of rotating and oscillating motions in a known way. The resultant energy imparted to the surface by the lap through a combination of mechanical abrasion, chemical attack, and thermal flow disrupt and remove the material. This process results in surfaces whose finish characteristics are small compared to the wavelength of light being applied and whose shape can be controlled to some extent(1).

The advantages of this process with respect to precision machining in general relate to the wide variety of materials that lend themselves to polishing and the relatively high quality finishes normally achieved. Optical polishing has been successfully applied to most all glasses, metals and crystals, as well as most all hard inorganic materials and semiconductors. It is a process that is insensitive to mechanical vibration, acoustic coupling, and in most cases, small variations in temperature(1).

Reflectance data for a number of coatings which had been diamond polished in silicon oil to 10Å RMS surface roughness or better ar shown in Figure 1 for the range between 0.40 and 2.5 μm wavelengths. Bright nickel and sulfamate nickel showed approximately 12% higher reflectivities than electroless nickel and tin-nickel. Although all four of thee coatings could be optically polished, only electroless nickel and tin-nickel deposits could be diamond turned without causing undue degradation of the diamond tool(2).

Precision Machining

Precision machining (also termed single point diamond turning or just diamond turning) is accomplished by combining the very hard and sharp edges obtained from certain crystalline (usually diamond) tools with extremely precise machine tools (either liquid or gas bearing) operating under closely controlled environmental conditions to produce finished or nearly finished optical surfaces. This technology removes some of the difficulties in forming optical surfaces encountered in conventional grinding and polishing, specifically for that family of materials both physically and chemically compatible with diamond tools. Because these tools are so hard and sharp, no cutting edge contact area is presented to the material. This promotes the cutting process by restricting it to a thin shear plane with a minimum of contact stress or friction and results in a process that minimizes material deformation. The result is a specular finish required for optical surfaces and a contour that is an exact copy of the tool path(1).

The materials that can be successfully diamond turned are limited in number. Table 1 lists those compatible with diamond tools and hence considered machinable. It is interesting to note that all of the metals listed in Table 1 except for beryllium-copper can be deposited from aqueous solutions or non-aqueous solutions (aluminum).

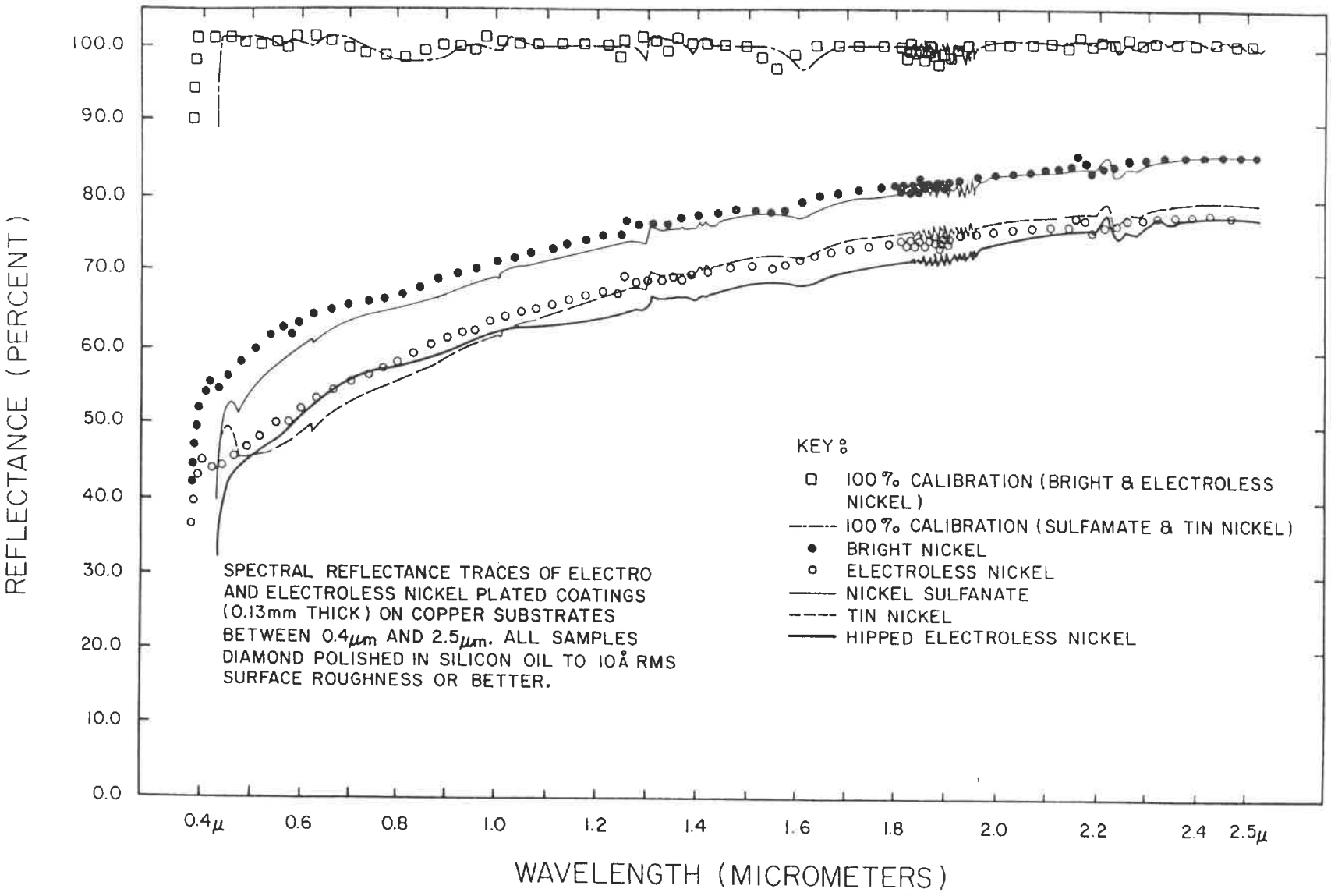

Figure 1 - Spectral reflectance traces of electrodeposited and electroless nickel plated coatings on copper substrates. From Reference 2.

Metals which are carbide formers such as iron, pure nickel, molybdenum, tungsten and titanium are not amenable to single point diamond turning because they cause rapid deterioration of the diamond tool. Metals with which carbon has very low or no solubility, such as aluminum, copper, gold, silver and tin lend themselves well to single point diamond turning(3).

Table 1
Diamond-turned materials*

Nonferrous metals	Infrared-transmitting materials	Polymers
Aluminum[a]	Germanium[a]	Acrylic[a]
Brass[a]	Silicon[a]	Nylon[a]
Copper	Zinc sulfide[a]	Polycarbonate[a]
Beryllium-copper[a]	Zinc selenide[a]	Polystyrene[a]
Electroless nickel[a]	Alkali halide	Polysulfone
Gold	Lithium niobate	Acetal
Silver	Cedium iodide	Fluoroplastic
Tin	Potassium chloride	Silicone
Tin-nickel	Calcium fluoride	
Platinum	Cadmium telluride	
	Mercury cadmium telluride	

[a] Most common lens or mirror materials
* From Reference 3

Adhesion

A wide variety of substrates are used in the manufacture of precision parts. A number of these such as aluminum, beryllium, beryllium-copper, molybdenum and glass are not the easiest materials to coat with adherent deposits. Special processing is required to ensure adhesion of the coating to the substrate. When properly prepared for plating, adhesion can be quite good as revealed in Figure 2 which shows failure in 7075 aluminum which was overplated with thick nickel.

The origin of the problem for most difficult-to-plate substrates is typically a thin, naturally forming oxide film that is difficult to remove and that reforms quickly when a clean surface is exposed to air or water. Techniques that have been used by electroplaters to prepare difficult-to-plate substrates for coating include:

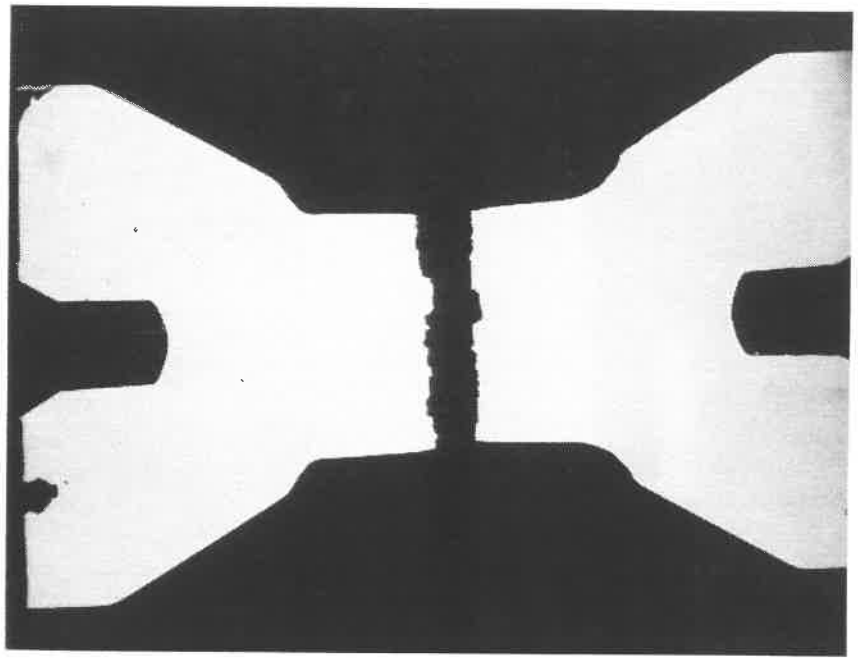

Figure 2. Cross-section of nickel plated 7075 aluminum conical head tensile specimen after testing (magnified 6X). Failure occurred in the aluminum at 83,000 psi (573 MPa).

etching to allow mechanical keying between the substrate and plated deposit, mechanical roughening such as glass bead or sand blasting to roughen the substrate surface, replacing the oxide film with a displacement coating, heating to allow for the interdiffusion between the substrate and coating, anodic oxidation of the substrate, and intermediate strike coatings to minimize coefficient of thermal expansion mismatches. With precision substrates many of these techniques are not very acceptable since they can noticeably alter the original surface. For example, chemical or mechanical etching can considerably change the surface finish and heating can induce distortion.

A relatively new approach that works very well and also eliminates the severe pickling, mechanical roughening or heating required of the processes just discussed is the use of augmented energy physical vapor deposition to provide an initial adherent coating and then electroplating over this to the required final thickness. Ion plating and hot hollow cathode deposition have been used successfully for providing the initial, adherent coating. Ring shear data (4) for three very difficult-to-plate metals, tungsten, molybdenum and titanium are presented in Table 2. In all cases, the adherence was considerably improved over that obtained without the use of PVD. Clearly, coupling augmented energy PVD processes with electroplating provides better adhesion than obtained with wet processes and also eliminates: 1) the need for roughening the surface chemically or mechanically, and 2) heating after coating.

Stress

Residual stresses which are inherent in deposition processes can result in distortion or be the cause of poor adherence of subsequently applied dielectric films (5-8). Some electroless nickel deposits on beryllium induce significant tensile stresses in the composite and these stresses can produce unacceptable distortions (5,8). Even room temperature relief of silver electroplating stresses can be a problem with optical parts. For example, a flat brass mirror plated with silver then diamond turned to better than 0.5 fringe deformed 9 fringes within 15 months after machining. Removing the silver by machining eliminated the distortion and essentially restored the original features (9). One technique used to minimize stress problems in these kinds of situations with silver and copper plated parts is to heat at 150°C prior to diamond turning. It is important to note, however, that with some electrodeposits this treatment could cause recrystallization and grain growth. For example, the grain size of silver deposited at 21.5 A/m^2 (2 asf) in a cyanide solution containing carbon disulfide increased from 2.36 to 3.22 x 10^{-6} cm during a three month storage period with a corresponding decrease in hardness from 148 to 130 VHN (10).

Table 2
Ring Shear Data Show the Value of Combining PVD with Electroplating for Coating Difficult-to-Plate Metals

Metal	Ring Shear Adhesion (MPa)	
	Electroplating	PVD & Electroplating
Tungsten	48[a](Cu)[b]	173[c](Cu)
Molybdenum	125[d](Au)	216[e](Cu)
Titanium	145[f](Ni)	252[g](Cu)

a) This process included etching in 3 parts HF, 1 part HNO_3, and 4 parts H_2O for 5 min. at 22°C followed by anodic treatment (1076 A/m^2) in 300 g/l KOH at 50°C for 5 min. prior to plating.

b) Metal in parenthesis was that used for building up the thick ring (1.5mm) required for ring shear testing.

c) The magnetron ion plating process included sputter etching in vacuum, magnetron ion plating with 6μm of copper and then electroplating to final thickness. Base pressure of the system was 5 x 10^{-6} Pa (10^{-8} Torr), etch power was 0.5 watts/cm^2, and bias power was 0.078 watts/cm^2 (but tapered to zero after deposition of about 20,000Å of copper).

d) This process included degreasing in perchlorethylene, firing in dry hydrogen (<2ppm H_2O) for 10 min., immersing in a solution containing four parts NH_4OH (28%) and one part H_2O_2 (30%) for 8 to 10 seconds at room temperature, rinsing in distilled water, gold striking to deposit 0.15 to 0.63 mg/cm^2 (0.08 to 0.32 μm), rinsing in distilled water, firing in dry hydrogen at 1000°C for 10 min., and then electroplating to final thickness.

e) The magnetron ion plating process included sputter etching in vacuum, magnetron ion plating with 6μ of copper and then electroplating to final thickness. Base pressure of the system was 5 x 10^{-6} Pa (10^{-8} Torr), etch power was 0.5 watts/cm^2 and bias power was 0.078 watts/cm^2 throughout the coating run.

f) This process included abrasive blasting, cleaning in hot alkaline solution, pickling in HCl, bright dipping in a solution containing 10% by vol. of HF (70%), 1% HNO_3 and balance water, followed by anodic etching for 6 min. at 162Å/m^2 in a 40°C solution containing 13% by vol HF (70%), 83% acetic acid and 4% water. Then 25 μm of Ni was plated in a sulfamate solution at 48°C. Specimens were heated at 480°C for 2 hours and then plated with approximately 1.5 mm of nickel.

g) This process included coating with 10 μm of copper by hot hollow cathode deposition and then electroplating to final thickness. Conditions for the etch cycle included a source power/rate of 10Å/sec, substrate voltage of 2 KV and pressure of 3 x 10^{-4} Torr. Conditions for the coating cycle were a source power/rate of 100 Å/sec, and a pressure of 3 x 10^{-4} Torr.

By judicious choice of plating operating conditions (e.g., current density, pH, solution composition, and additive content) it is possible to deposit coatings that are in a stress-free state. For example, Figure 3 shows deposit stress as a function of current density for a plating solution used to deposit up to 1 mm of copper on glass. This plot defines the current density to use to produce zero stress in the deposit and this information was utilized to coat neutral density glass substrates (15 cm by 15 cm) with 1 mm of copper and pyrex optics (22 cm diameter) with 0.4 mm of copper. This deposit was capable of withstanding single point diamond turning to provide an optical surface (Figure 4). it was also able to withstand heating at 250°C for four hours without degradation of the metal-glass bond (11).

One technique utilized to provide for real time control of stress that has been used in the electroforming of optical components is plating on a strain gage simultaneously with the actual part (Figure 5). As the plated surface of the gage bends in response to compressive or tensile forces, an analog is produced. The strain signals are analyzed by computer programs which vary the output of the power supply up or down to compressive or tensile bending of the plated surface. Stress control with this method is reported to have been held sufficiently close to zero so that dimensional accuracy in optical nickel electroforms was 0.15 μm (12).

If one has the chance to provide input on the substrate material at the design stage, this can considerably help in minimizing stress problems with subsequent coatings. An example is Figure 6, which shows the stress in electroless nickel deposits as a function of phosphorus content for aluminum and brass which have high expansion coefficients, and steel, beryllium and titanium, which have low expansion coefficients. Besides showing that the substrate has a very distinct influence on stress, the curves also show that for each metal, a deposit with zero stress can be obtained by controlling the amount of phosphorus in the coating (13).

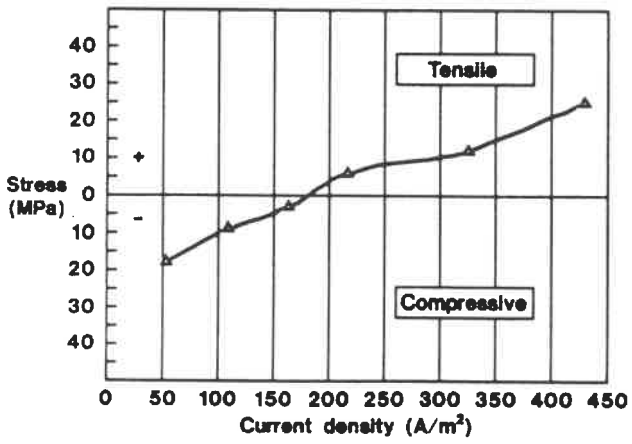

Figure 3 - Deposit stress as a function of current density for a high copper/low sulfuric acid solution containing a proprietary brightener. From reference 11.

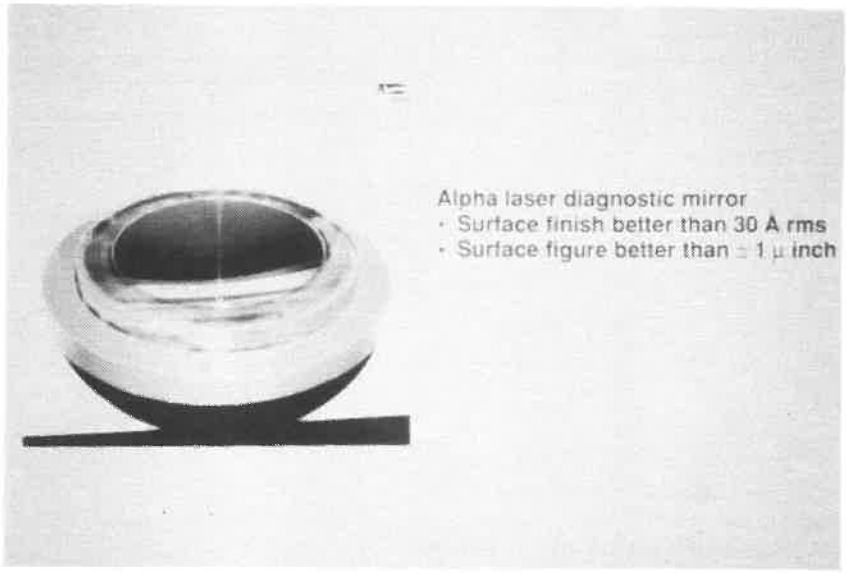

Figure 4 - Diamond machined electrodeposited copper on a glass substrate.

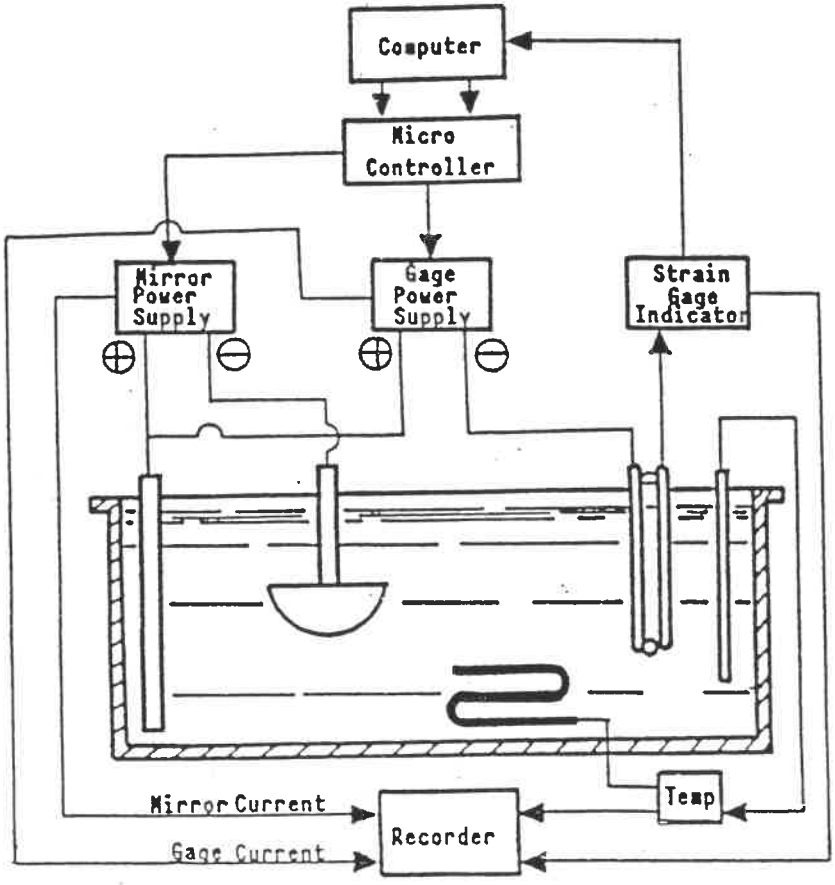

Figure 5 - Strain gage technique for measuring stress in electrodeposits. From reference 12.

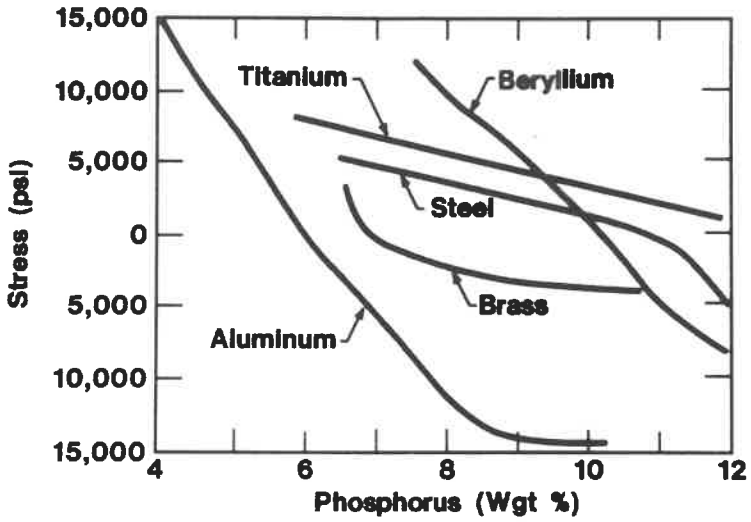

Figure 6 - Stress in electroless nickel as a function of phosphorus content for metals with a high expansion coefficient (aluminum and brass) and a low expansion coefficient (steel, beryllium, and titanium). From reference 13.

Electroless Nickel - A Brief History

Abner Brenner and Grace Riddell of the National Bureau of Standards are typically credited with starting electroless nickel on the road to commercialization (14). Their work, with solutions containing glycolate and hypophosphite and first reported in 1946, had been preceded by Wurtz in 1844 who reported that nickel metal could be produced from a solution containing nickel salts and hypophosphite (15) and the first patented report of thick, adherent nickel deposits in a hypophosphite solution by Roux in 1916 (16). General American Transportation Company in the mid 1950's established the first commercially feasible electroless nickel process, known as the "Kanigen" process utilizing solutions containing lactate and hypophosphite (17). They developed stabilizers which prevented dissociation of the solution by masking catalytically active nuclei (18). Small amounts of lead, tin, arsenic, molybdenum, or thiourea were effective in stabilizing the solution and this led the way to effective commercialization of the process.

The Kanigen patents have long since expired and today there are many dozens of suppliers who market formulations for electroless nickel plating. For that matter, there are any number of electroless nickel deposits that can be commercially deposited, including the engineering types with high phosphorus content, the more decorative middle phosphorus deposits and the recent low phosphorus deposits for improved wear resistance. Also, other metals or compounds can be incorporated in the deposit for enhanced properties in specialized applications. As Stevenson recently stated, "Today, electroless nickel truly is a family of coatings:" (19), and this is shown in Figure 7.

Figure 7

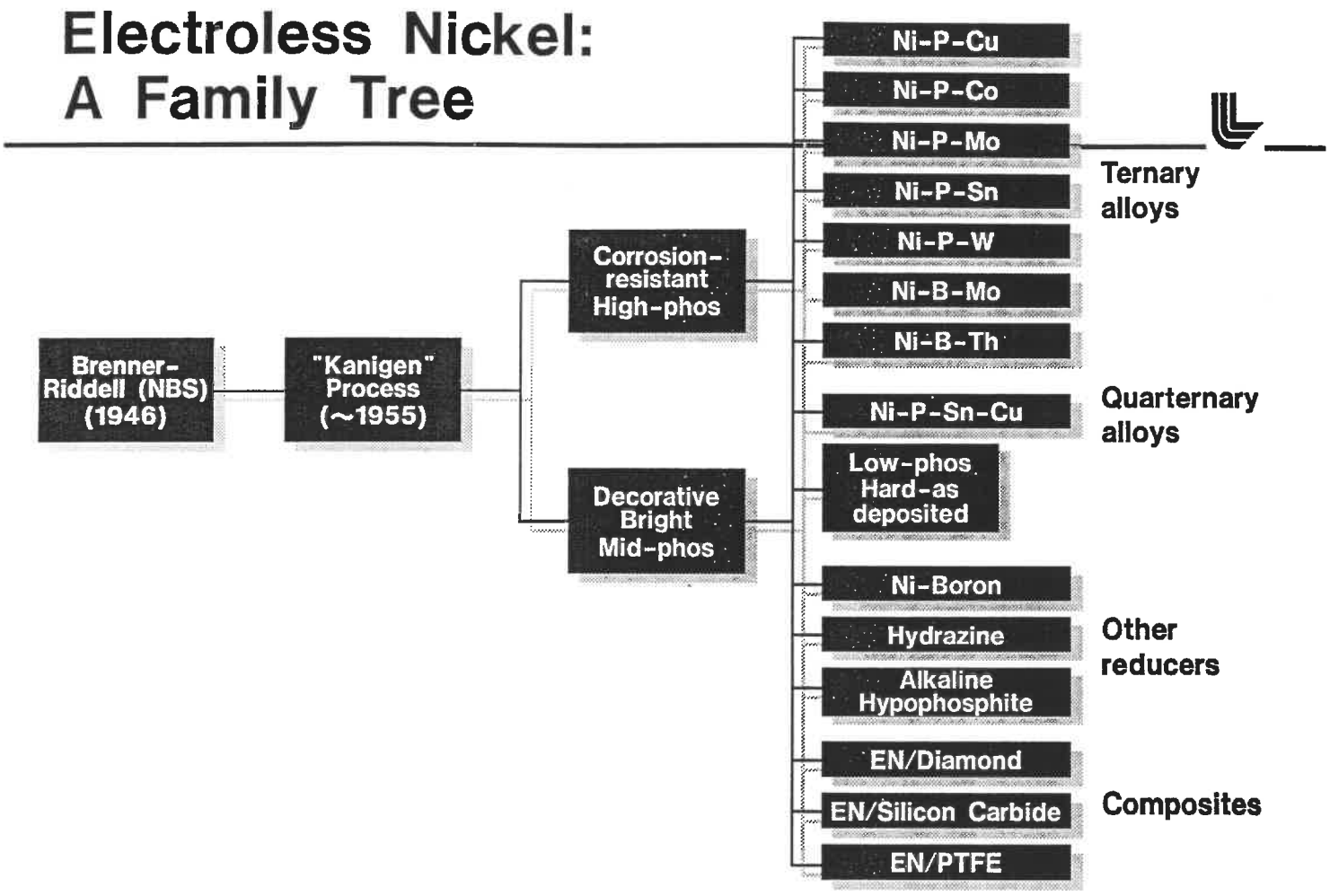
Electroless Nickel:
A Family Tree
Brenner-Riddell (NBS) (1946)
"Kanigen" Process (~1955)
Corrosion-resistant High-phos
Decorative Bright Mid-phos
Ni-P-Cu
Ni-P-Co
Ni-P-Mo
Ni-P-Sn
Ni-P-W
Ni-B-Mo
Ni-B-Th
Ni-P-Sn-Cu
Low-phos Hard-as deposited
Ni-Boron
Hydrazine
Alkaline Hypophosphite
EN/Diamond
EN/Silicon Carbide
EN/PTFE
Ternary alloys
Quarternary alloys
Other reducers
Composites

Electroless Nickel-Influence of Phosphorus Content

Electroless nickel deposits for single point diamond turning should contain at least 11% (wgt) phosphorus to minimize tool damage (Figure 8). A stress relief treatment at 200°C for 2 hours even further enhances the cutting characteristics of deposits containing greater than 11% phosphorus (20).

Electroless Nickel-Pitting

A general requirement for electroless nickel for optical use is that it have no porosity since porosity on the finished surface would result in a void on a mirror surface or a "pip" in the molded surface. Both of these are degrading to optical performance (21).

Typically, with precision parts, the plater does not have the luxury of an endless supply of parts or for that matter sometimes even one practice part that could be used for characterizing the deposition process. This means that occasionally parts have to be stripped and re-plated because of defects such as pits in the coating. Obviously, this is not an ideal situation. What clearly is needed is some manner of characterizing the plating operation so that when the actual part is coated, the chance for defects is minimized to the highest degree possible. A methodology for handling this type of situation is one of the goals of the organizers of this conference.

In the thin film rigid memory disk industry where electroless nickel plays an important part, much effort has been directed at understanding the cause and influence of defects (22). Microscopic examination of both as-plated and lightly polished electroless nickel surfaces has revealed that the surface defects that contributed to yield and magnetic performance problems were pits which could be classified into two groups. The first type (class A) were small (2-10 μm) circular pits of varying depths. The second type (class B) were considerably larger (10-30 μm) and irregularly shaped. Class A pits were found to be the most frequent in number and process related due to chemical imbalance in the plating solution. Class B pits were often only one or two per surface and related to prior physical handling damage in the aluminum substrate and particulate matter in the electroless plating solution.

Another example is random micropits on the surface of computer discs that were driving electroless platers "buggy". They had prepared solutions carefully, using deionized water, clean room conditions, carefully cleaned discs, and effective filters. Still pits of very small size were causing about six percent of the computer discs to be rejected, with one or more random pits on the surface (23). After much analysis it was finally discovered that the pits were caused by a micro-organism that was able to live in the plating solution. Once this discovery was made, the platers checked the system and found organisms in the deionized water. These nematodes were originally in the "raw" water. As the water went through the ion exchanger they multiplied and remained in the carbon filters, eventually escaping into the deionized water. By irradiating the water with UV light, the platers were able to kill the organisms and eliminate pitting of the discs (23,24).

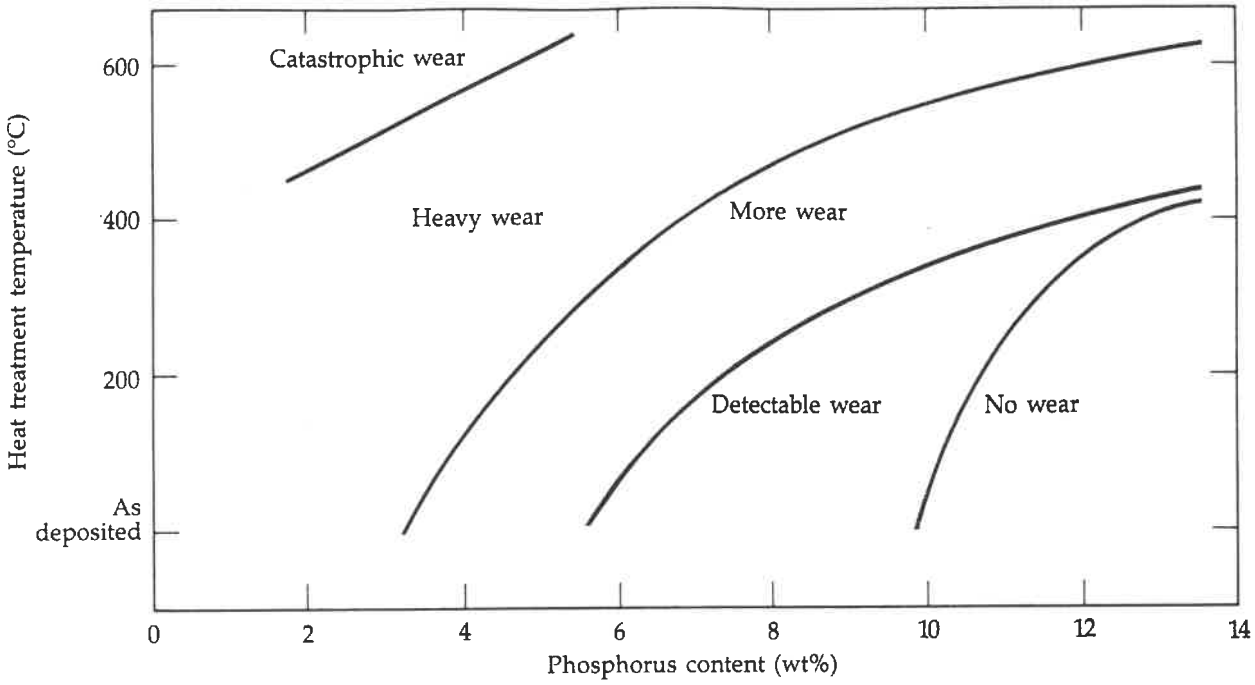

Figure 8 - Map of diamond tool flank-face wear and damage vs. electroless nickel phosphorus content and heat treatment conditions, based on scanning electron microscopy. From reference 20.

Recently, American Metaseal Corporation of Maryland discovered that in its area of the country (mid-Atlantic region) electroless nickel plating on aluminum required DI water. Hard water left mineral deposits in the solution that caused pitting and roughness on parts (25).

The purpose of the above discussion on pitting is to show the insidious nature of the problem. It can be a very complex issue and require a considerable amount of time and effort to understand and control.

Microstructural Stability of Electroless Nickel, Copper and Silver Deposits

A potential problem in using coatings for precision finishing applications is metallurgical instability. Electroless nickel, copper and silver deposits all have the possibility of undergoing changes that could seriously affect precision parts.

As-deposited electroless nickel is metastable and undergoes a crystalline transition at moderate temperature (240 to 400°C). This change causes a rapid increase in the hardness and wear resistance of the coating while reducing the corrosion resistance and ductility (26,27). The transition also causes an increase in density and accordingly a decrease in volume. This volume change, which can vary from 0.1% to 1.3% (28-30), coupled with differential thermal expansion is the cause for cracking or fissuring often found in deposits after heat treatment (30). The extent of the crystalline transition is a complex function of a number of factors including: 1) temperature and time at temperature, 2) heating rate, 3) previous temperature history, and 4) phosphorus content (31). Figure 9 provides a time/temperature profile which illustrates the transition from an amorphous to a crystalline structure for electroless nickel containing 11% phosphorus. If thermal exposure is maintained in the time/temperature envelope below the dotted curve, then the electroless nickel will remain entirely amorphous. However, if exposure conditions fall above this curve, then partial or complete crystallization will occur(31).

Copper deposits have been shown to markedly soften after storage at room temperature for 30 days (32). Interferometric tests on copper mirrors revealed a change in the optical surfaces over a period of six months. Metallographic analysis revealed that recrystallization had occurred in the copper, accompanied by a shifting of the surface along individual grain boundaries(33). In the most extreme cases this was visible to the eye as an orange-peel effect which scattered the laser beam and degraded reflectance measurements. Figures 10 and 11 show the roughening of a single point diamond turned copper electrodeposit as a result of recrystallization. The problem is caused by the high density of defects in the electroplated copper, often much higher than that achieved by cold working. Differential scanning calorimetry (DSC) showed that copper plated at 5 asf had a very high recovery energy exotherm of 1.97 J/g at 148.5°C and a much lower recrystallization energy exotherm of 0.529 J/g at 283.8°C (Figure 12). A DSC of copper plated at 15 asf appeared to have a joined recovery/recrystallization energy exotherm of 1.27 J/g at 306.2°C (Figure 13). To

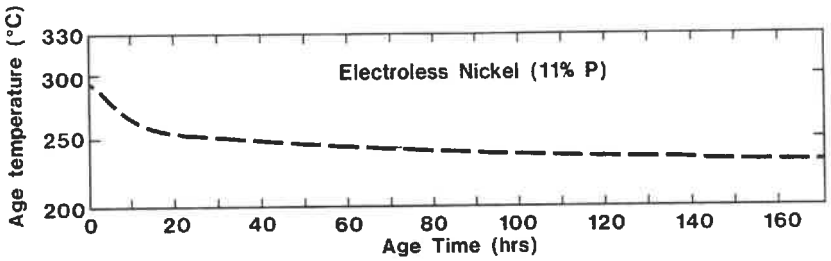

Figure 9 - Time/temperature profile illustrating the transition from an amorphous to a crystalline structure for electroless nickel containing 11% phosphorus. From reference 31.

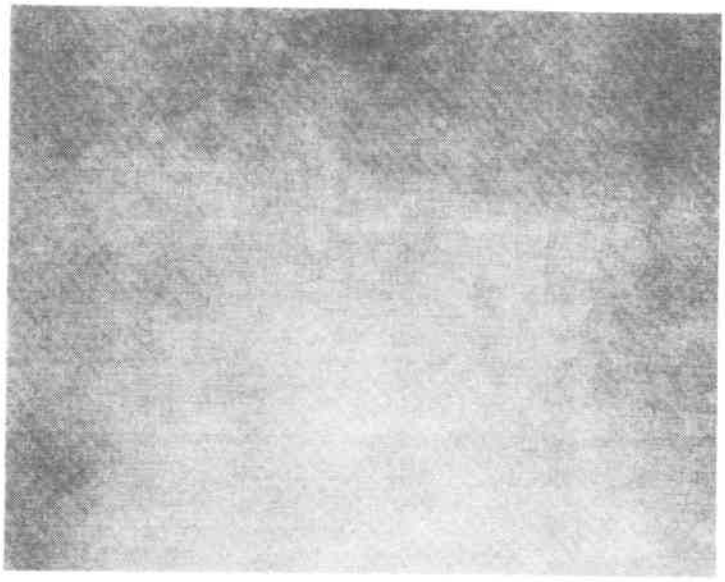

Figure 10 - Nomarski micrograph of a diamond turned copper surface before recrystallization (100X). From reference 33.

Figure 11 - Nomarski micrograph of a diamond turned copper surface after recrystallization (100X). From reference 33.

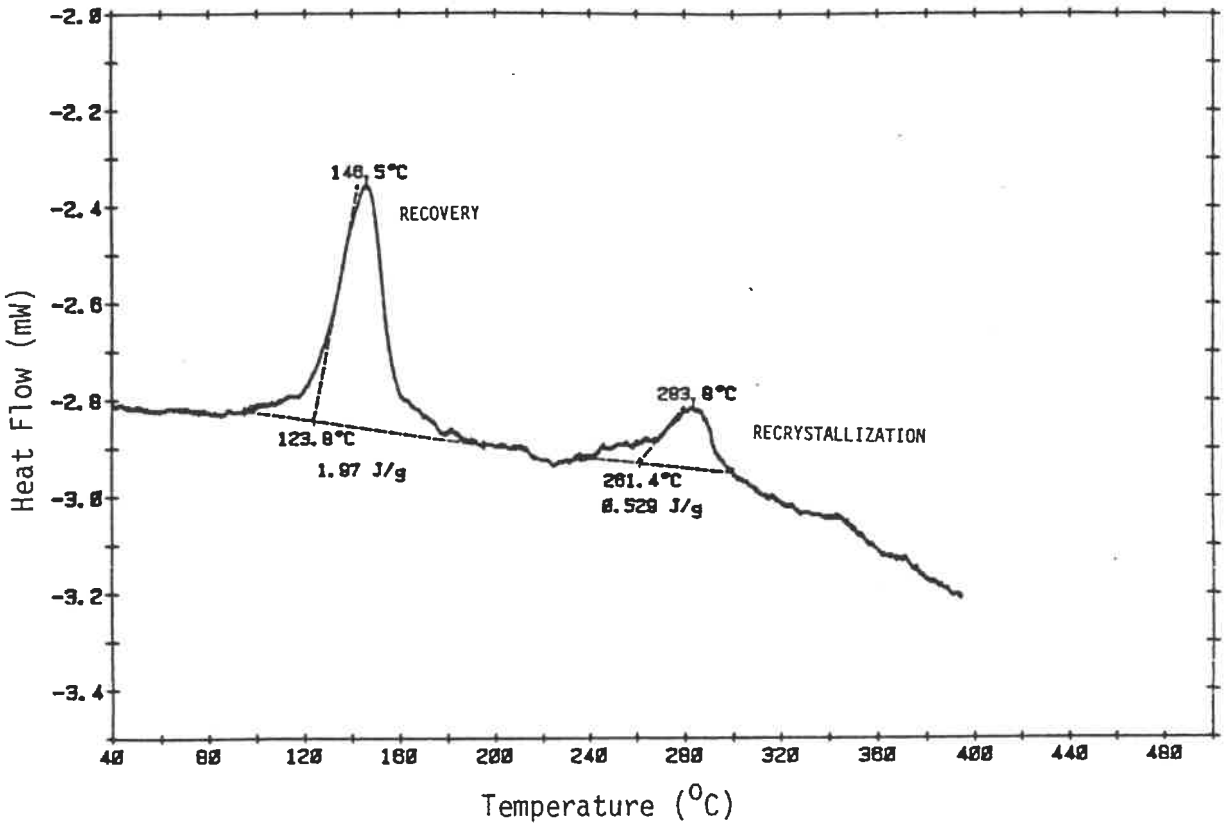

Figure 12 - DSC showing exotherm at 146.5°C and 283.8°C for copper plated at 5 asf. From reference 33.

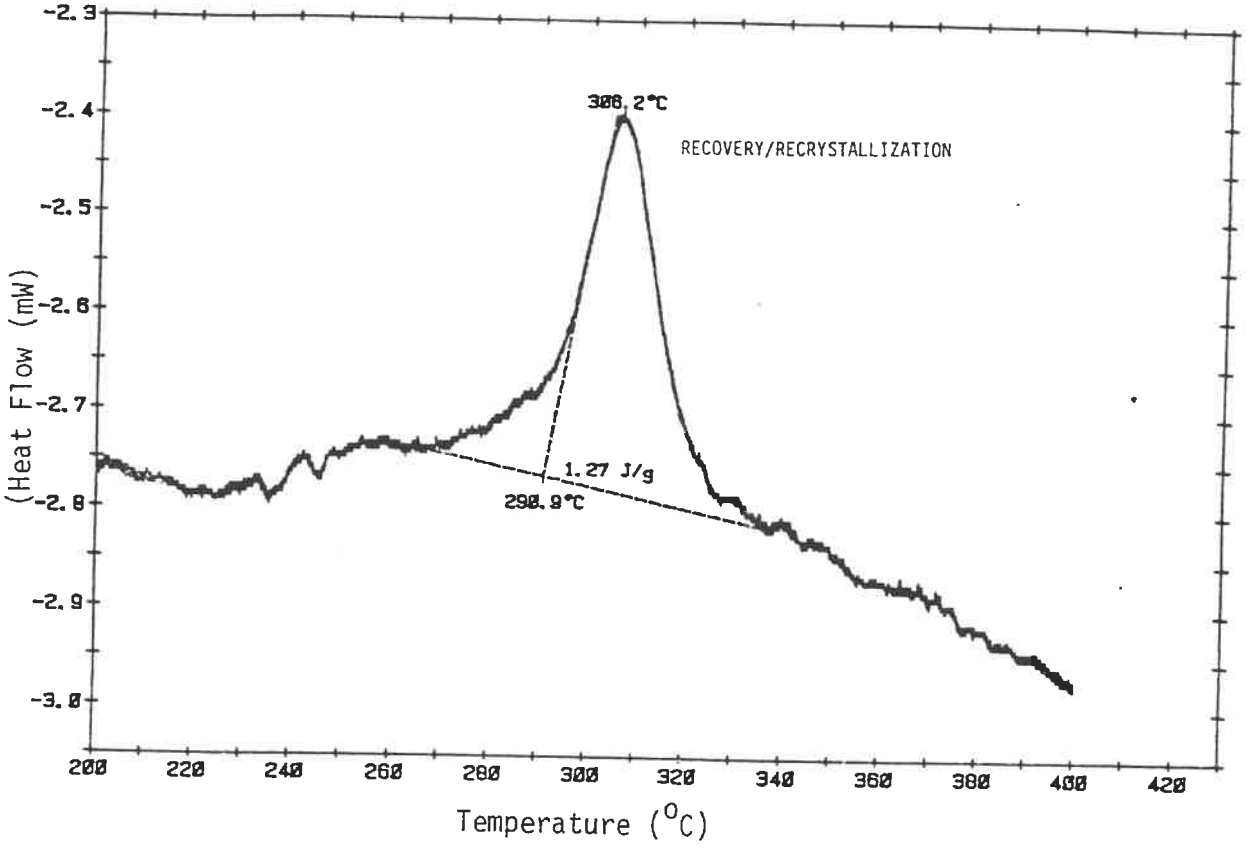

Figure 13 - DSC showing energy release at 306.2°C for copper plated at 15 asf. From reference 33.

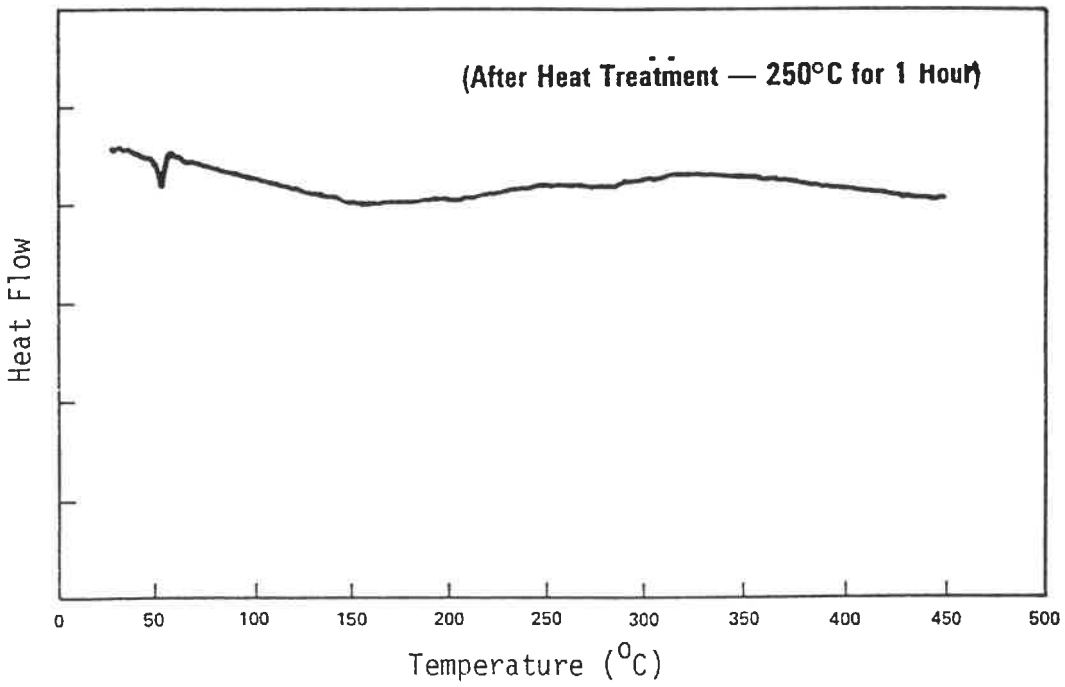

Figure 14 - DSC of copper which had been plated at 5 asf and then heat treated. From reference 33.

eliminate the problem of recrystallization at room temperature, the low current density copper is given a low temperature heat treatment (1 hour at 250°C) to remove the recovery energy without causing recrystallization and grain growth (33). The DSC of low current density copper which had been heat treated did not have any retained recovery energy and the recrystallization energy also appeared to be reduced (Figure 14).

Silver deposits have also gone through changes on precision parts. This was discussed earlier in this paper in the section on stress in coatings.

Potential Future Coatings

Electrodeposited Nickel-Phosphorus Alloys

Recently, increased attention has been directed at electrodeposition as an alternate to electroless deposition for producing Ni-P alloys. The electrodeposition process offers a number of potential advantages:

1) alloys with 14-15% P which is higher than that obtainable with electroless nickel are possible, and as shown in Figure 8, higher P means less tool wear.

2) an order of magnitude greater deposition thickness can be produced.

3) noticeably less expensive than electroless deposition since electrodeposition is not a batch process.

4) the possibility of reduced porosity

Preliminary work at three different establishments has shown the viability of substituting electrodeposition for electroless deposition of Ni-P alloys. At LLNL an electrodeposited Ni-14P coating compared quite favorably with electroless nickel coatings even after a cutting distance of 25 km (15.3 miles). Figure 15 shows a collection of surface roughness profiles, 500 microinches in length at cutting distances from 15 to 60,000 ft. for electroless Ni-13P, illustrating the variety of profile shapes and amplitudes that occur. Figure 16 shows a similar measurement for electrodeposited Ni-14P at the end of the test after a cutting distance of 81,000 ft. Comparison of the two figures reveals that for the tools used in these studies, the electrodeposited Ni-P was not as damaging to the tool as the electroless Ni-P. With electrodeposited Ni-P, rms roughness after cutting 81,000 ft was 15.7 Å versus 83.2 Å for electroless nickel after 60,000 ft of cutting (34).

Researchers at NIST also reported good results with electrodeposited Ni-15P. After 40 km (24.8 miles) of machining, no change in surface finish was noted (35). Recent results published in Australia also suggest that electrodeposited Ni-P is a viable alternative to electroless Ni-P in the high quality finishing of mirrors (36).

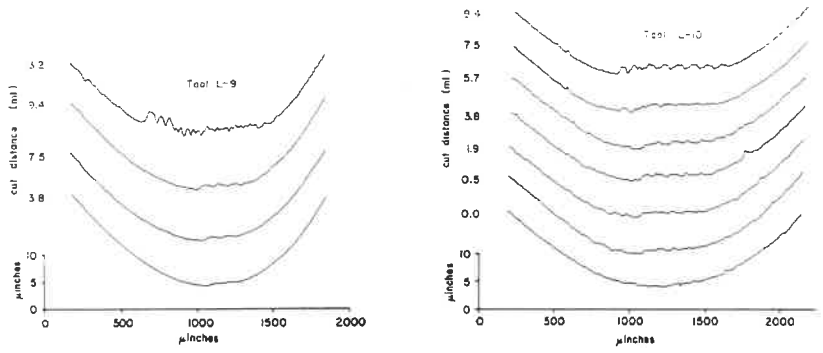

Figure 15 - Talystep profiles of replication grooves for electroless nickel labeled with cutting distance in miles. The leading edge of the tool is toward the left. From reference 34.

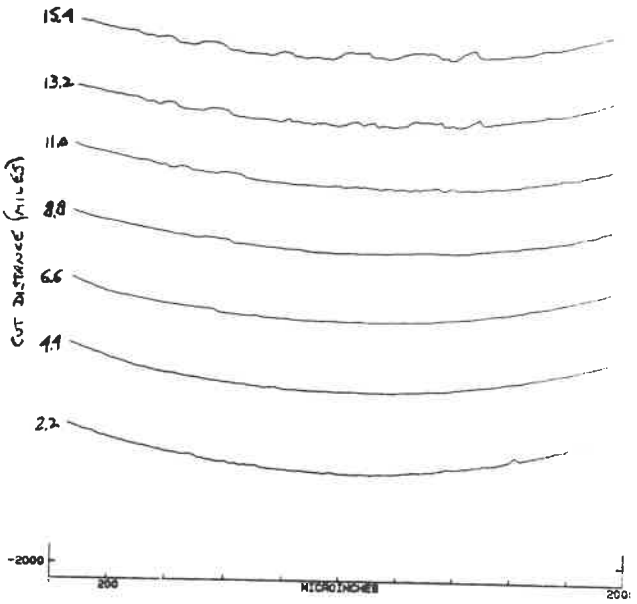

Figure 16 - Talystep profiles of replication grooves for electrodeposited Ni-P with cutting distance in miles. The leading edge of the tool is toward the left. From reference 34.

Also of interest are some data from Lashmore et al., who have reported that pulse plated alloys can contain greater than 20% P with a layer spacing that is much finer and more uniform in appearance than that in the dc alloy (37, 38). This would be an interesting material to evaluate for diamond turning applications.

However, it has recently been discovered that electrodeposited Ni-P transforms at relatively low temperatures and short incubation times to a two phase material, with intermetallics in a crystalline nickel matrix (39, 40). Evans at NIST noted that electrodeposited Ni-P completely transformed in 3 hours at 250°C whereas electroless Ni-P took 50 hours at 250°C to transform (40). Figure 9, discussed earlier, provides some additional data on stability of electroless nickel deposits. Clearly, more work needs to be done with electrodeposited Ni-P to determine how to improve the stability of these alloys before they will be entirely suitable for diamond turning applications.

Electrodeposited Silver Alloys

Silver, which surpasses other metals in terms of reflectivity in the spectral region from 15 to 0.4 μm, is widely used in optical instrument manufacture as a mirror coating. However, silver coatings must be protected in order to prevent a loss of their reflectivity in air. Some Russian researchers have reported that it is possible to electroplate alloys of silver-antimony (2.7%) which are about 2 times harder than pure silver and 10-15 times more abrasion resistant. Tests under natural climatic conditions for two months with ambient relative humidities of 65 ± 15% and temperatures of 25 ± 10°C showed that silver was covered with a continuous black film after a month, while the silver-antimony coating suffered practically no change (41). Some work directed at determining the practicality of depositing silver-antimony alloys and also determining if these alloys are diamond turnable might prove fruitful.

Silver alloys containing 10 to 27% tin also are worth some consideration. Alloys containing 10% tin reportedly exhibit good ductility and solderability and have a low coefficient of friction. They also exhibit considerably improved tarnish resistance when compared with pure silver (42). Another potential coating is the intermetallic Ag_3Sn (73 Ag-27 Sn). Electrodeposited coatings of this alloy could be polished to high luster and were more resistant to tarnish in sulfide mixtures than pure silver (43).

References

1. G. M. Sanger, "Some Thoughts on the Role of Electroplated Coatings in Optics and Some Considerations for Their Production", Proceedings SUR/FIN 82, American Electroplaters & Surface Finishers Soc. (1982).

2. G. M. Sanger and J. W. Dini, "A Perspective on Electrodeposited and Electroless Nickel Coatings Used in Optical Applications", Proceedings SUR/FIN 82, American Electroplaters & Surface Finishers Soc. (1982).

3. R. E. Fischer, "Diamond Turning", ENCYCLOPEDIA OF MATERIALS SCIENCE AND ENGINEERING, VOL. 2, Co-E, M. B. Bever, Editor, Pergamon Press (1986).

4. J. W. Dini, W. K. Kelley and H. R. Johnson, "Ring Shear Testing of Deposited Coatings", TESTING OF METALLIC AND INORGANIC COATINGS, ASTM STP 947, W. B. Harding and G. A. DiBari, Editors, American Society for Testing and Materials 320 (1987).

5. R. M. Shemenski, J. G. Beach and R. E. Maringer, "Plating Stresses from Electroless Nickel Deposition on Beryllium", J. Electrochem. Soc., 116, 402 (1969).

6. R. A. Hoffman, W. J. Lange, J. G. Gowan and C. J. Miglionico, Optical Engineering, 17, No 6, 578 (Nov/Dec 1978).

7. J. R. Buckmelter, T. T. Saito, R. Esposito, L. P. Mott and R. Strandlund, "Dielectric Coated Diamond Turned Mirrors", Laser Induced Damage in Optical Materials, July 29-31, 66 (1975).

8. J. T. Bloxsom and J. B. Schroeder, "Preparation of Optical Surfaces on Beryllium", Applied Optics, 9, 539 (1970).

9. T. T. Saito, "Polishing and Characterizing Diamond Turned Optics", Lawrence Livermore Laboratory, UCRL 51951, Nov 1975.

10. N. P. Fedotov, P. M. Vyacheslavov and V. I. Gribel, Journal of Applied Chemistry (USSR), 37 (6) 1368 (1964).

11. W. C. Cowden, T. G. Beat, T. A. Wash and J. W. Dini, "Deposition of Adherent, Thick Copper Coatings on Glass", METALLIZED PLASTICS 1, FUNDAMENTALS AND APPLIED ASPECTS, K. L. Mittal and J. R. Susko, Editors, Plenum Press, New York, 93 (1989).

12. R. W. George et al., "Apparatus and Method for Controlling Plating Induced Stress in Electroforming and Electroplating Processes", U. S. Patent 4,648,944 (March 1987).

13. K. Parker and H. Shah, Plating, 58, 230 (1971).

14. A. Brenner and G. E. Riddell, Journal Research NBS, 37, 31 (1946) and 39, 385 (1947); U. S. Patent 2,532,283 (1950).

15. A. Wurtz, Ann. Chim. et Phys., 3, 250 (Nov 1844), and 16, 198 (March 1846); Compt. Rend., 21, 149 (1845).

16. F. A. Roux, U. S. Patent 1,207,218 (1916).

17 K. Parker, "Electroless Nickel-State of the Art", Proceedings SUR/FIN 90 American Electroplaters & Surface Finishers Soc., 1425 (July 1990).

18. G. O. Mallory, private communication, Jan 1991.

19. M. Stevenson, Jr., "Electroless Nickel: No Longer Just a Coating", Proceedings SUR/FIN 90 American Electroplaters & Surface Finishers Soc., 1273 (July 1990).

20. J. W. Dini, C. K. Syn, J. S. Taylor, G. L. Mara, R. R. Vandervoort and R. R. Donaldson, "Influence of Phosphorus Content and Heat Treatment on the Machinability of Electroless Nickel Deposits", Proceedings Electroless Nickel Conference IV, April 1985, Products Finishing Magazine, Cincinnati, Ohio.

21. E. Ulph, "Electroless Nickel Coating for Diamond Turning Applications", Proceedings SUR/FIN 84 American Electroplaters & Surface Finishers Soc., (1984).

22. J. E. Williams, Jr. and C. Davison, "Review of the Capabilities and Properties of Electroless Plated Thin Film Media for Rigid Memory Disks", J. Electrochem. Soc., 137, 3260 (1990).

23. G. T. Miller, "Bugs in the Computer Disc", Electroless Nickel News, 7, No 2, 6 (Fall 1990).

24. G. T. Miller, "Unsuspected Factors that Affect EN Plate Quality", Proceedings Sur/Fin 90 American Electroplaters & Surface Finishers Soc., 1259 (1990).

25. C. Daniels, "So you want to Plate EN?", Products Finishing, 54, 66 (Nov 1990).

26. "Electroless Nickel Plating", Metals Handbook, Ninth Edition, Vol. 5, Surface Cleaning, Finishing and Coating, ASM, Metals Park, Ohio (1982).

27. H. G. Schenzel and H. Kreye, "Improved Corrosion Resistance of Electroless Nickel-Phosphorus Coating", Plating & Surface Finishing, 77, 50 (Oct 1980).

28. "The Engineering Properties of Electroless Nickel Deposits", INCO, New York, NY (1977).

29. D. H. Johnson, "Thermal Expansion of Electroless Nickel, Report 28-670, Y-12 Plant, Oak Ridge National Laboratory, Oak Ridge, TN, (Jan 2, 1982).

30. D. H. Killpatrick, "Deformation and Cracking of Electroless Nickel Cladding on Large Metal Mirrors", AFWL-TR-83, Air Force Weapons Laboratory, Kirtland Air Force Base, NM, (Jan 1983).

31. M. W. Mahoney and P. J. Dynes, "The Effects of Thermal History and Phosphorus Level on the Crystallization Behavior of Electroless Nickel", Scripta Metallurgia 19, 539 (1985).

32. H. J. Wiesner and W. J. Frey, Plating & Surface Finishing, 66, 51 (Feb 1979).

33. B. M. Hogan, "Microstructural Stability of Copper Electroplate", Proceedings SUR/FIN 84, American Electroplaters & Surface Finishers Soc., (1984).

34. J. W. Dini, R. R. Donaldson, C. K. Syn and D. J. Sugg, "Diamond Tool Wear of Electrodeposited Nickel-Phosphorus Alloy", Proceedings SUR/FIN90 American Electroplaters & Surface Finishers Soc., (1990).

35. C. J. Evans, R. S. Polvani and A. Mayer, "Diamond Turned Electrodeposited Nickel Alloys", OSA 1990 Technical Digest Series, 9, 110 (1990).

36. N. Currie, "High Quality Finishing of Mirrors Using Nickel-Phosphorus", Coatings in the Age of Technology, Expo 88, Australian Inst. of Metal Finishing, Queensland, Australia.

37. D. S. Lashmore and J. F. Weinroth, "Pulse Electrodeposition of Nickel-Phosphorus Metallic Glass Alloys", Plating & Surface Finishing, 69, 72 (August 1982).

38. A. W. Ruff and D. S. Lashmore, "Dry Sliding Wear Studies of Nickel-Phosphorus and Chromium Coatings on 0-2 Tool Steel", SELECTION AND USE OF WEAR TESTS FOR COATINGS, ASTM STP 769, R. G. Bayer, Editor,

39. A. Mayer, R. D. Bramlett, R. A. Day, C. J. Evans and R. S. Polvani, "Electrodeposited Coatings for Diamond Turning Applications", Proceedings ASPE Spring Topical Meeting, Metal Platings for Precision Finishing Operations, April 1991.

40. C. J. Evans, Private communication, May 1991.

Machining Forces in Diamond Turning of Plated Copper and Unplated Substrates

J. D. Drescher, T. A. Dow
North Carolina State University,
Precision Engineering Center
Raleigh, NC 27695-7918

Tool forces were measured during diamond turning of a number of materials including plated copper. A 3-axis piezoelectric transducer with 0.02N resolution was used to monitor the magnitude of the cutting and normal force components as a function of the depth of cut. A model of these tool forces indicating the sources of the components is presented which includes the influence of the change in geometry of the tool due to wear. The force components are a sensitive measure of the wear on the clearance face of the tool and a comparison of the measured and predicted wear shows excellent agreement. The tool wear experienced cutting 6061-T6 aluminum was 200 times more severe than when cutting hard plated copper. Specific cutting energies for several materials are presented along with a qualitative explanation of their performance based on the combined effects of material strength and ductility.

Introduction

Metal platings are used extensively in diamond turning (DT). They enable the combination of structurally strong substrates with surfaces suitable for optical finishing. Platings also provide small grain size which is desired for optimum finish in DT. Strict specifications on surface finish and dimensional accuracy often lead to DT as a manufacturing process. The desire to relate some measurable process output to these part qualities has led to the work reported here on tool force measurement and prediction. An understanding of how the tool forces change with cutting conditions, material, and tool wear provides a basis for the machine tool controller to maintain figure accuracy and surface finish.

A model of tool forces including material properties, tool geometry and cutting parameters is being developed. The goal is to base this model on the material properties and deformation mechanics and not to rely on empirical relationships. The primary material chosen for analysis is an electroplated copper. This copper is homogeneous, does not work harden, and causes minimal tool wear. In this paper the force measurement system is described and the model of the tool forces including tool geometry and material parameters is presented.

Force Measurement System

Figure 1 is a schematic of the force measurement system. The main component is a piezoelectric, quartz transducer which is sensitive in three perpendicular directions. A preload is required so that transverse forces can be transmitted by friction. This preload is applied by a 6 mm bolt through the center of the transducer clamping it between the toolholder and dovetailed block. Time varying temperature changes cause strains of the piezoelectric element in all directions which can not be separated from strains caused by cutting force. This effect is greatest along the

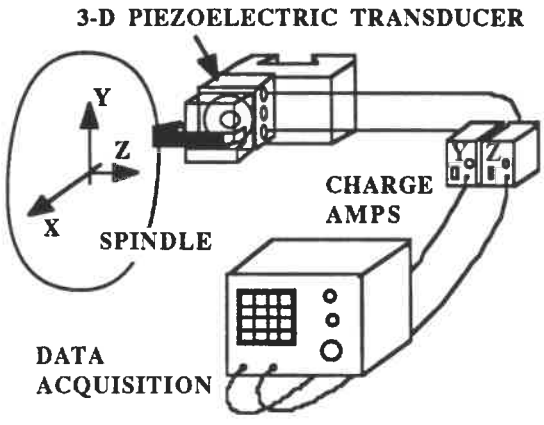

Figure 1:Force measurement system

preload axis. In the cutting force measurements described in this report, forces were measured in the two directions perpendicular to the preload axis. In this way the temperature effects on force were avoided. The directions of interest are labeled Y and Z in Figure 1.

Experimental Cutting Geometry

The schematic in Figure 2 shows the orthogonal cutting geometry which is used in many turning applications. This geometry is best for studying the turning process. The chip produced has uniform thickness and width, unlike the round-nose, crossfeed geometry. In this orthogonal geometry, the cutting parameters are limited to cutting depth and edge length. The feed is in the Z-direction so that feed/revolution is equal to cutting depth, d. The edge length, L, is determined by the length of tool employed in the cut. A tool with 0° rake and 6° clearance angle was used for the experiments. A steady flood of light machine oil was directed at the tool edge to entrain the continuous chip and carry it away.

Tool Force Model

One important use of force measurement is to develop and validate a tool force model. The simplest tool force model includes only forces at the tool rake face. The normal force on the rake face has been shown to be proportional to the area of the uncut chip, L d [1]. When depth of cut is small relative to edge sharpness, however, measured forces do not scale linearly with depth of cut. This is due to the forces on the tool edge. These forces are not related to depth of cut, because they are not associated with material removal. There are four force components; two normal and two tangential. These can be added as vectors to describe the forces in the cutting and thrust directions. The force model is:

$$F_Y = F_{Yr} + F_{Ye} = C_1 \, d \, L + \mu \, C_2 \, L \qquad (1)$$

$$F_Z = F_{Zr} + F_{Ze} = \mu \, C_1 \, d \, L + C_2 \, L \qquad (2)$$

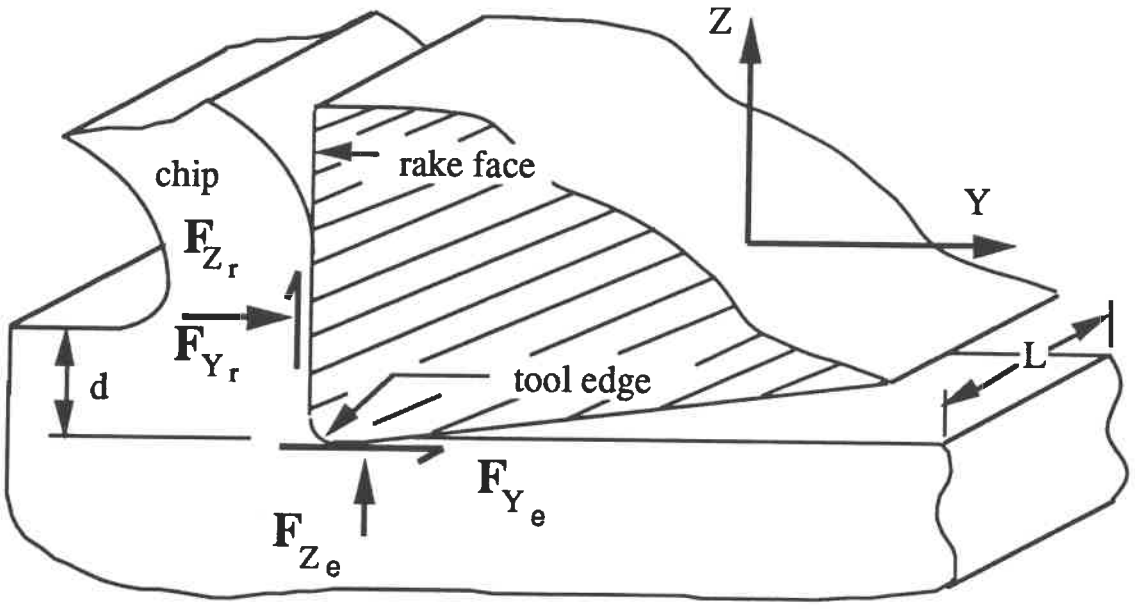

Figure 2: Orthogonal tool force model; The force components are not measured directly but deduced from the total forces using the model of Equations (1) and (2).

There are three variables in this model, C_1, C_2, and μ. With experimental force data, where d, L, F_Y, and F_Z are measured, C_1, C_2, and μ are found which optimize the correlation between measured forces and the model. The friction coefficient, μ, is assumed to be equal on the rake and clearance face. Figure 3 shows measured tool force data (points) in the Y-and Z- directions as a function of the depth of cut. The best fit lines are also plotted using Equations (1) and (2). The values for the friction coefficient (μ= 0.21), and the parameters (C_1 & C_2) are included in the graph as well as the correlation coefficient of the data fit. The coefficient C_1 represents a flow stress and has units of pressure (GPa) while C_2 has units of force / unit width (N/mm).

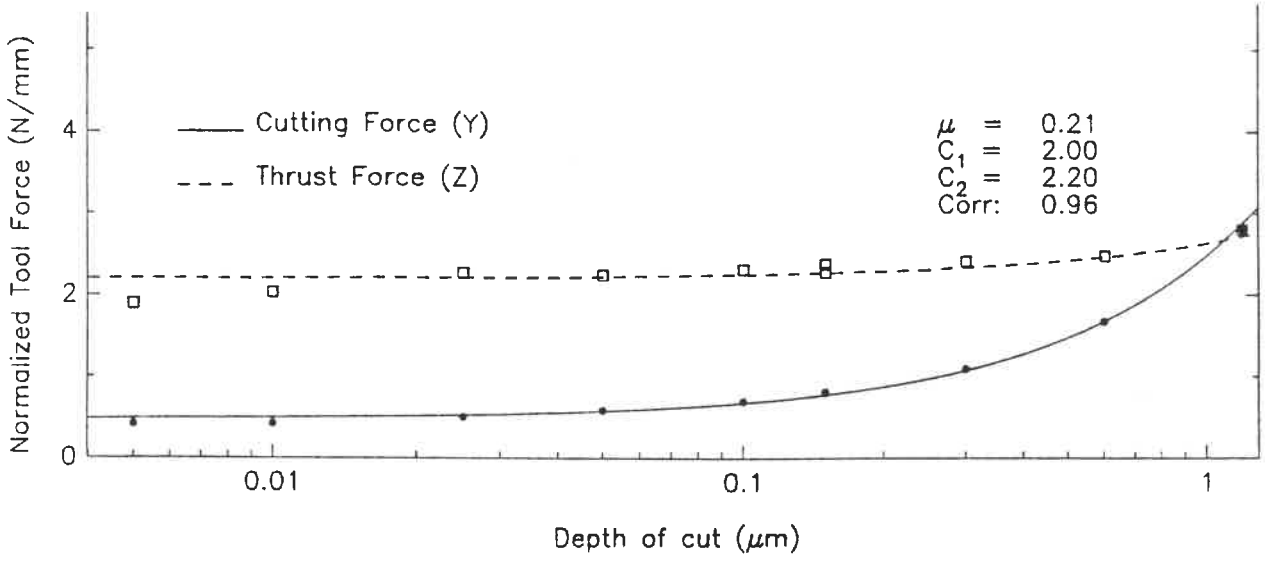

Figure 3: Curve fit for 3-parameter model

In the force model, the friction coefficient is the only one of the three parameters whose physical significance is readily apparent. However, the units on C_1 and C_2 give insight into their physical significance. C_2 (force / unit length) when multiplied by edge length, L , gives the normal force on the tool edge in the thrust direction. The area of the tool in this direction is A_2 (A_2=wL) so that the stress on this area is C_2 / w. C_1 is the stress acting on the rake face area, A_1 (A_1=L d).

Wear Effects on Tool Force

The forces on the tool for the same cutting conditions change as a result of wear on the edge. The model described in Equations (1) and (2) can be used to indicate the source of these changes. To match the cutting data, the magnitude of the parameter C_2 must be increased while C_1 and μ do not change. By comparing the variation in this parameter with changes in the shape of the tool as measured using a high-resolution field-emission SEM, the tool condition can be incorporated into the model. Figure 4 is a schematic of a tool on which a flat area is worn on the clearance face. Assuming homogeneous, isotropic flow resistance, the plastic stress on the rake face and the clearance face should be equal. With this assumption, the relationship between the parameters C_1 and C_2 and the width of the worn region,

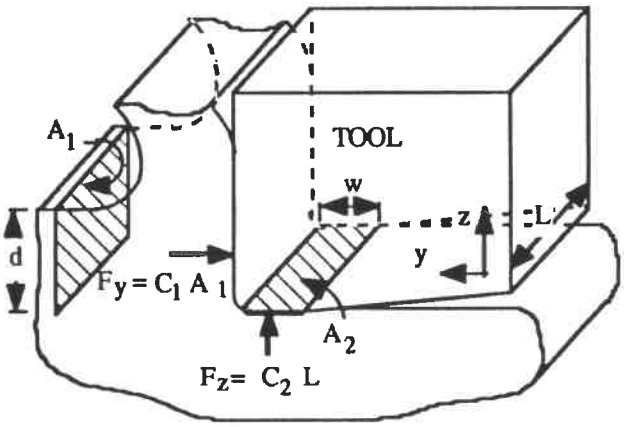

Figure 4: Tool edge diagram with edge wear

w, can be calculated. C_1 is the stress acting on the area A_1 which is equal to L d. The normal force on the area A_2 can be written as C_1 L w by the constant plastic stress assumption and is also equal to C_2 L. Therefore:

$$w = C_2 / C_1 \tag{3}$$

Equation (3) indicates that the flank wear can be calculated based on parameters derived from experimental force data. Equivalently, the flank wear can be included in the model for tool forces. Equations (1) and (2) become:

$$F_Y = C_1 [L d + \mu L w] \tag{1}'$$

$$F_Z = C_1 [\mu L d + L w] \tag{2}'$$

The parameter C_2 in the model has been replaced by the new parameter, w, which has physical significance. Force data can now be used to find the wear width, w, which best fits the data in the same manner as was done for C_2. The wear width, w, can be checked by careful measurement.

Measured forces were used to predict the wear width, w, in two separate series of wear tests. In the first series, a straight-edge tool was used to cut plated copper for a total cutting length of 28 km. Periodically, force measurements were made over a range of cutting depths and the best fit parameters were found using the model of Equations (1)′ and (2)′. The values of w are plotted as +'s in Figure 5. The width of the wear land as predicted by this procedure suggests that tool wear was small, but no measurements of the tool were made.

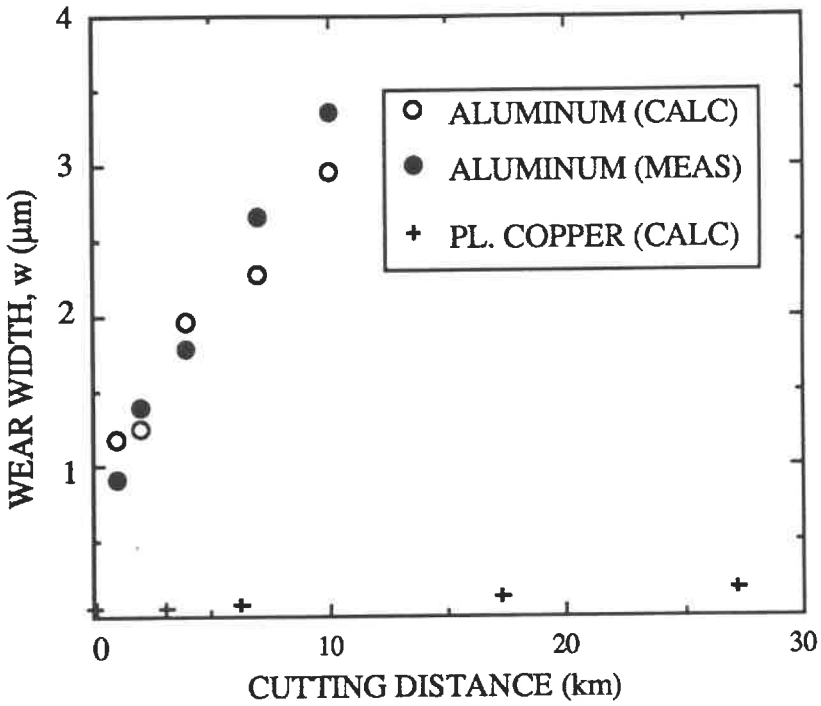

Figure 5: Calculated and measured tool wear vs. cutting distance

A second series of tests was performed using Al 6061-T6 as the workpiece. The hard constituents in this material produced much higher tool wear than was observed cutting the plated copper. The same tool was used for both series of experiments but was relapped after the copper tests. Force measurements were made using the same procedure as the first series of tests.; that is, while

aluminum was used for the wear experiments, forces were measured cutting the same hard, plated copper after certain distances of cutting the aluminum. The values for w were calculated and are plotted in Figure 5 as the open circles. Note that after 1 km of cutting the aluminum, predicted wear is greater than that predicted after 28 km of cutting the hard copper.

At the end of each cutting experiment, the tool was examined in a field-emission scanning electron microscope (SEM). Images of the uncoated tool edge at 20,000X magnification were obtained. Charging effects, typical when imaging low conductivity diamond, were avoided by using digital acquisition at high-speed scan rates. A sample of the SEM micrographs used for the edge measurements is given in Figure 6. Figure 6(a) provides a schematic of the tool orientation in the SEM. It was necessary to know this fixturing geometry to obtain geometric measurements from the projected lengths in the micrographs. Figure 6(b) is the image of the tool after 2 km of cutting aluminum. Lapping marks are visible on both the clearance face and rake face of the tool. These have been worn away at the edge as the flat area on the clearance face developed. The wear dimension of interest is perpendicular to the rake face. Lines can be seen along the cutting direction on this wear area.

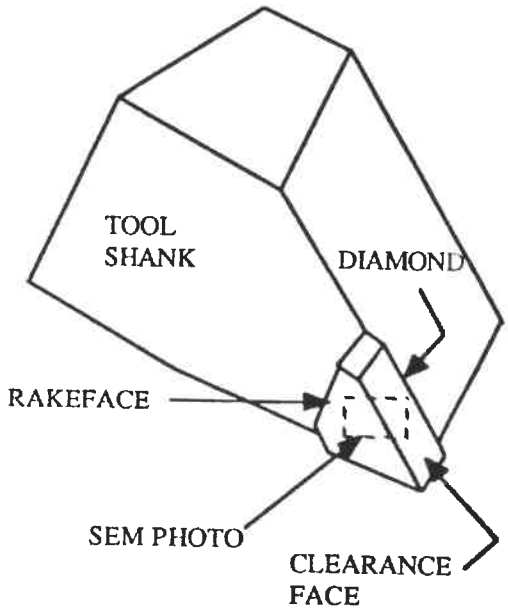

Figure 6(a): Top view of straight edge, diamond tool orientated in SEM

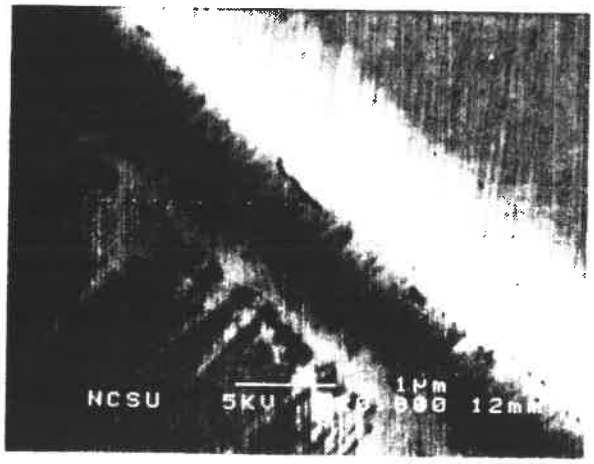

Figure 6(b): Micrograph of tool edge after 2 km of cutting Al 6061-T6

The measured values of the wear width are plotted in Figure 5 as the filled circles. These values are in excellent agreement with the geometric changes predicted from the tool forces and indicate that the force model presents an accurate picture of the changes on the tool. Based on these experiments, the tool wear rate cutting 6061-T6 aluminum was approximately 200 times greater than the wear rate cutting the plated copper.

Each calculated wear land width plotted in Figure 5 was obtained from tool force vs. depth of cut measurements such as shown in Figure 3. These measured forces can be combined into a single plot to show force vs.depth of cut and wear. The data covers nearly two decades of wear width from 41 nm to 3 µm. Figure 7 is a plot of the normalized force components (Force/unit edge length) as functions of depth of cut and clearance face wear width. Note that the cutting force is most influenced by depth of cut and to a lesser degree by tool wear while the thrust force is

dominated by the tool edge condition. The ratio of measured thrust force to measured cutting force changes continuously along a line of constant cutting depth. Therefore, using the model represented by Figure 7, a single force measurement at a known cutting depth has enough information to assess the tool condition.

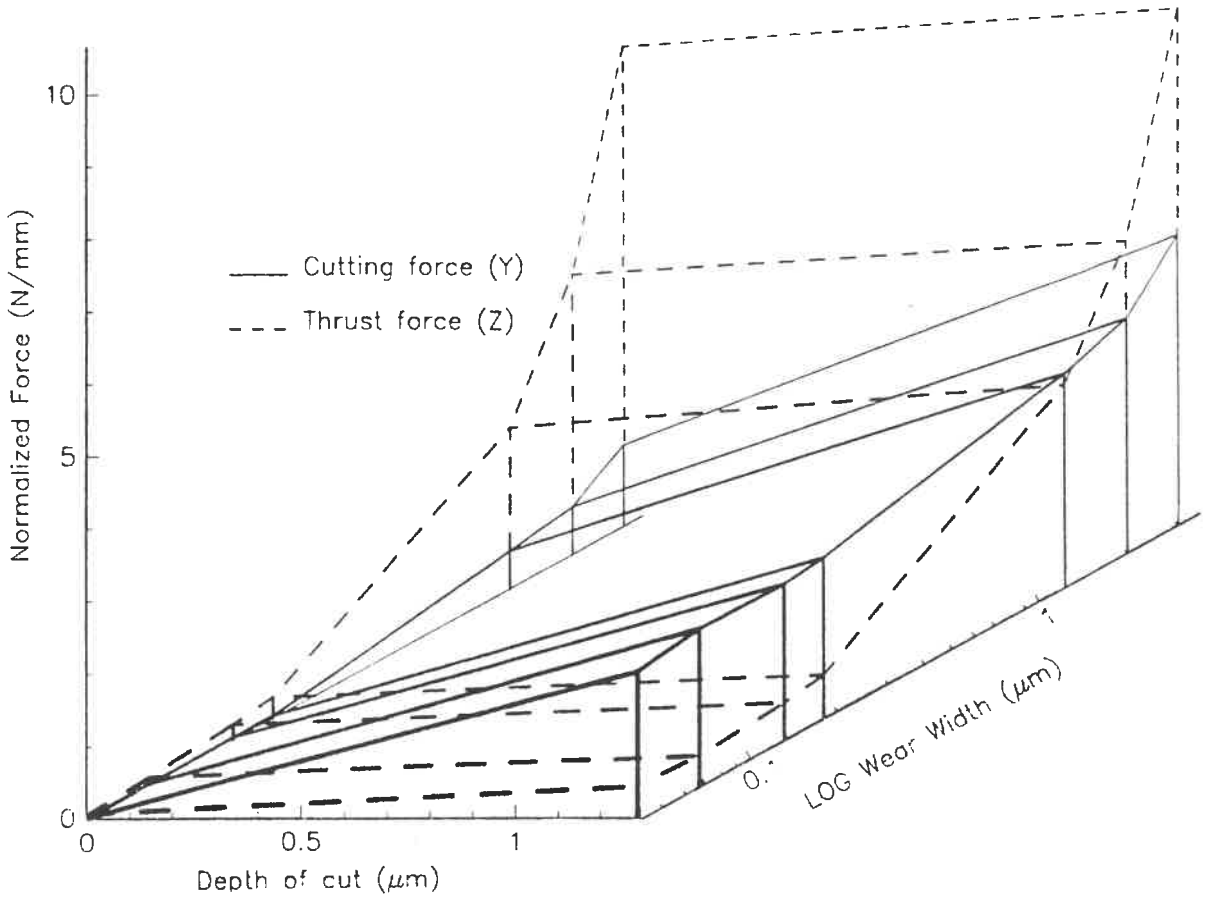

Figure 7: Tool force vs. edge wear and depth of cut using the model of Equations (1) and (2) with parameters derived from experimental data at the various wear stages

Discussion

Flow Stress: The terms flow stress and dynamic shear stress have been used interchangeably in metal cutting analyses [3]. In metal cutting, flow stress is defined as the cutting forces resolved onto the shear plane divided by the shear plane area. Traditionally, the forces at the tool edge are considered negligible so that in terms of measured cutting force, F_c, and thrust force, F_t, the flow stress can be written:

$$\tau_s = \frac{F_s}{A_s} = \frac{F_c \cos\phi - F_t \sin\phi}{A_0 / \sin\phi} \qquad (4)$$

where:

ϕ = shear plane angle
F_s = shearing force on shear plane
A_s = shear plane area
A_0 = cross-sectional area of uncut chip

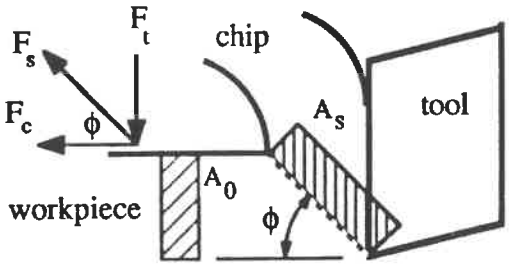

Figure 8: Forces on shear plane

The dynamic shear stress, or flow stress, has been shown to be a material dependant constant for wide ranges of cutting parameters. Using the nomenclature of Figure 2, the flow stress can be written in terms of forces acting on the rake face.

$$\tau_s = \frac{F_s}{A_s} = \frac{F_{Y_r} \cos\phi - F_{Z_r} \sin\phi}{A_0 / \sin\phi} \tag{5}$$

which can be simplified using the relationships $A_0 = Ld$ and $F_{Zr} = \mu F_{Yr}$.

$$\tau_s = \frac{F_{Y_r}}{L\,d}\left[\sin\phi \cos\phi - \mu \sin^2\phi\right] \tag{6}$$

In terms of the model parameter, C_1, where $C_1 L d = F_{Yr}$:

$$C_1 = \frac{\tau_s}{\sin\phi \cos\phi - \mu \sin^2\phi} \tag{7}$$

C_1 can be expected to stay constant if the geometrical factor, $1 / (\sin\phi \cos\phi - \mu \sin^2\phi)$ does not change. This factor depends solely on the shear angle if the friction coefficient remains constant. The Merchant theory [3] predicts a shear angle of 40^o using $\phi = 45 - \beta/2 + \gamma/2$ where:

β = friction angle = $\tan^{-1}(\mu)$ (11^o with $\mu = 0.2$)

γ = tool rake angle (0^o for the experiments reported here)

Chips from the cutting tests were collected and measured in the SEM to calculate the shear angle from the ratio of cutting depth to chip thickness. The uncut chip thicknesses (cutting depths) were 0.3, 0.6, and 1.2 μm. Examinations at 20,000X yielded chip thicknesses from which shear angles of 39^o, 41^o, and 39^o were calculated respectively. A variation of shear angle from 30^o to 50^o in Equation (7) only produces a variation from 2.4 to 2.7 in the geometrical factor relating C_1 to τ_s. Therefore, it is not surprising that C_1 was found to be constant for depth of cut and tool wear. C_1 can be considered as a material property related to flow stress by a constant.

The value of C_1 can be estimated for any material with force data from only two cuts if the depth of cut is varied. Equation (1)′ can be written for each cut and these can be combined into one equation, $(F_Y)_2 - (F_Y)_1 = C_1 [L d_2 - L d_1]$ where only C_1 is unknown.. The uncertainty in this calculation can be reduced by using data from several experiments covering a range of cutting depth.

The parameter C_1 was obtained for the electroplated copper, OFHC copper, and 70/30 brass to compare. The ranking of these three materials according to the values of C_1 was the inverse of the ranking according to Knoop hardness. Both C_1 and Knoop hardness for each material are plotted in Figure 9. Two other materials are also included, single crystal germanium and lead, Pb. The ratio of indentation hardness to C_1 was calculated for all five materials. This ratio is included in Figure 9 in the column to the right of the bargraph. A pattern in this ratio is not apparent but a qualitative explanation can be found in the interpretation of C_1 as specific cutting energy.

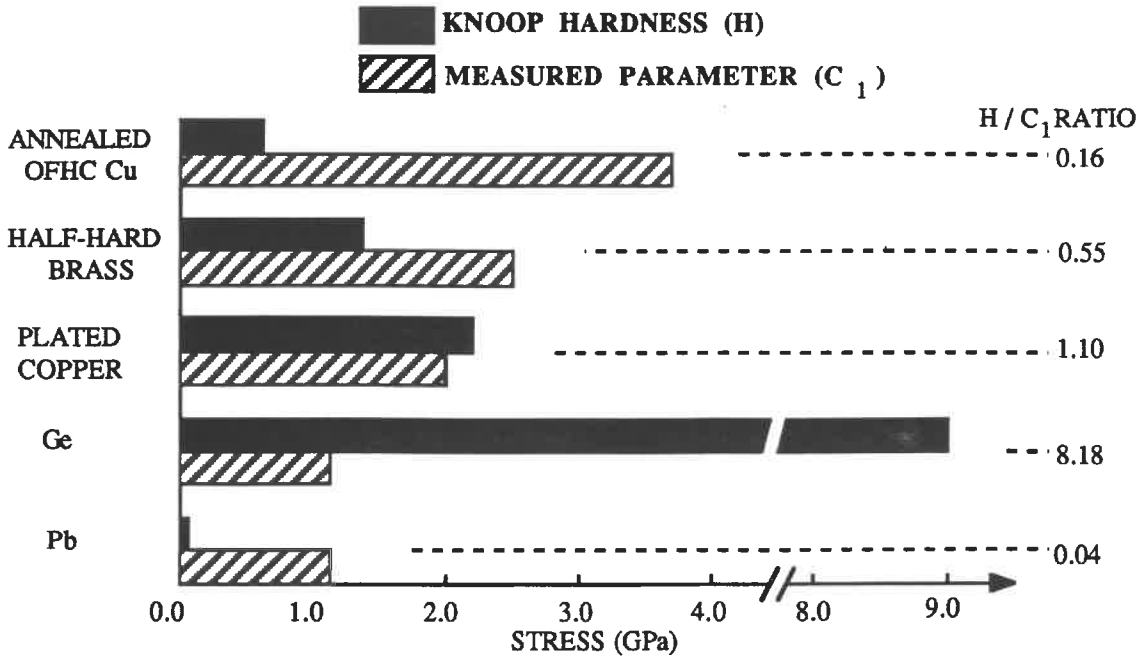

Figure 9: Knoop hardness and flow stress for various materials

Specific Cutting Energy: Force in the cutting direction divided by uncut chip cross-sectional area, is commonly called specific cutting energy [4]. The cutting force multiplied by cutting velocity is power and cross-sectional area multiplied by velocity is volumetric removal rate. The ratio of these is force per unit area and also work per unit volume. It is common to use the measured force in the cutting direction in the calculation of specific cutting energy. However, this force includes the effect of the friction at the tool edge contact area. Therefore, both the depth of cut and the tool edge condition influence the energy calculated. As a result it is not uncommon for a range of specific cutting energy values to be reported for a single material. C_1 in the model presented here can be interpreted as specific energy without tool edge contributions.

The interpretation of C_1 as volumetric work suggests that it is related to the area under the stress strain curve. It is the work necessary to deform the material both elastically and plastically to the point of failure. This area is a function of both a strength of the material and its strain at separation. The latter is a measure of the ductility. Figure 10 is a schematic showing this interpretation of the flow stress, strength, and ductility relationship.

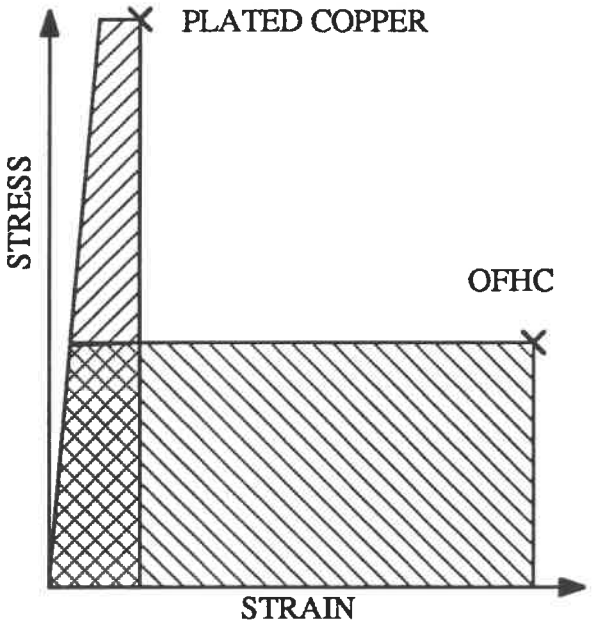

Figure 10: Schematic stress-strain curves

Since metals do not generally have both high strength and high ductility, it is possible for the area under the stress-strain curve to be larger for a material with a lower yield strength. Thus, the inverse relationship between hardness and flow stress, or C_1, can be explained. The data for Ge and Pb were included in Figure 9 as extremes to emphasize the importance of both ductility and strength to the measured flow stress. Germanium is very hard but brittle. In contrast, lead is soft and very ductile. It is the combination therefore which could lead to the equivalent values of C_1, measured in the cutting experiments and shown in Figure 9.

Unfortunately, the interpretation of C_1 as stress times strain does not account for its magnitude. For annealed OFHC copper the area under the stress-strain curve can be approximated as tensile strength 0.22 GPa, times 45% elongation at fracture (0.45) or 0.1 GPa. This value is only about 3% of the 3.5 GPa value shown in Figure 9. Similar comparisons give similar results for the plated copper, brass, and lead. The measured flow stresses are much greater than predicted from the stress-strain curves.

Other published data for specific cutting energy in diamond turning is also higher than predicted by tensile test information. Rhorer has recently presented data for OFHC copper where, above 1 μm depth of cut, the specific cutting energy was approximately 2.0 GPa [5]. This value should correspond to C_1 in the model presented here, since at the highest cutting depths used by Rhorer, edge forces become negligible. While these two numbers are reasonably close, less than a factor of 2 different, both are much higher than the 0.1 GPa calculated from the stress-strain curve for annealed copper.

The discrepancies between published values of flow stress from cutting experiments and the stress-strain data point to the difficulty in establishing quantitative descriptions of the metal cutting process. Reasonable explanations do exist for the discrepancies; for example, prior cold work as it relates to ductility could be a factor. Also, material behavior in the quasi-static tensile test and the highly compressive, rapid shearing process of cutting are potentially very different. Explanations are possible, but quantitative prediction is the goal. It is not difficult to understand why, after so much has been done, there is still much work to do in this area.

Conclusions

Tool force modeling can lead to understanding of the process which can be applied to improving the product quality. For example, calculation of forces might enable positioning correction to be made based on cutting loop stiffness to maintain form accuracy. The model can also be used with experimental data to monitor tool wear quantitatively. Finally, tool forces can be used in the analysis of properties for platings and other metals which are being developed.

Acknowledgements

The authors wish to thank the faculty and students of the Precision Engineering Center at NCSU who have participated in helpful conversations regarding this work. Ronald Scattergood has been especially helpful with his understanding of the material effects in metal cutting mechanics.

References

[1] J. T. Carroll, T. A. Dow, J. S. Strenkowski; *"Tool Force Measurement and Prediction in Diamond Turning"*, SPIE Vol 676, Ultraprec.Machng. & Automtd. Fabrctn. of Optics, 1986

[2] J. T. Black; *"Flow Stress Model in Metal Cutting"*, Journal of Engineering for Industry, Vol.101,pp403-415; Nov.1979

[3] M. E. Merchant; *"Mechanics of the metal cutting process. I. Orthogonal cutting and a type 2 chip,"* Journal of Applied Physics, Vol.16,pp267-275; 1945

[4] G. Boothroyd, W. A. Knight; Fundamentals of Machines and Machine Tools, 2nd Ed. McGraw-Hill,Inc , 1975

[5] R. L. Rhorer, D. A. Lucca; "An Experimental Procedure for Studying Diamond Turning Chip Mechanics", Proceedings of the ASPE 1990 Annual Conference, pp51-54

Sputtered Beryllium Coatings for the Precision Fabrication of Optical Components

C. M. Egert
J. B. Arnold

Optics MODIL
Oak Ridge National Laboratory

Abstract

Beryllium, because of its low density and high stiffness, is an excellent material for the fabrication of lightweight optical components. However, beryllium is a difficult material to precision machine, in part due to its high impurity content and rapid tool wear. Previous investigators have demonstrated that some improvement in the finish of beryllium is obtained when precision machining is conducted within an evaporated, pure beryllium coating using cubic boron nitride tools. However, this improvement still results in poorer quality finish than obtained by precision machining more conventional materials such as electroless nickel.

Recent advances in understanding the columnar microstructure of sputtered beryllium coatings and its dependence on thickness have suggested further ways to improve surface finish of precision machined beryllium. These studies have shown that the average column size of sputtered beryllium coating grains increases nearly linearly with increasing thickness. Also, above a critical thickness of ~25 μm the columnar grain structure becomes increasingly porous and the grain shape more anisotropic with increasing thickness. These results suggest that precision machining of thinner coatings, with smaller grain size and more isotropic shape, would result in further improvement in surface finish. This advance in understanding beryllium coating microstructure, combined with recent advances in diamond turning process for beryllium, have resulted in several orders of magnitude improvement in light scatter (BRDF at 10.6 μm wavelength) from precision turned beryllium surfaces.

1. Introduction

Precision fabrication technologies such as diamond turning are expected to play an important role in deterministic, low cost manufacture of high quality optical components. Recently, considerable improvements have been made in the precision fabrication of beryllium metal - an important material for space-based optical components - through the use of dense, sputtered beryllium coatings. These improvements have resulted in more than an order of magnitude improvement in optical scatter from precision machined beryllium surfaces. This paper describes these results with emphasis on the beryllium coating process which is in part responsible for this remarkable improvement.

Early attempts to diamond turn beryllium metal were unsuccessful due to the extremely high tool wear and poor surface finish. Several hypotheses were proposed to explain this failure; most of these suggesting that the extreme temperatures and pressures at the diamond-metal interface during machining resulted in degradation of the diamond tool through graphitization or reaction with the freshly cut beryllium surface. These difficulties with diamond tools eventually led to the use of polycrystalline cubic boron nitride (CBN) tools. Use of these tools eliminated the catastrophic tool wear observed with the diamond tools, resulting in a considerable improvement in beryllium surface contour and finish. Typical reported rms surface roughness values, measured by a Talystep profilometer, where in the range 250 to 500 Å.[1] Even the best of these samples were not of good optical quality, a consequence of the polycrystalline nature of the CBN tools and impurities in the beryllium.

While the precision fabrication process was being optimized progress was also being made in improving the beryllium material used for precision machining. Bulk beryllium used for precision optical applications is typically produced by hot isostatic pressing of beryllium powders. The resulting consolidated material contains as much as 1 wt. % oxygen, mostly in the form of oxide particulates located at grain boundaries. These particulates can be pulled out during a machining operation and dragged across the surface thereby limiting the final surface finish. To eliminate this problem high purity, thick beryllium coatings have been applied to lower grade beryllium substrates by e-beam evaporation. These coatings were then precision machined using CBN tools. Typical roughness values were obtained in the 220 to 300 Å rms range. These surface finishes were not significantly better than those obtained by CBN turning of bulk beryllium. Pullouts of the columnar coating grain structure and intrinsic coating porosity appeared to be the limiting factors in improving the surface finish of thick evaporated beryllium components.[2]

These diminishing returns in improving beryllium finish led to a re-examination of diamond tools for precision fabrication of beryllium. It was hypothesized that moderating the severe environment at the tool-surface interface might greatly reduce or even eliminate the diamond tool wear. This was done by reducing the rotational speed, feed rate, and depth-of-cut during diamond turning. This test was remarkably successful, producing an immediate improvement in surface finish without significant tool wear. Roughness measurements of diamond turned HIPed beryllium surfaces where obtained in the range 150 to 240 Å; a significant improvement over similar CBN turned surfaces.

While this breakthrough in precision machining of beryllium was being made, advances in understanding of the material and structural properties of beryllium coating related to machinability were also being made.[3] This paper describes these advances in understanding sputtered beryllium coating structure and its impact on machinability. Understanding of beryllium coating structure combined with the breakthrough in diamond turning beryllium have produced an optical quality, low-scatter, precision machined beryllium surfaces.

2. Sputtered Beryllium Coatings

A major influence on machinability of beryllium coatings is the microstructure of the coating. It is generally recognized that a very fine grain or near-amorphous microstructure produces a superior machined surface finish compared to the same material with a larger grain size. Sputter deposited coatings have a microstructure consisting of columnar grain extending through the thickness of the coating. The size and shape of these columnar grains are affected by a number of deposition parameters. For example, increasing temperature during deposition increases column size while ion bombardment during deposition generally reduces column size. However, the single greatest effect on column size is simply coating thickness, a parameter often ignored in studying coating microstructure. Beryllium coatings exhibit a considerable differences in columnar structure and size with increasing thickness which is described in greater detail below.

2.1 Sputter Deposition of Beryllium Coatings

Beryllium coatings produced for this study where deposited by a physical vapor deposition process known as magnetron sputtering. Compared to evaporation, another commonly used technique for producing beryllium films, sputtering is a slower, but more stable process. This greater stability allows for more control over the deposition process and more reproducible coating quality. In the sputtering process the source material, in this case a hot isostatically pressed beryllium disk, is placed inside a vacuum chamber in a low pressure (~ 10 mtorr) argon environment. A negative voltage applied to the beryllium disk produces a glow discharge plasma in the chamber. A glow discharge is a low energy plasma consisting primarily of neutral argon atoms with a small percentage of positively charge argon ions and negatively charged electrons. The positive ions are attracted to the negatively charges disk and strike the surface with sufficient energy to remove beryllium atoms. The sputtered beryllium atoms travels freely through the plasma and are deposited onto the substrate being coated. In magnetron sputtering the normal sputtering process is enhanced by a magnetic field above the beryllium disk which serves to enhance the glow discharge and increase the removal rate of beryllium atoms from the disk.

A schematic diagram of the sputter deposition system used to produce beryllium coatings is shown in Figure 1. The main deposition chamber is a 10" ID stainless steel 6-way cross suitable for high vacuum operation. A Torus-10 magnetron sputter source with a 6" diameter target is located in the top arm of the cross and a substrate holder is mounted on a linear motion feedthrough in the lower arm of the cross. Rough pumping of the system is performed by two LN_2 sorption pumps attached through a vacuum manifold to the main chamber. High vacuum is produced and maintained by a CTI-8 cryo-pump. The high vacuum pump can be isolated from the main chamber by a gate valve in order to allow access to the main chamber without requiring lengthy restart of the high vacuum system. A second baffle butterfly valve, placed in series with the gate valve, is used to throttle the crypopump during deposition. The design of this system allows operation in complete isolation, an important consideration when working with hazardous materials such as beryllium.

Samples to be coated are loaded into the system through a side arm of the chamber. Access is through a contamination control glove box located in front of the this arm of the chamber. The glove box is continuously purged with argon gas during operation. The use of a glove box for everyday loading and unloading of samples limits access of water vapor to the interior chamber walls so that water vapor levels inside the vacuum system are extremely low. The vacuum system is routinely capable of reaching base pressures in the mid 10^{-7} torr range after pumping overnight.

Beryllium coatings were produced by sputtering at approximately 10 mtorr argon pressure with an operating power of between 5 kW and 9 kW depending on the required deposition rate. The sputter source material used for these studies is Brush-Wellman grade S65-B with an oxide content of 0.7 wt%. Deposition rates varied with operating power and thickness requirements, but were in the range from 3 Å/s to 45 Å/s. Samples being coated were attached to a substrate holder, but otherwise were allowed to float thermally. Temperature measurements made during some early deposition runs using a thermocouple attached to the substrate holder. These measurements indicated a maximum temperature of 200 °C during deposition.

2.2 The Evolution of Beryllium Columnar Structure

Figure 2 and 3 show a series of scanning electron micrographs of the surfaces of beryllium coatings produced with increasing thickness. Care must be taken when comparing these micrographs due to the differences in magnification necessary to illustrate coating structural features; magnification generally decreases with increasing thickness. The increasing surface roughness of the coatings with increasing thickness is clearly evident in these micrographs. Thin coatings exhibit a smooth surface structure even at the high magnification shown here and visually these coatings are specularly reflecting. As thickness increases a more faceted, increasingly rougher surface morphology arises. Porosity, produced by mismatch between adjacent columns growing together, also becomes more pronounced as thickness increases.

For thicknesses beyond about 10 μm the shape of the columnar grains becomes increasingly anisotropic. This anisotropy increases with increasing thickness so that for 230 μm thick coatings the columns are several times longer than they are wide. The cause of this anisotropy is uncertain, but it may be related to the preferred rapid growth of certain crystal planes on the already highly faceted surface of a beryllium columnar grain. This preferred growth combined with shadowing produced by the faceted surfaces might be responsible for the evolution of this anisotropic grain shape with increasing thickness.

2.3 Column Size-Thickness Relationship for Sputtered Beryllium Coatings.

The micrographs of sputtered beryllium coatings in Figures 2 and 3 clearly show the increase in column size with increasing thickness. To quantify this relationship, the line-intercept method of measuring grain size was applied to cross-section scanning electron micrographs of sputtered beryllium coatings with varying thicknesses. In applying this method a line is drawn parallel and near the surface of the coating in a cross-section micrograph. The number of intersections with grain boundaries along this line are counted. The column size is then given by the

total length of the line divided by the number of intersections. Despite the simplicity of this method, the unusual nature of beryllium coatings makes accurate determination of column sizes difficult in many cases. Where possible this method was applied to several micrographs and the results given as a range of values obtained from these measurements.

The results of these grain size measurements are plotted on a log-log plot in Figure 4. Above a critical thickness of 2 μm there is a simple power law dependence between column size and thickness for sputtered beryllium coatings. A least squares fit to the data in the range of thicknesses between 2 and 300 μm results in the following power law for column size:

$$CS = 0.079 * Thk^{(0.9\pm 0.1)} \quad (1)$$

where CS denotes the column size and Thk the coating thickness both in μm. Care must be used in applying this relationship since other coating parameters known to affect column size (e.g. temperature) are not included in this relationship. Also presented in Figure 4 are measured columnar grain sizes obtained where possible from the literature for sputtered beryllium coatings. These results are in good agreement with the column size results reported here, despite the differences in sputter deposition conditions among the different studies.

For thicknesses below about 2 μm, the column size appears to be independent of coating thickness. These results indicate that for thicknesses down to approximately 1000 Å, column size is constant at about 0.1 to 0.2 μm diameter. The previously mentioned difficulties in measuring column size for thin beryllium coatings makes more accurate determination of sizes in this thickness regime difficult. This behavior implies that a different coating growth mechanism is dominant over this thickness range.

3. Precision Machining of Sputtered Beryllium Coatings.

The observed dependence of coating column size on thickness has important implications for improving the machinability of beryllium. As suggested earlier, a material with a fine-grain or nearly amorphous structure is considered most desirable for optimum machinability. Indeed a great deal of emphasis in our early coating efforts was applied to reducing column size through modification of the sputtering process. These attempts, as well as others reported in the literature,[4,5] have never affected column size to the extent that thickness can. The use of extremely thick beryllium coatings in earlier investigations results in column sizes of about 10-15 μm; not much different than the grain size of many bulk beryllium materials. However, a 20 to 30 μm thick, sputtered beryllium coating is expected to have a column size of 1 to 2 μm, significantly lower than previous beryllium materials used in precision machining studies. This insight, combined with the recent use of very small depth-of-cuts for diamond turning beryllium led to our using these thinner beryllium coatings to further improve the performance of precision machined beryllium optical components.

This hypothesis was tested by depositing a 25 μm thick beryllium coatings on 5 cm diameter, diamond turn aluminum substrates. Aluminum was chosen as the substrate both because of its low cost and immediate availability. Our experience in sputter depositing beryllium coatings shows essentially no difference in beryllium coating structure deposited on either beryllium or aluminum substrates. Two I-70A HIPed beryllium coupons were also obtained from Hughes-Danbury and used as uncoated control samples for comparative machining studies. These four coupons were divided into two sample sets, each set consisting of a coated and an uncoated coupon. The first set was CBN machined, while the second set was CBN machined, followed by diamond machining. The machining runs were performed with the modified process using slow speed and light depth-of-cut. The actual diamond machining parameters were: 60 rpm, 0.006 in/min feed rate, and 40 to 100 μin depth-of-cut. Only about a 2.5 cm diameter central region of the HIPed beryllium sample in the second set was diamond turned. Surface finish of the precision machined coupons was evaluated by a Talystep mechanical profilometer and optical scatter by the ORNL Complete Angle Scatterometer.

Table 1. Roughness Measurements for Precision Machined Beryllium Samples

Material	Measurement Type and Location	Roughness (rms P-V in A) CBN	Diamond
Bulk Be (I-70A)	perpendicular	218 1585	149 1417
	parallel	240 1802	213 1903
Sputtered Be on Al	cloudy, perp.	484 3129	117 1306
	cloudy, para.	524 3213	141 2432
	clear, perp.	247 1600	101 989
	clear, para.	234 1973	106 1468

Figure 5 is a photograph of the four samples after machining. The diamond turned samples exhibited a specular appearance compared to the CBN turned samples. However, the diamond turned coated samples show a "cloudy" wedge shaped region often observed on diamond turned single crystal surfaces. This cloudiness may be reduced by strategic positioning of the sample while machining or by deposition a finer grain coating. Surface roughness measurement for these samples are summarized in Table 1. Because of the anisotropic nature of precision machined surfaces two roughness profile measurements were performed: one perpendicular and one parallel to the local machining direction. For the coated samples, roughness measurements were also made in the cloudy and clear regions of the surface.

Table 1 shows that overall, the rms roughnesses of the diamond machined samples are better than CBN surfaces. There was however, a significant difference between the two beryllium material types. The roughness value obtained for the sputter coated beryllium sample was 100 Å rms. This is about 60% the roughness of the next best sample: diamond turned bulk beryllium. Generally, the differences observed between roughness measurements made parallel and perpendicular to the machining grooves were not statistically significant, especially for the smoother surfaces. This indicates that machining grooves are not a major source of roughness from these surfaces. The difference between the clear and cloudy areas of the machined coated samples is also less for the diamond turned surface compared to the CBN turned surface. This difference is roughly a factor of two for the CBN turned surface, but less than 30% for the diamond turned surface.

BRDF scatter measurements were also performed on the four samples in this study. The measurements were made at 10.6 μm wavelength and a 10° angle of incidence. Again measurements were made with the plane of incidence parallel and perpendicular to the machining direction; and for the coated samples, in both the cloudy and clear regions. Results of these measurement are shown in Figures 6 and 7.

The scatter measurements indicate the same relative ranking of the different materials and machining techniques, with diamond turned, sputter coated beryllium exhibiting the lowest scatter. The BRDF at 5° ranges from about 10^{-4} to $5x10^{-5}$ for this sample depending on location of the plane of incidence with respect to the machining direction. This is at least a factor of three lower than the next lowest scatter material: diamond turned bulk beryllium. It is interesting to note that a significant difference is observed for scatter from precision machined surfaces with respect to the machining direction; the perpendicular direction being a factor of two higher than the parallel direction for the diamond turned, sputtered beryllium surface. This is in contrast to the Talystep roughness measurements which indicated very little difference in roughness with respect to machining direction. This discrepancy between the two characterization techniques is most likely due to the existence of different spatial frequency bandwidths of the two surface characterization techniques.

Scatter from the cloudy regions of the coated samples was also found to be higher for large scatter angles compared to the clear regions (Figure 8); indicating that relatively small surface features are responsible for the higher scatter level in the cloudy region. This implies that the disruption of the smaller columnar coating structure during machining may be responsible for the cloudy regions on the coated samples.

4. Conclusions

These relatively low scatter levels for as-turned beryllium surfaces are comparable to required levels for beryllium mirrors in some IR sensors. Figure accuracy of the modified diamond turning process described here as yet to be assessed; however, the figure accuracy achieved to date using CBN tools under normal machining conditions are still worse than those required for most optical systems. Preliminary results using the modified diamond turning process has shown improvement in figure accuracy for small beryllium mirrors, but extension of this improvement to larger, more complex mirrors must be demonstrated.

A number of materials related issues also remain to be resolved before sputtered beryllium coatings can be widely used in precision optical fabrication. Perhaps the most important issue is the elimination of the cloudy wedge-shaped region on the precision machined beryllium coated surfaces. The behavior is often observed in machining materials with preferred grain orientations and is believed to be related to crystallographic orientation of the grains with respect to the direction of cutting. This cloudiness may be reduced strategic positioning of the sample during the machining process, or perhaps be deposition of a still finer grain, more randomly oriented coating structure.

Finally, this paper has discussed the relationship between coating thickness and structure for beryllium coatings and applied these observations to improving the machinability of beryllium. This combined with complimentary advances in the use of diamond tools for precision fabrication of beryllium has resulted in the fabrication of beryllium surface finishes with BRDFs below 10^{-4} at 10.6 μm and 5°.

5. References

1. T. O. Morris, *Beryllium Machinability*, Hardened Passive Optical Components Technology Development Progress Report for May 1986, p. 8, MMES/USASDC/MR-86-5.

2. G. L. Copeland and L. A. Harris, *Hot Isostatic Pressing*, Hardened Passive Optical Components Technology Development Progress Report for June 1986, p. 6, MMES/USASDC/MR-86-6.

3. C. M. Egert and J. G. Gooch, *Sputtered Beryllium Coatings*, Hardened Passive Optical Components Technology Development Progress Report for June 1988, p. 4, MMES/USASDC/MR-88-6.

4. C. M. Egert and J. G. Gooch, *Structure Modification by Sputtering in Reactive Environments*, Advanced Optical Materials and Components Technology Development Progress Report for January 1989, MMES/USASDC/MR-89-1

5. R. J. Burt et. al., J. Vac. Sci. Tech., 17, 407, (1980)

Acknowledgements

Research sponsored jointly by the Optics MODIL (under Interagency Agreement No. 1855-1562-A1) and the U. S. Army Strategic Defense Command (under MIPR No. W31RPD-9-54535) at the Oak Ridge Y-12 Plant. Oak Ridge National Laboratory and the Y-12 Plant are managed by Martin Marietta Energy Systems, Inc. for the U. S. Department of Energy under Contract No. DE-AC05-84OR21400.

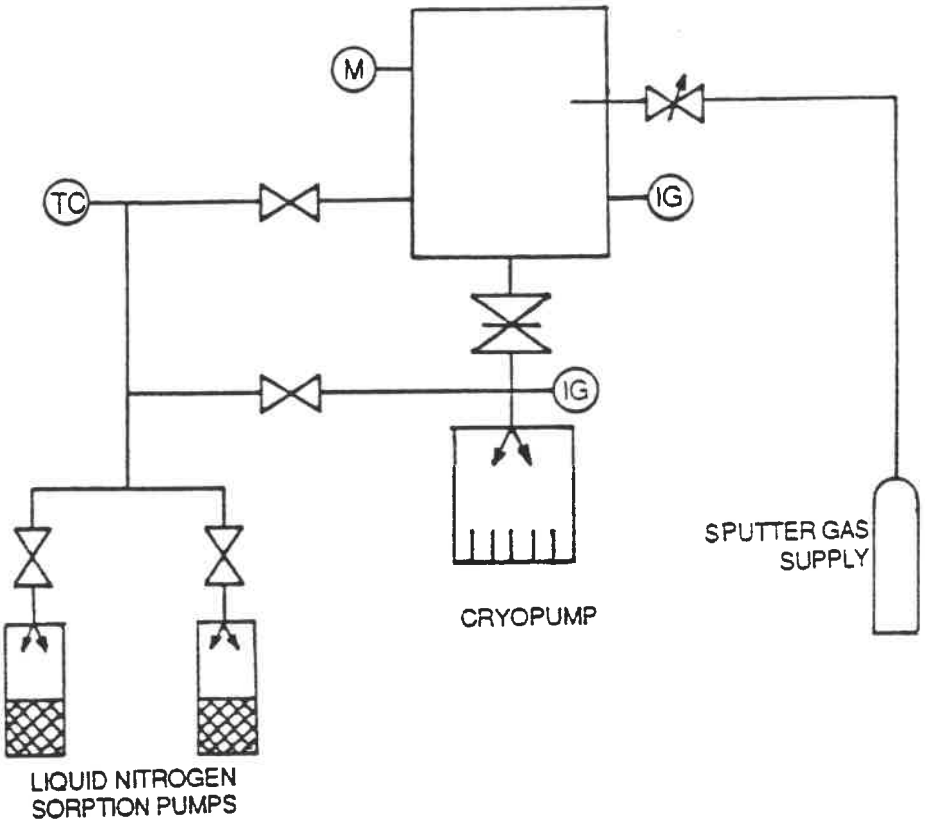

Figure 1. Schematic diagram of the sputter plating system.

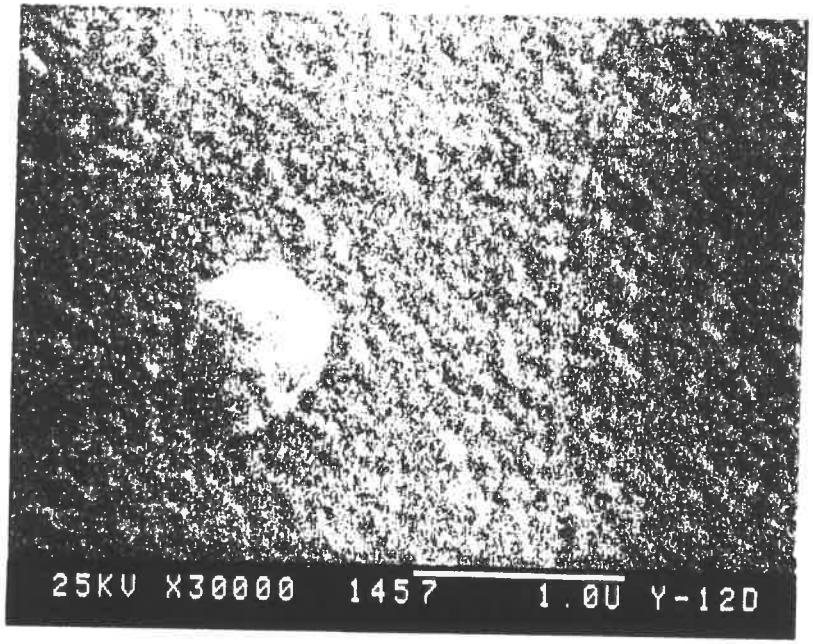

0.4 μm thick

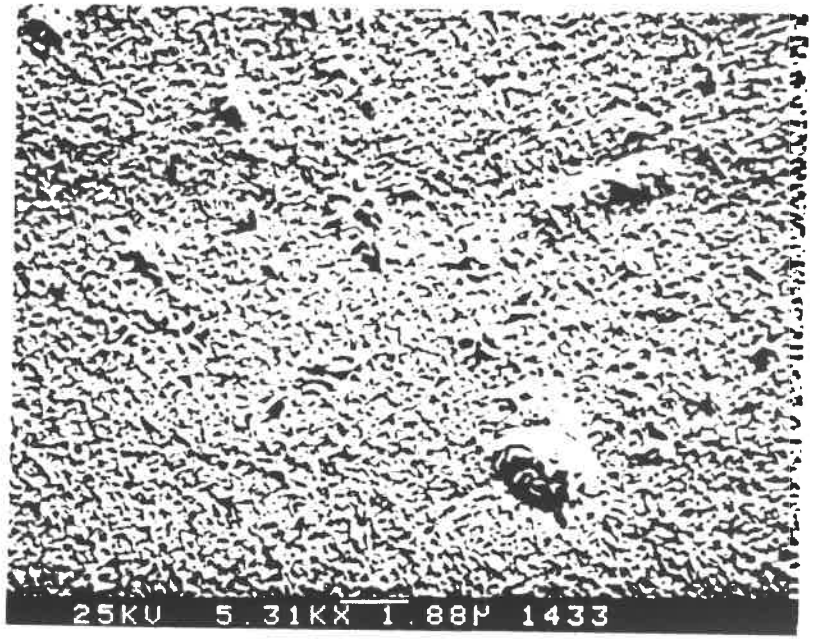

2.5 μm thick

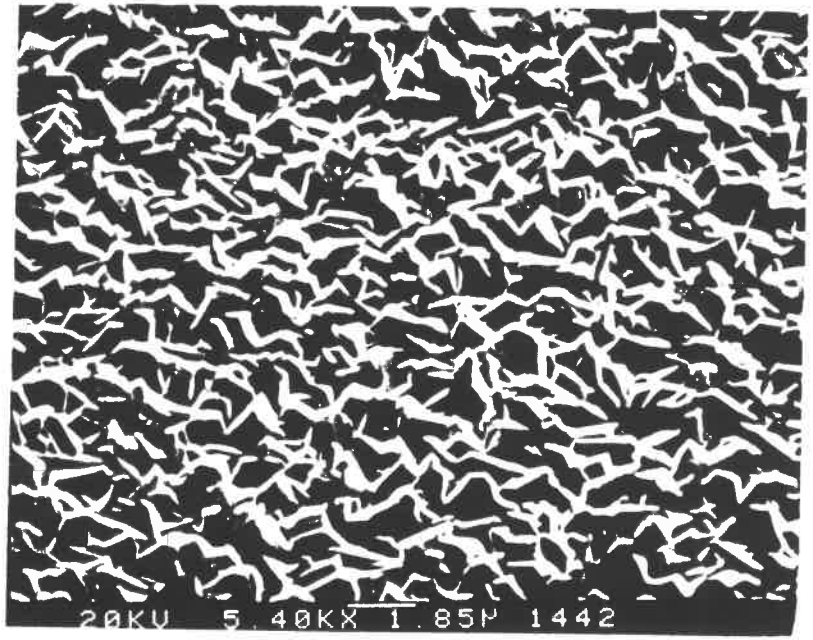

10 μm thick

Figure 2. Scanning electron micrographs of sputter deposited beryllium coatings with varying thicknesses - note the different magnifications used: a) 0.4 μm thick, b) 2.5 μm thick, and c) 10 μm thick.

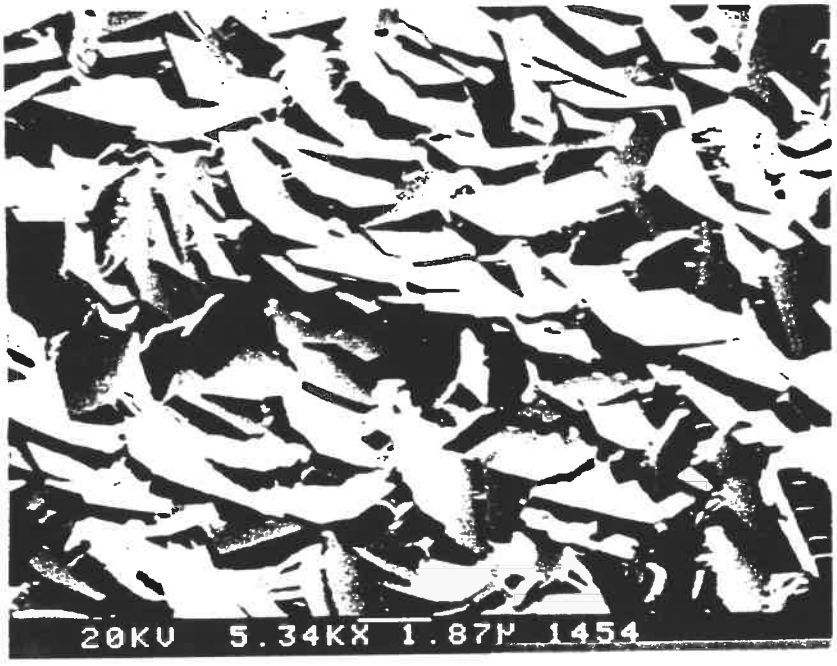

25 μm thick

230 μm thick

Figure 3. More scanning electron micrographs for thicker coatings showing the evolution of an anisotropic columnar shape: a) 25 μm thick, b) 230 μm thick.

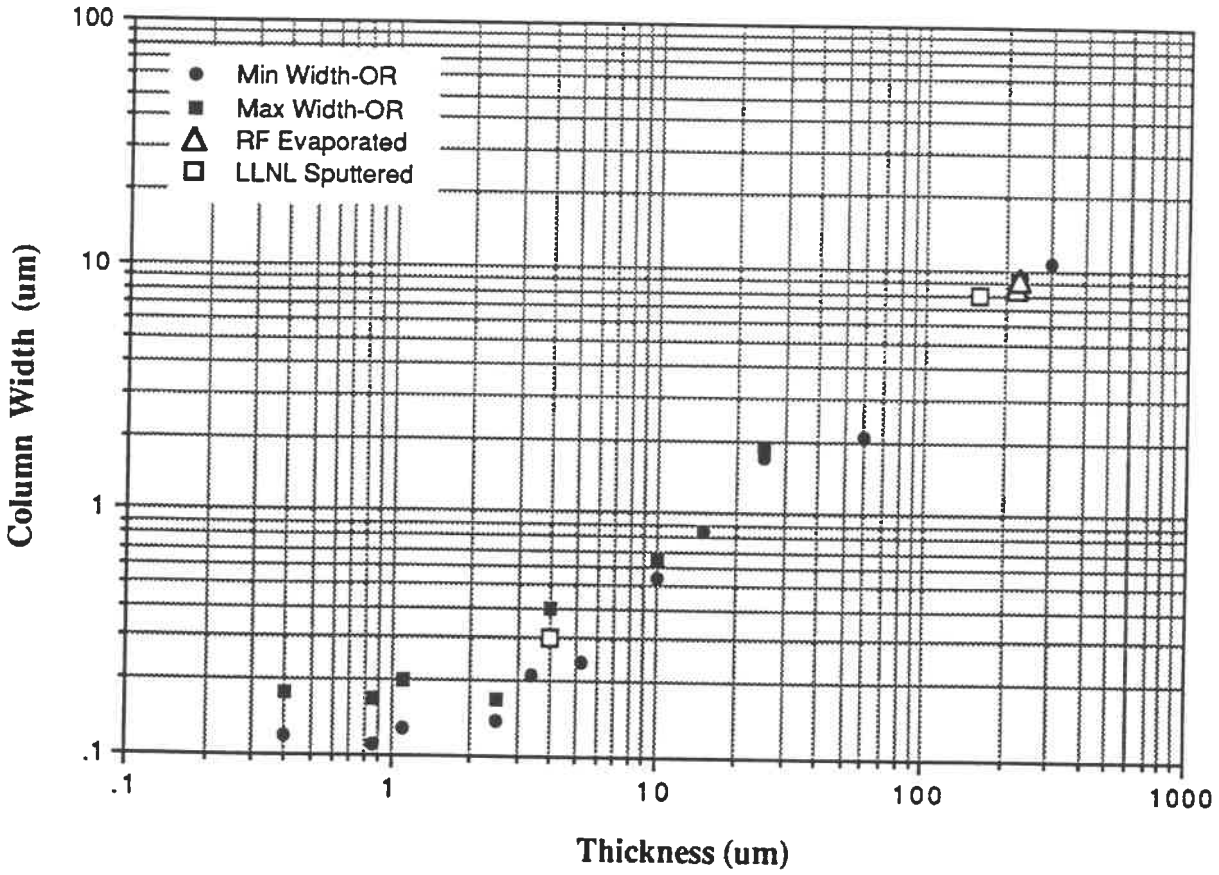

Figure 4. Estimated column size vs. thickness for sputtered beryllium coatings.

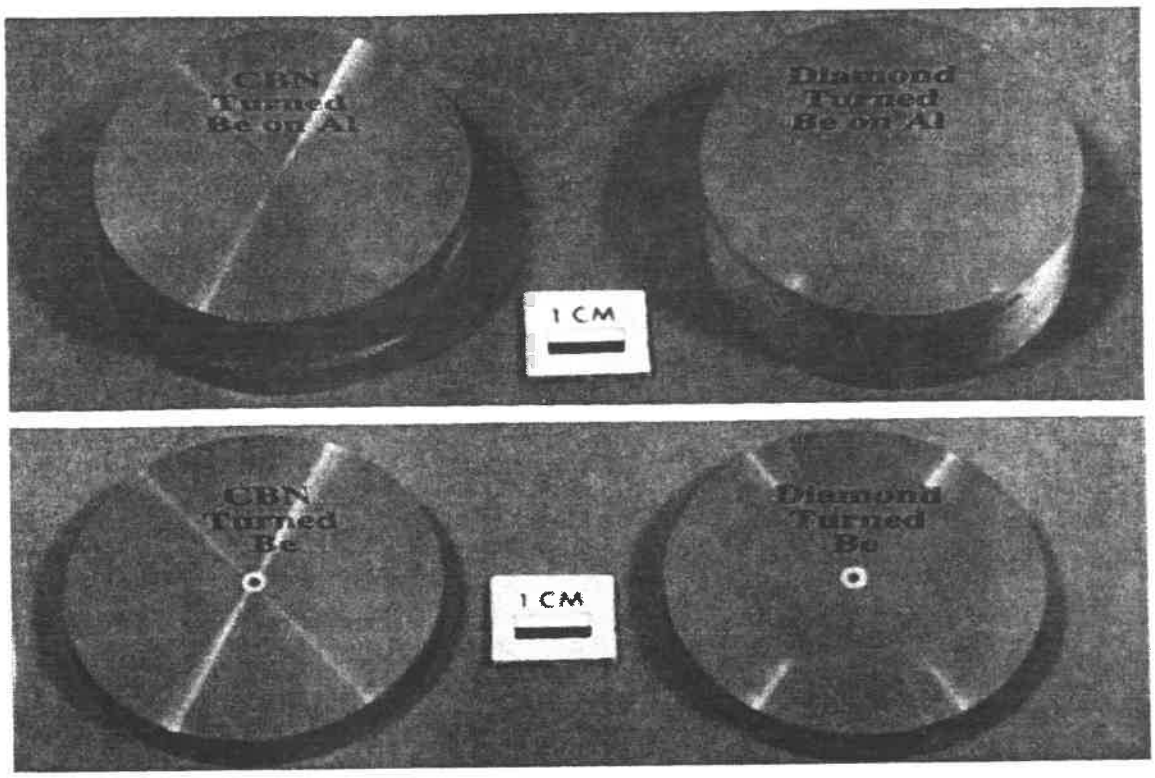

Figure 5. Photograph comparing the appearance of four coupons used in this study after precision machining.

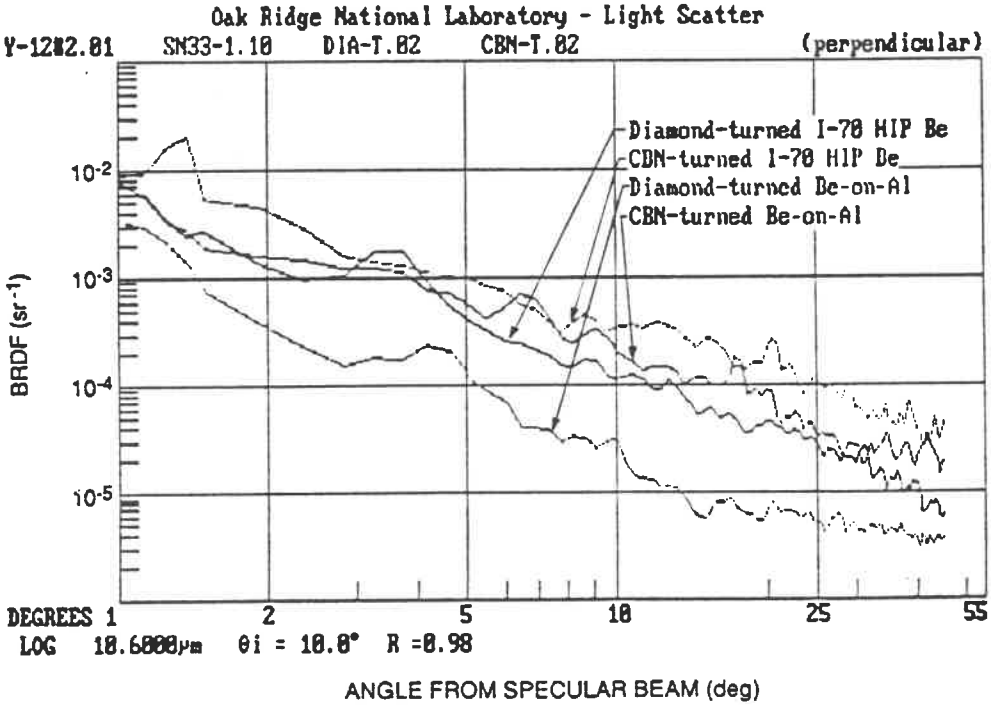

Figure 6. BRDF scatter data at 10.6 µm and 10° angle of incidence for precision machined beryllium surfaces measured perpendicular to the turning direction.

banded structure, the high probability of gradients in the phosphorus content as a function of the thickness and for amorphous alloys the possibility of creating the same composition in two different amorphous configurations each with different physical and chemical properties.

References

1. Abner Brenner and Grace Riddell, J. Research NBS 37,31 (1946) RP1725: AES Annual Proceeding, P. 23 (1946)
2. A Benner, J. Res. N. B. S., 39 ,5, (1974)
3. A. H. Graham, R. W. Lindsay, and H. J. Read: J. Electrochem. Soc. 1965, Vol 112, p 401
4. A. W. Ruff and D. S. Lashmore, in "Selection and Useof Wear Tests for Coatings", ASTM STP 769, R. G. Bayer, Ed. ASTM 1982, pg. 134-156
5. M. Ratzker, D.S. Lashmore, Plating and Surface Finishing, Sept. 1986 pg. 74
6. J. W. Dini, Electroless Nickel Conference II, Cincinnati, Ohio March (1981) UCRL 84976 Preprint
7. C. K. Syn, J. W. Dini, J. S. Taylor, G. L. Mara, R. R. Vandervoort, and R.R. Donaldson,Electroless NIckel Conferene IV Ap (1985) UCRL 91148 Preprint
8. D.S. Lashmore, L. H. Bennett, J. E. Schone, P. Gustafson and R. E. Watson, Phy. Rev. Letter Vol 48, No. 25 (1982) 1760
9. L. H. Bennett, H. E. Schone and P. Gustafson, Phys. Rev. B, Vol. 18, No. 5 Sept. (1978)
10. A. I. Goldman, G.G. Long, L. H. Bennett, D. S. Lashmore and M. Kuriyama J. Electrochem. Soc. Vol 135, No. 8 (1988) 1919
11. E, Vafaei-Makhssos, Edwin L. Thomas, and L. E. Toth Metal. Trans. A ,**9a**, Oct. (1978)
12. D.S. Lashmore and J. F. Weinroth, Plating and Surface Finishing Aug. 1982 pg. 82
13. C. C. Nee and R. Weil, Surface Technology, 25 (1985)7
14. F. Ogburn and C. E. Johnson, Plating and Surface FInishing, 60 (1973) 1043

coarsening. Both types of grains are randomly oriented. For alloys with high phosphorus contents, the amorphous to crystalline state transformation involves complex morphologies of Ni-P(glass) to Ni_xP_y and Ni. Two types of Ni_xP_y grains have been observed; in one type the individual grains are heavily striated with the striations being perpendicular to the transformation front; in the other type the grains are not striated. The Ni_xP_y is a metastable phase . Crystallization occurs by nucleation and growth mechanisms in which a distinct crystallization front advances onto the amorphous matrix. In transformations caused by electron beam heating in a TEM, the front grows radially with a sharp boundary between crystallized Ni_xP_y and the amorphous regions [3,11].

Amorphous alloys produced by electroless processes seem to have a higher free energy than those produced by ordinary electrodeposition because low temperature heat treatments irreversibly change the phosphorus Knight shift to that of the electrodeposited alloy. This structural change may explain why low temperature heat treatments have been an industry practice for the electroless alloys for many years. Both the electroless and the electrodeposited alloys exhibit a banded structure consisting of zones parallel to the substrate of generally small but measurable differences in phosphorus content. The banded structure was shown to be transport phenomena that can be eliminated by forced convective transport such as rapid and uniform stirring or by pulse electrochemical deposition [12-14]. The banded structure continues down to nearly the atomic scale. The band spacing is a function of the deposition potential in electrodeposited materials and likely is a result of oscillating electrochemical reactions involving pH, desorption of atomic hydrogen, and transport. This structure typically has band spacings of about 1 to 3 μm in the acid sulfate electrolytes whereas in alkaline electrolytes, the bands are about 500 nm thick. The banded structure has been correlated with the corrosion behavior. Non banded alloys exhibit a lower corrosion rate in chloride media [5]. The corrosion rate for the alloys exhibiting a higher phosphorous Knight shift (electroless or pulse plated] is higher than alloys produced by normal electrochemical deposition [5]. The microhardness is also higher for the same material [12].

Summary

Alloys of nickel phosphorus have very complex structures and because of the nature of the deposition process these microstructure are often not in thermodynamic equilibrium. Among the more important microstructural characteristics of the material are the existence or absence of a

agent, often sodium hypophosphite, in aqueous solutions at elevated temperatures and involves a catalyst for the reduction process. Once deposited the alloys themselves are capable of catalyzing the reaction. An important by product of the reduction reaction is hydrogen which affects mass transport and may also effect substrate properties. Upon heat treatment, nickel phosphorus alloys,which may deposit in an amorphous structure, can recrystallize with the resulting alloy containing a oriented microdispersion of nickel phosphides in a nickel matrix.[3] This latter structure has been shown to exhibit extraordinary wear performance [4]. The amorphous unheat-treated nickel phosphorus alloys have applications as protective coatings, particularly in chloride containing environments [5], and as soft magnetic materials that have potential for magnetic memories and transformer cores. They have application as brazing materials and finally as a materials capable of being diamond turned [6,7]. Because a wide variety of compositions and because two types of amorphous microstrutures for the same composition can be produced, it is important to understand the microstructure and how it is affected by the processing parameters.

Metallurgy

Nickel phosphorus is the oldest and perhaps the most extensively studied metal system forming a metallic glass [2]. The amorphous state occurs between 10 and 42 atomic percent phosphorus [8]. These glass structures are metastable arrangements of atoms frozen into position. When subjected to elevated temperatures (over 250 °C) the low activation energy barrier for nucleation is overcome and they pass through a sequence of metastable structures to a final, stable well ordered phase. On an atomic scale the amorphous alloys possess short range order with the atoms densely packed in a semi-random pattern but with very well defined first and second nearest neighbor distances, beyond this, order is rapidly lost.The deposition process seems to affect this short range order and two discrete atomic configurations are observed which can be selected by appropriate choice of deposition parameters [8,9,10]. A transition between these amorphous structures is possible and seems to occur at temperatures near 150 °C [8].

For alloys with low phosphorus contents, the deposits is supersaturated fcc nickel whose grain size, in general, decreases as the phosphorus content increases. Upon heat treatment these supersaturated solutions recrystallize to an alloy consisting of fcc nickel with Ni_3P particles dispersed throughout the structure. Nucleation and growth of the Ni_3P grains occurs with Ni grain

The Metallurgy of Nickel Phosphorus Alloys

D. S. Lashmore
Metallurgy Division
National Institute of Standards and Technology
Gaithersburg, Maryland 20899

Abstract

The metallurgy of electrochemically produced Nickel Phosphorus will be reviewed. The structure and properties of both autocatalytically and electrolytically deposited nickel phosphorus are compared. Clear differences in the atomic configurations for amorphous alloys of the same compositions have been observed using phosphorus Knight shifts and these different structural configurations manifest different physical properties including microhardness, and corrosion performance. In addition the electrochemically produced alloys typically have a banded structure resulting from small differences in phosphorus content between layers. This banded structure can be suppressed by appropriate control over the deposition parameters. Its importance lies in its effect on the properties, in particular corrosion behavior.

Introduction

The discovery of the autocatalytic deposition of nickel phosphorus alloys by Abner Brenner and Grace Riddell in 1944 and published in 1946 [1] has led to the development of a multimillion dollar industry, whose product, mainly nickel phosphorus alloys, are established in many critical areas of the U.S. economy [2]. The process makes use of a suitable reducing

and electroless. We have established procedures for each of these base metals. As long as the plater knows which base metal they are plating, bonding is not a problem.

Adhesion failures due to preplating solutions being out of operating limits rarely happens since our solutions are checked weekly by our Plating Laboratory. With our current production rate that means that the solutions are checked for every 250 or less parts produced.

Failure to completely remove all the maskant from the area to be plated occurs occasionally causing partial bonding failure. Experienced platers seldom have this problem.

CONCLUSION

The successful heavy buildup of electroless nickel relies on several factors. Two important ingredients to our success may not be obvious, which are our platers, and the type of electroless nickel bath. The long run times for heavy buildup requires around-the-clock attention of knowledgeable platers. This also requires a stable electroless nickel bath. When these two requirements are met, the heavy buildup of electroless nickel just becomes a matter of time to reach the desired thickness.

2. Electroless Nickel Solution : The stabilizers and other additives used in one solutions cause pitting in heavy deposits. These solutions appear to produce pit free plating when plated 0.002 inches per side or less, but pitting will become obvious by 0.005 inches thickness. The solutions as described early have been found to provide consistent pit free plating.

3. Deionized Water: Our most difficult to find pitting problem was due to our make up water. Severe pitting began after we had installed a new deionized water unit. Within a week of a new bath make up, we would begin to have pits in everything we plated. One of our suppliers told us that it was due to silicon build up in the solution. Our tests showed pitting when the solution contained from 2 to 5 parts per million (ppm) of silicon. Additional water purification equipment allowed us to plate longer, but we still had pitting when the silicon reached a maximum of 5ppm. We determined that the silicon was getting into our deionized water from sand being pumped up with our well water. We were trying to provide ultra pure water, but we were still having the pitting problem. Our Plating Chemist told us that we were producing silicon ions in our back flush operation of the deionizing process. At that time we quit using the deionized water and started using tap water. This eliminated the pitting problem even though we reached over 95 ppm of silicon. We are currently using distilled water with no problems.

Bonding: We plate titanium, aluminum, low alloy steels, carbon steels, stainless steels (300 & 400 series), nickel based alloys, nickel plating,

transfer which can be accomplished in about fifteen minutes. When required, a backup new solution is on hand and a complete change of solution and tank can be made in less than an hour. Most suppliers have a trouble-shooting list for their solution and the plater must become familiar with these. The plater is essential to the successful operation and control of the electroless nickel plating when heavy build up is required.

PROBLEMS AND SOLUTION WITH THICK DEPOSITS

Pitting : has been a recurring problem for us. It has been caused by many different and sometimes hard to find things. We have encountered the following causes:

1. Base Metal : The bases metal can be one factor contributing to pitting, but it may be at fault for different reasons. The corrosion that commonly occurs in low allow steels causes pits in the bases metal which will causes pits in the electroless nickel plating. These corrosion pits may occur even though the part was premachining to remove pits. If the parts are allowed to remain unprotected in a corrosive atmosphere or if the copper sulfate solution used to insure all old plating was removed is left on the part, pitting will occur. Applying a corrosion inhibiting coating will eliminate environmental corrosion and rinse of parts tested with copper sulfate will prevent corrosion due to the solution.

4. Acid Etch: We use several different acid etches depending on the base metal. They are fairly standard in the industry for the particular metal.

5. Nickel Strike: We apply a nickel strike to all our parts except aluminum. This insures plating activity as soon as the parts are placed in the bath. We use a non-attached internal anode on some ID's.

6. Electroless Nickel Plate: We plate using standard operating parameters for a high phosphorous bath to the desired thickness. The plating rate is usually from 0.0005 to 0.0003 inch an hour and we plate 0.002 to 0.003 inch per side over finish dimensions.

CONTROL PARAMETERS

Control of the electroless nickel plating bath is the prime factor in successfully plating heavy deposits. We do not have controllers on our plating tanks, yet. The platers have to maintain around-the-clock checking of the electroless nickel bath and the quality and rate of plating. They must have a wide knowledge of potential problems and solutions to those problems. Our platers receive as much classroom and on the job training as our resources will allow. The platers are in control of the bath running their own hourly analyses and rate determinations. When something is occurring which they are not trained or equipped to handle, they request assistance from our Chemical Laboratory or our Process Engineering Section. The platers check nickel content, pH, plating rate and make visual observations. If an immediate-action problem is found, such as a leaking tank or excessive seeding out, they have a backup tank available for

cause chipping during handling or grinding. While our rates and hardness are not at the maximums possible, they are at an optimum for our repair of a wide range of engine and aircraft parts with a wide range of plating thicknesses needed.

PREPLATING PREPARATION AND PROCEDURES

Our preplating preparation and plating procedures for electroless nickel plating are as follows :

1. Masking: Primarily we use an organisol for masking. Due to our long run times, we have to use an additional thin coat of an organisol with excellent adhesion or an epoxy primer covered with several layers of a heavy organisol. We had plating in unauthorized areas before we started these procedures. We prefer the all-organisol masking combination since both can be removed by vapor degreasing with perchloroethylene. If the epoxy primer is used, the part must be glass bead blasted after vapor degreasing.

2. Presoak: An alkaline presoak is used on all parts to remove any residual organics from the maskant. Parts are soaked about ten minutes in the solution operated at about 120 deg F.

3. Electrocleaning: The parts (except aluminum and titanium) are placed in an alkaline cleaner operated at 120 deg F using a periodic cycle from anodic to cathodic.

0.002 inch per side. The keys to this success has been using the right kind of electroless solution and dedicated platers.

We will be discussing some of the procedures established that allow us to have success when plating thick deposits. Also, we discuss some the problems that we have encountered during the repair/overhaul of aircraft engine components.

SOLUTION TYPE

For our operation, the type of electroless nickel solution is very important to a success in thick deposit plating. We have tried many different solutions from various suppliers, but we come back to the same type of solution. We currently have three approved suppliers of the solution with the following general characteristics:

1. Provides a minimum of 11 % phosphorous in the deposit
2. Self regulating pH
3. Very stable, able to operate for extended times with 0.1 square foot surface area per gallon of solution or less
4. Produce heavy buildup deposits without pitting
5. Compressively stressed as plated

These types of solutions are slow plating with rates from 0.0003 to 0.0005 inch per side per hour. Even though there are faster plating baths available such as those with 7 to 9% phosphorous, we find the lower phosphorous solutions produce brittler deposits. We have found that brittle deposits from either low phosphorous or from a high hardness bake

THICK DEPOSITS WITH ELECTROLESS NICKEL

G.H. Graham
Process Engineering Section
Oklahoma City Air Logistics Center

INTRODUCTION

Oklahoma City Air Logistics Center (OC-ALC) at Tinker AFB has for over ten years plated electroless nickel in thick or heavy deposits. Thick or heavy deposits can be defined according to ones experience, but we plate 0.015 to 0.030 inches per side of finish-ground electroless nickel plating. We have developed criteria which give us a very high success rate with these repairs. These thick deposits of electroless nickel plating for repairs have proven to be very acceptable through in-service use.

Initially, at OC-ALC, electroless nickel plating was for corrosion coating or plating to size, with 0.002 inch per side or less of plating. The initial electroless nickel solution was an in-house mixture. As we began to explore the possibility of buildup plating repair using electroless nickel, we found a supplier who claimed success with his solution with buildup of 0.010 inch per side of plating. Successful implementation of this electroless nickel plating solution in our plating shop was the beginning of our current operation. We have continued to increase deposit thickness on parts until, today, many parts routinely require 0.020 inch per side of electroless nickel plating with some requiring as high as 0.030 inch per side. Meanwhile, we have maintained our workload for corrosion coating and plating to size with less than

FROM THE KECK TELESCOPE TO WHERE...?

A derivative process of Laser Gold is presently lowering power cost and increasing production efficiency in some 20 infrared automotive paint drying ovens for General Motors assembly plants. As the use of water-borne paints accelerates throughout industry, thanks to the new EPA Solvent Regulations, more and more ovens will be built with, or converted to, this vastly more efficient reflective coating.

At the same time, the name Laser Gold was trade-marked; Laser Gold was so called because of its then near universal use as the coating on NDYag lasers. With their main pump band at 1.06 microns, this was an ideal material for pump cavity reflectors.

Continuous improvements in the process has pushed the total reflectivity over 97% at the benchmark wavelength of .7 microns and higher than 99% from 3 microns out. The coating is 99.99% pure, yet at 150 Knoop is hard enough to be physically cleaned (pure gold generally has a Knoop hardness that does not exceed 85).

THE KECK TELESCOPE AND LASER GOLD

The Xerox application and continuous improvements in the Laser Gold process that were driven by their engineering requirements opened up the applications for a hard, reflective coating that was not line-of-site dependent (as is evaporative gold) and could be applied in various thicknesses.

In the mid 1970's, Laser Gold became the sole process for the Tow missile guidance reflector and as of this writing more than 500,000 have been produced. A custom designed helium neon laser is the key inspection tool for these critical components.

In the recent Gulf action, most of the IR Maverick seeker scan mirrors were coated with Laser Gold after diamond turning the internal facets.

Other military and aerospace applications followed as the coatings' reputation spread through the engineering community. Reflectors and chopper blades for infrared counter-measures used to protect both helicopter and fixed wing aircraft from heat seeking threats is a key application for Laser Gold. Substrates of stainless or aluminum are either buffed or optically polished and electroless nickel plated before the gold is applied.

The process is used in a broad spectrum of industries from IR lightpipes or wave guides used to measure the temperature of the human body through the ear, to sandblasted, diffuse, intergrating spheres for a device that measures the protein value of grain by infrared spectroscopy.

The SDI high energy laser program, commonly known as Star Wars, used Laser Gold on beam clippers and strut protection hardware, some of which were quandrants of a 4 foot diameter diamond machined toroidal mirrors.

Early in 1991, Epner Technology was approached to coat the Infrared Secondary Mirror on the giant Keck Telescope in Hawaii. While the primary mirror, constructed in sections, is some 33 feet in diameter and aluminum coated, the IR secondary is 20" in diameter. It's fabricated in beryllium and plated with an optical quality electroless nickel-phosphorous to a thickness of .004" and then diamond machined to the final optical figure.

After careful activation of the nickel, a .000020" minimum thickness of Laser Gold is applied. Because of the great value of this mirror, the entire process is rehearsed on a nickel plated pathfinder blank made of aluminum.

The IR specification called for a minimum thickness of 10 microns of gold with a hardness that would permit the field tech service rep to periodically clean the toner residue. It had to meet a minimum of 91% total reflectivity at the just visible wavelength of .7 microns.

Although the functional wavelength of the fuser was closer to 2 microns, .7 was chosen because of it's position on the gold reflectance curve, i.e., below the "knee". Thus greater resolution of the spectrophotometer's scan, made small differences in reflectivity very apparent.

Epner's engineering staff explored the two most obvious controllable aspects of an electroplating system - the chemistry and the power. Options such as pulsed, periodically reversed, and AC over direct current were part of the research matrix as were some 16 basically different gold bath chemical formulations.

When production finally began, disaster soon struck in the form of a trailer truck of gold plated rejects...the reflectivity was low. It was apparent that Epner would need the same inspection tooling that Xerox used.

A Beckman DK-2A spectrophotometer with an integrating sphere was purchased, and with this inspection tool for measuring total reflectivity, it became evident that only a few hundred parts could meet specification before contamination of the plating bath degraded reflectivity. Gold baths were in a constant rotation of one bath plating parts, and one bath being refined.

The Epner Spectrophotometer was being calibrated to an NBS vapor deposited Gold Reference Standard and some years into the project another major reject occurred...

Again for low reflectivity. Epner's QC Manager protested based on a favorable comparison of a rejected part to this NBS Reference Standard. David Epner, company President, hand carried the NBS Standard to Rochester for a comparitive reading on the Xerox Spectrophotometer.

Incredibly, the Xerox Optical Lab Manager said "The NBS Standard is 2 percentage points off." The "gauntlet was dropped" and an appointment was made to have the NBS recalibrate the Standard.

Much to the dismay of both Epner and Victor Weidner of the NBS Metrology Lab, the standard had indeed "drifted". As a result, the NBS immediately withdrew these reference standards from the market.

By this time Epner's gold was hard, and was consistently achieving 93% at the critical .7 micron wavelength, so the suggestion was made that this plated gold be considered for replacement of the old Standard. Optically flat nickel plated copper substrates were gold coated and submitted to the NBS. They were calibrated and stored. A year later, they were rechecked and stored for 3 more years. It took some 7 years before Epner's mirrors became the official NBS Reference Material and offered to the world scientific community.

LASER GOLD® PLATING FOR DEVELOPING AN NBS (NIST) STANDARD AND A COATING FOR THE KECK TELESCOPE SECONDARY MIRROR

David Epner, President
Epner Technology Incorporated
25 Division Place
Brooklyn, NY 11222

This paper will review the serendipitous discovery of the need and of the development of an electrodeposited proprietary process called Laser Gold®, a highly reflective, hard, infrared coating by a small company in Brooklyn, NY called Epner Technology Incorporated.

WHO IS EPNER TECHNOLOGY AND WHAT IS LASER GOLD?

Epner Technology (Incorporated) is a direct descendant of a company founded in 1910 under the name of Cohan-Epner, after the two founders, Emmanuel Cohan and Louis Epner. Initially, the company did the repair and gilding, (as gold plating was then called,) of jewelry.

In 1985, the name was changed to Epner Technology which closer describes the high-tech specification contract plater it has become. Epner Technology currently employs about 50 people. Approximately half its sales are the plating of precious metals, nickel, electroless nickel, tin and copper. These are primarily plated on substrates such as titanium, molybdenum, and beryllium, as well as the more routine metals such as aluminum and stainless.

The other half of Epner Technology's sales comes from a proprietary process known as Laser Gold and this paper will trace the path of the development of this process from its birth, thanks to Xerox Corporation, to its current use as the Infrared Standard for the NIST (NBS) and the coating for the Infrared Secondary Mirror on the Keck Telescope under construction in Hawaii.

HISTORY OF THE PROCESS

In 1971, a Xerox design engineer visited the Epner Company display at the Design Engineering Show in Chicago. At that time, Xerox had a need for a plater that could polish, nickel and gold plate a 4 pound aluminum extrusion to be used as an IR Reflector for a quartz halogen lamp used to heat-fuse toner to the copy.

The competing process was a vapor deposited gold directly over the polished aluminum extrusion. This was not only costly, but the gold would soon diffuse or migrate into the substrate destroying its reflective function. It was also very fragile.

Xerox had had little success in finding a company that had both expertise in buffing and plating the aluminum to withstand high temperature and gold plating.

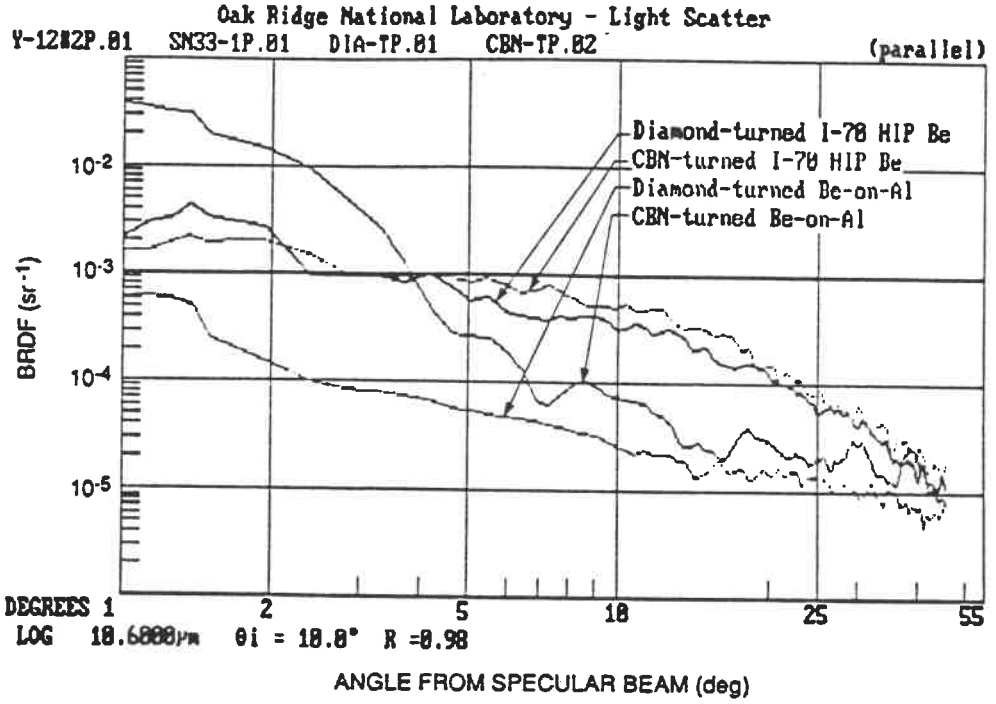

Figure 7. BRDF scatter data at 10.6 μm and 10° angle of incidence for precision machined beryllium surfaces measured parallel to the turning direction.

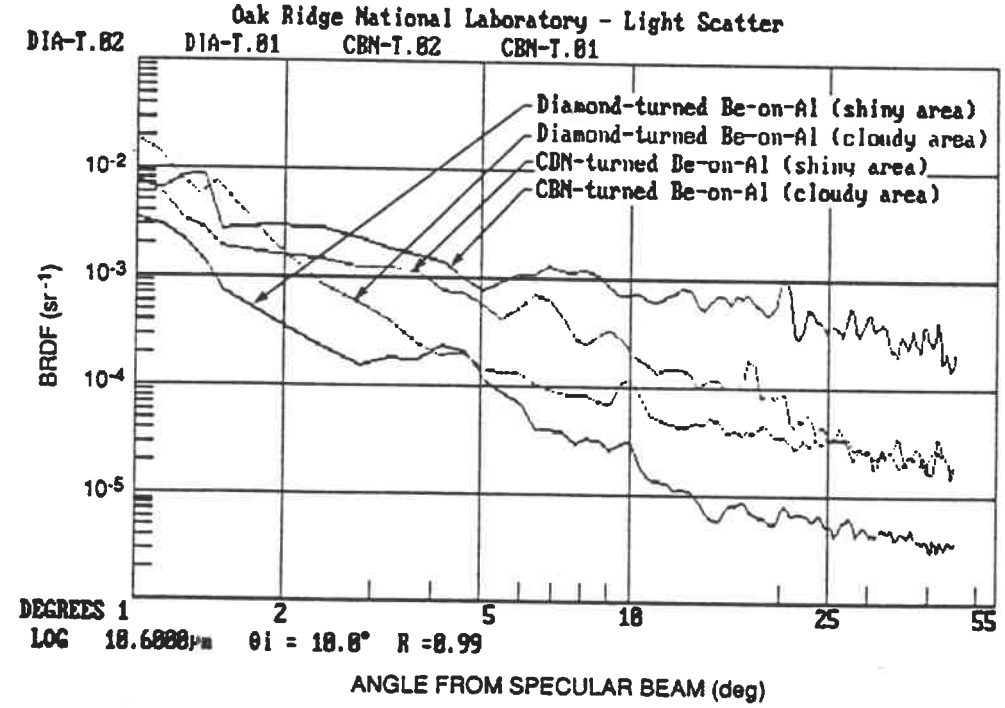

Figure 8. A comparison of BRDF scatter data at 10.6 μm and 10° angle of incidence for precision machined sputtered beryllium on aluminum the cloudy and clear regions of the finished parts.

Glenn A. Malone
Electroformed Nickel, Inc.
Corona, California 91720

ELECTROFORMING COMPLEX INTERNAL SURFACES IN HIGH POWER COMPONENTS

In early 1990 Electroformed Nickel was awarded a contract to fabricate a 500.00 MHz Buncher Cavity Assembly for the High Power Modular Component - Free Electron Laser System being fabricated by TRW in Redondo Beach, California for The Office of Naval Research. This cavity assembly is a high power RF device consisting of a thin wall copper shell with a precise internal shape that represents a resonant cavity to RF energy at 500.00 MHz. The inside of this oblate spheroid must be capable of evacuation to 1 x 10 Torr. Various components are attached to the unit via high vacuum flanges with ports for connection to other components and insertion of RF couplers, probes, and other devices. Other features of the cavity provide for cooling mechanical loading to change the spheroidal shape for RF tuning. Internal surface finish of 4 to 8 microinch RMS was required.

The plan for fabrication consisted of electroforming the oblate spheroid shell over a suitable mandrel using thigh purity copper, growing the main four stainless steel vacuum flanges to the copper shell by electrodeposition with copper, high temperature brazing of the vacuum flanged access ports to holes in the cavity shell, low temperature brazing of the manifolded water cooling systems to the outside of the assembly wall, and polishing the interior surfaces to the required finish for proper RF wave performance.

OFHC copper was selected for the cavity wall because of the requirements that the metal be highly conductive - both thermally and electrically - and non-magnetic. An acid sulfate copper electroforming bath was selected for the application. This electrolyte contained a pentose additive known to act as an oxygen inhibitor at surfaces being plated. This electrolyte has been found to produce copper deposits containing less than 10 ppm oxygen while having ultimate tensile strength exceeding 30 ksi with over 30 percent elongation in a two inch gauge length. Addition of a small amount of tri-isopropanolamine, or use of periodic current reversal, will permit deposition of copper in great thicknesses while retaining a fine grain structure.

The mandrel for electroforming the oblate spheroidal shape was made from an epoxy-glass cloth lay-up with a polished surface finish. The epoxy extensions forming the minor axis poles of the oblate spheroid were sufficiently long so as to accommodate attachment of stainless steel half nipples which would serve as vacuum mounting flanges to the rest of the vacuum system. The epoxy mandrel was made conductive by spraying several coats of an electronic grade silver pigmented paint with hand rubbing for smoothness after each coat was air dried.

The polar half nipples were copper plated over the tubular surfaces to provide a bonded deposit for later growing onto the cavity wall during electroforming. These plated surfaces were masked to prevent plating with a poor bond during the initial copper build-up of the cavity wall on the epoxy mandrel. A gear driven rotating fixture was built to rotate the mandrel about the polar axis during electroforming. The two polar half nipples were masked with PVC plates and rings to prevent copper deposition on the stainless steel vacuum sealing surfaces. The use of a threaded rotating shaft through the mandrel allowed accurate fixturing of the half nipples for precise fit-up to the experiment vacuum system after fabrication. After electroforming about 0.050 inch of copper on the mandrel, the part was removed to mechanically dress the deposit at the mandrel-half nipple interfaces. The masking was removed, and all copper surfaces were activated for electroform bonding with copper. Electroforming was resumed until a cavity wall thickness of about 0.150 inch was achieved.

The cavity wall was next machined to the 0.125 inch wall thickness required by design. The following operation was to electroform grow pedestals 180 degrees apart at the equator of the oblate spheroid. PVC tubular shields were fabricated to confine electroform growth to these particular areas - the balance of the cavity wall being masked. The copper pedestal thus grown were milled to flat surfaces for mechanically mounting the next generation of stainless steel half nipples. These were pre-plated with copper so that electroform joining could be accomplished on like metals. Following this operation, the part was machined to provide access ports in the equatorial half nipples for electronic probes. Additional holes were machined in the cavity wall for RF couplers, probes, and other equipment.

The next fabrication stage required vacuum brazing of half nipples onto the machined openings and brazing of stainless steel reaction rings used to mechanically adjust the cavity shape for RF tuning. It was necessary to remove the epoxy mandrel to permit the brazing which would involve heating the part to 1550 F. The ports were all closed with masked aluminum plates so the cavity could contain a solvent needed to strip the epoxy and allow withdrawal of the glass cloth reinforcement. The cavity was installed on a rotating fixture for the stripping operation. Following the removal of the mandrel, it was necessary to clean and polish the interior surfaces. This was performed using plastic tumbling cones and a soap solution.

The reaction rings were torch brazed unsuccessfully. Localized overheating led to distortions which necessitated removal of the first ring. Brazing of the second ring was assisted by induction heating which led to a more uniform and controlled heating. This joining operation was very successful. The area of distortion required correction, and a fixture incorporating an internal compression roller was made which permitted roll-forming the copper wall to the correct contour - as verified with a template. All remaining vacuum components were successfully brazed in place using a copper-silver braze alloy. Other lower temperature alloys were not permitted due to potential for the alloying ingredients such as tin or zinc to volatize as a contaminant in high vacuum and possible damage to the cathode gun device.

The final fabrication stage consisted of silver soldering the water cooling system to the exterior of the Buncher Cavity. Two water manifolds and 24 copper cooling tubes were joined to form the coolant flow system. The interior surfaces were again polished with plastic cone medial and electropolished in concentrated phosphoric acid. System leak tests demonstrated that the various component joining processes were of high integrity.

ELECTRODEPOSITED COATINGS FOR DIAMOND TURNING APPLICATIONS

A. Mayer, R. D. Bramlett and R. D. Day
Los Alamos National Laboratory

C. J. Evans and R. S. Polvani
National Institute of Standards and Technology

Electrodeposited coatings are attractive for precision machining operations because thick coatings can be economically applied, with good adhesion, to a variety of substrates. Approximately 20 pure metals and a large number of alloys can be deposited from aqueous solutions. Fused salt and organic solvent electrolytes can be used to lengthen the list of metals that can be electrodeposited. However, both the choice of the metallic coating and the control of the plating process are critical for success in precision finishing of electrodeposited coatings. Some preliminary results at the National Institute of Standards and Technology[1] and at the Lawrence Livermore National Laboratory[2] suggest that electrodeposited nickel-phosphorus alloys are excellent coatings for single point diamond turning from the standpoint of material properties and low tool wear. Electrodeposited aluminum and aluminum alloy coatings also merit consideration for precision finishing where weight is an important factor.

NICKEL-PHOSPHOROUS ELECTRODEPOSITION

Amorphous nickel-phosphorus alloys were first electrodeposited by Brenner et al.[3] These coatings have high hardness[4], good corrosion resistance,[5,6] and dry sliding wear resistance comparable to that of hard chromium.[7] Our interest in NiP was in synthesizing thick metallic glasses for structural characterization and in fabricating free standing electroforms for possible use as unique structural materials. We also were interested in investigating the machining characteristics of these deposits and their resistance to solid-particle erosion.

Amorphous NiP alloys with a composition range of 12 to 15 w/o were electrodeposited from a 125 liter phosphorus acid electrolyte. The solution contained $NiSO_4$, $NiCl_2$, $NiCO_3$, H_3PO_4, and H_3PO_3. The solution was operated at 75°C at a current density range of 5-20 A/dm^2. The pH was maintained between 1.0 and 1.5. We used platinum anodes for most of our work. If soluble nickel anodes are used, the nickel concentration in the solution rises rapidly with a corresponding rise in pH caused by the lower cathode than anode efficiency in this electrolyte. The plating cell had two external filters housings connected in series with course (10 μm) followed by fine (3 μm) cartridge filtration. The filter pump discharge stream was directed towards the cathode to provide vigorous agitation and to minimize particulate inclusions.

An x-ray diffraction scan (Fig. 1) of the NiP deposit shows the material to be a single phase amorphous alloy. A typical TEM image of NiP viewed normal to the deposit surface (Fig. 2) shows no structure. Detailed TEM examination of NiP viewed parallel to the electrodeposited layer (Fig. 3) revealed extremely fine layers on the order of 10-20 μm thick. The light and dark bands are the result of variations in etch rates due to compositional variations within the layers. Amorphous electrodeposited NiP transforms at relatively low temperatures and short incubation times to a two phase material, with intermetallics in a crystalline nickel matrix. These transformations are observed in both electrodeposited and electroless high phosphorus nickel alloys. Figure 4 shows partial crystallization, in the shape of rosettes, of a NiP deposit heated to 265°C for 2 hours. The hardness of the as-plated amorphous phase was 595 DPH while the crystalline phase was 945 DPH. The cracks visible in some of the rosettes in Figure 4 are caused by a volume contraction during crystallization. The hardness and high wear resistance of amorphous nickel-phosphorous coatings suggested that they may also be resistant to solid particle erosion. In our study,[8] NiP and pure electrodeposited nickel was subjected to angular alumina particles at various impingement angles from 15° to 90° at particle velocities from 50-100 m/s. For all experimental conditions, the erosion rate of the amorphous alloy was higher than that of the pure nickel. The material removal in the amorphous NiP was attributed to the formation of plastic shear bands below the impact areas resulting in spallation.

The results of our single point diamond turning experiments showed that thick NiP coatings were essentially pore free and typically showed less tool wear than electroless nickel deposits.[1] Our preliminary results indicate that electrodeposited nickel-phosphorous may be useful for some opto-mechanical applications.

ALUMINUM AND ALUMINUM ALLOY ELECTRODEPOSITION

Practical electroplating processes for active metals such as Al, Mg, Ti, and Be would have applications for both functional and decorative coatings and also for fabricating light weight, high strength structures of high value such as optical components and space hardware. The metals cannot be plated from aqueous solutions because the hydrogen ions of the water are preferentially reduced over the active metal ions. Attempts to plate the active metals from aprotic solvent solutions have been made since the beginning of this century. Of the four metals mentioned above, only organic solvent aluminum plating processes have had limited commercial success.

We were interested in electrodepositing aluminum for electroforming of low Z components and for barrier coatings for metals such as uranium. We selected an aluminum plating process developed by Ziegler and Lehmkuhl[9] for our evaluation. The

solutions are based on trialkyl aluminum/alkali metal fluoride complexes dissolved in aromatic solvents. High purity (> 99.99) aluminum deposits with relatively fine grain structures can be obtained from these solutions. Because of the high purity, small grain size, and absence of inclusions in electrodeposited aluminum, high quality mirrors can be fabricated by single point diamond machining. Figure 5 shows a scanning electron micrograph of diamond turned electroplated aluminum. For comparison, diamond-turned commercial grade 6061 aluminum is shown in Figure 6. Chip removal during machining high purity aluminum was difficult. We explored the feasibility of hardening the deposits by alloy plating. We developed plating solutions for depositing Al/Mg alloys spanning the total composition range.[10] The solutions contain trialkyl aluminum/potassium fluoride complexes and dialkyl magnesium dissolved in toluene. A fivefold increase in deposit hardness over the pure Al deposits was observed on an alloy containing approximately 20 at % magnesium. The harder deposits suggest an increase in strength and perhaps improved diamond point machinability. Because some of the organometallic compounds are pyrophoric in air and react violently with water, all operations were carried out in a glove box under positive pressure of dry nitrogen or argon.

SUMMARY

Two classes of electrodeposited coatings were discussed for possible use in precision machining operations. Thick, pore free, high phosphorus content NiP alloy deposits can be electroplated. The high phosphorus electrodeposited alloys appear to extend diamond tool life over that of conventional electroless nickel deposits. The low thermal stability of electrodeposited NiP may preclude its use in some applications. Because electrodeposition of aluminum and aluminum alloys from organic solvent electrolytes are complex processes requiring specialized equipment, the use of these deposits for precision finishing may only be justified for very high value components.

REFERENCES

1. C. J. Evans, R. S. Polvani, and A. Mayer, "Diamond Turned Electrodeposited Nickel Alloys," 1990, Technical Digest Series, Vol. 9, pp. 110-113.

2. J. W. Dini, R. R. Donaldson, and C. K. Syn, "Diamond Tool Wear of Electrodeposited Nickel-Phosphorus Alloy," UCRL-Preprint 102050, Feb. 1990.

3. A. Brenner, D. E. Couch, and E. N. Williams, J. Res. Natl. Bur. Stand. 44, 109 (1950).

4. W. H. Safranek, in "The Properties of Electrodeposited Metals and Alloys" (American Electroplating and Surface Finishing Society, Orlando, FL, 1986), 2nd ed., p. 346.

5. C. Rajagopal, D. Mukherjee, and K. S. Rajagopalan, Met. Finish. J. 82, 59 (1984).

6. M. Ratzker, D. S. Lashmore, and K. W. Pratt, Plating Surf. Finish. 73 (9), 74 (1986).

7. A. W. Ruff and D. S. Lashmore in "Selection and Use of Wear Tests for Coatings," edited by R. G. Bayer (American Society for Testing and Materials, Philadelphia, 1982). p. 134.

8. K. C. Goretta, J. L. Routboard, A. Mayer, and R. B. Schwarz, "Erosion of Amorphous Nickel-Phosphorus," J. Mater. Res. 2 (6), Nov/Dec 1987, pp. 818-826.

9. K. Ziegler and H. Lehmkuhl, Z. Anorg. Allg. Chem., 283, 414 (1956).

10. A. Mayer, U.S. Pat. 4,778,575 (1988).

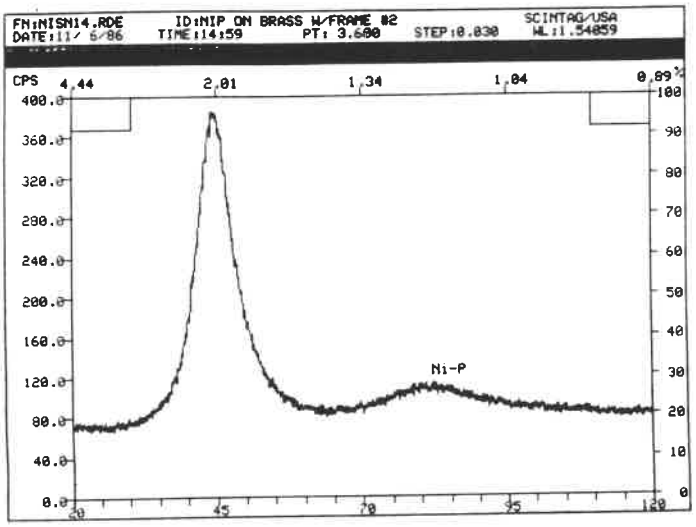

Fig. 1 X-ray diffraction scan of electrodeposited nickel-phosphorus alloy.

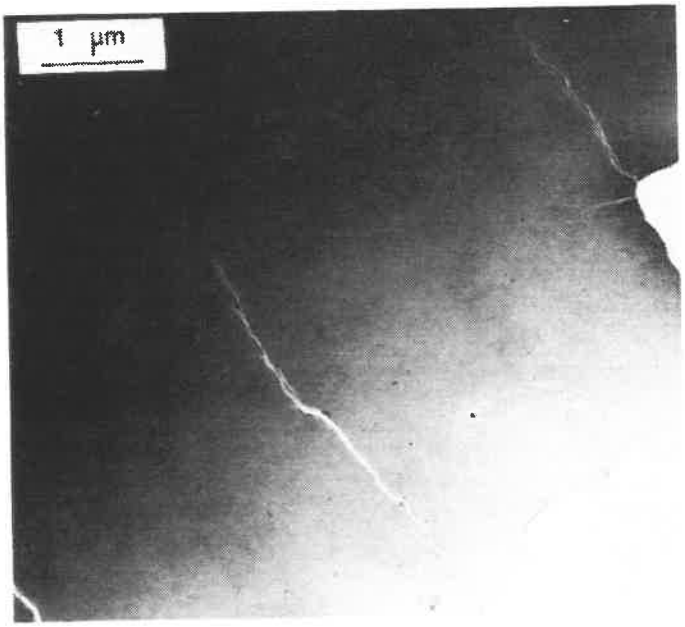

Fig. 2 TEM of NiP alloy surface viewed normal to the deposit layers (parallel to growth direction). Crack occurred as a result of thinning during specimen preparation.

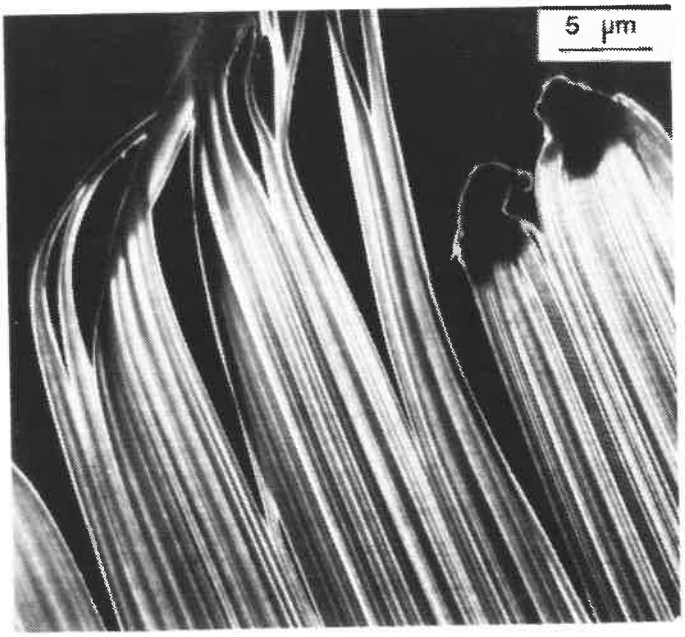

Fig. 3 Dark-field TEM photograph shows cross section of NiP alloy viewed parallel to electrodeposited layers (normal to growth direction).

optical wavefront because of the differing effects on the long and short axes of the ellipse. For a front surface reflector used at or near normal angles of incidence, the temperature effects are uniform (nonastigmatic) enough to be used for athermalization.

More experimentation needs to be done to determine if modifying the mirror geometry could cause the deformation pattern to become more deterministic. Also unknown at this time is whether the apparent power created by the temperature effects are deterministic enough to be used as a design tool for the optical designer. The geometry of the webbing on the back of the part, the thickness of the mirror sections, the thickness of the electroless nickel plating, the chemical composition of the electroless nickel,[4] and the amount of material machined from the front surface of the mirror are all variables which must be explored for their effects on the mirror geometry at various temperatures.

REFERENCES

1. Taylor, H., "Metal mirrors in the Large," *Proc. SPIE* Vol 35, 77 (1975).
2. "Engineering Properties of Electroless Nickel Deposits," a booklet by INCO.
3. Caithness, W., "Some Fundamentals of Metal Mirrors." *Proc SPIE* Vol 35, 8 (1975).
4. Syn, C. et al., "Influence of Phosphorus Content and Heat Treatment on the Machinability of Electroless Nickel Deposits." Lawrence Livermore National Laboratory.
5. Sanger, G., "The Precision Machining of Optics," *Applied Optics and Optical Engineering* Vol X, 339–345. Shannon, R. and Wyant, J., ed. Academic Press, 1987.

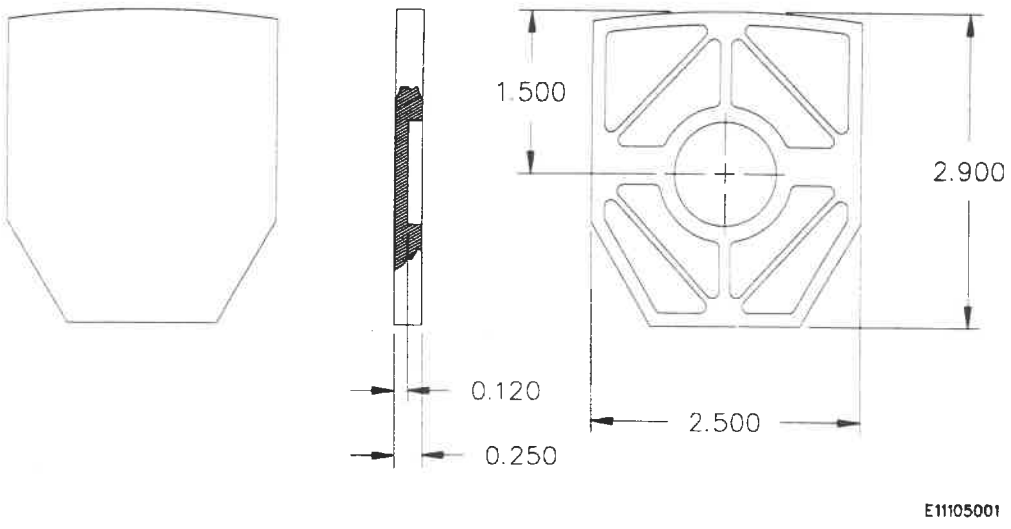

Figure 1. Mirror Geometry

AN ATHERMALIZATION MIRROR?

Although further thermal cycling of the mirror did not permanently affect the optical surface figure, it is interesting to note how changes in temperature affect the mirror. At approximately 200°F, the mirror deformed to approximately 15 fringes of convex power (Figure 8). On return to room temperature, the figure of the mirror returned to the approximately 1-fringe convex figure (Figure 9). Cycling the mirror to 5°F caused the figure to become concave by approximately 12 fringes (Figure 10). Again, the figure returned to the approximately 1-fringe convex condition after room temperature stabilization. Surface figure changes are summarized in Table 2.

TABLE 2. MIRROR SURFACE FIGURE

	Spherical power (fringe)	Irregularity (fringe)
Before thermal cycling	0.89 concave	0.64
After thermal cycling	>10 concave	N/A
After re-diamond machining	0.11 convex	0.45
After thermal cycling	0.61 concave	0.39
After enhanced gold coating	1.25 convex	1.17
At approximately 200°F	15 convex	N/A
After 200°F	1.11 convex	0.84
At approximately 5°F	12 concave	N/A
After 5°F	0.94 convex	0.93

Note: Measured with Zygo Mark II interferometer

Consider the case of an optical system for use in an environment where the temperature approaches 150° to 200°F (supersonic speed, a tank in the desert sun, etc.). Such a system expands at rates that depend on the material properties and geometry of the system. In most cases, the image plane (detector) shifts away from the system's optical elements. Many passive and active athermalization designs have been incorporated into systems to ensure that focus and image size on the detector remain constant over such temperature changes. The enhanced gold mirror might be considered as a passive athermalization element: at increased temperature, the mirror deformed convex with very spherical power. This would tend to shift the image toward the detector plane (or expand the size), thus counteracting the temperature effects. Because the mirror deforms concave at reduced temperatures (Figure 10), the desired effect is accomplished. It is important to remember that athermalization is wavelength-dependent (a system can only be athermalized at one wavelength). This mirror was tested in the visible (HeNe, 0.633 μm) but the effects of the power changes will be felt in the infrared wavelengths (7.6 to 11.9 μm).

One major disadvantage of the mirror for athermalization use is the elliptical-shaped optical "foot-print" created when a front surface reflective mirror is used at a 45-degree angle of incidence. This elliptical effect will introduce astigmatism on the

PROCESSING

The mirror was single-point diamond machined before nickel plating to limit material removal rates of the nickel plating in subsequent diamond-point machining operations. Surface figure at this operation was held to less than 2 fringes (1 wavelength) spherical power and 1 fringe (0.5 wavelength) irregularity. The diamond machining process produces a slightly concave part because the tool-holding spindle tilts with respect to the traverse axis to ensure that the tool does not interfere with the part at the back of the tool's rotational path.

The surface finish of the mirror was not measured at this time but could be expected (from statistical data) to be from 0.3- to 0.4-microinch RMS. The major contributor to the roughness of the unplated aluminum mirror is material defects such as iron and silicon nodules and precipitation hardening grain boundaries (minor differences in elastic moduli). Process related parameters are not significant contributors. This conclusion was reached after using identical machining parameters for a microscopic comparison of the surface finish obtained on the diamond-machined nickel-plated mirror and the surface finish obtained on the 6061 aluminum substrate. The characteristic diamond tool marks (cusps) add to the surface roughness of the electroless nickel mirror when compared to polished samples (Table 1), but the surface of the nickel is much "cleaner" because there are no point defects, which are seen on aluminum (Figure 2).

TABLE 1. RMS SURFACE ROUGHNESS

Polished electroless nickel	0.14 microinch
Diamond-machined electroless nickel	0.21 microinch
Diamond-machined 6061-T6 aluminum	0.38 microinch

Note: Average of five 20× objective Wyko 2D measurements

After diamond machining of the blank, the mirror was completely electroless nickel plated using a Niclad 1000 bath of approximately 10-percent phosphorous to a thickness of approximately 0.003 inch. The surface figure was distorted and had a general concave figure. The mirror was again diamond-point machined to 0.89 fringe concave power and 0.64 fringe irregularity (Figure 3). On thermal cycling to 350°F for 1 hour and back to room temperature, the surface figure "sprang" to approximately 10 fringes of spherical power due to release of plating stresses in the mirror (Figure 4). Subsequent diamond machining of the mirror with minimum material removal (0.0002 in.) returned the mirror to optical specifications. Additional thermal cycling of the mirror had little effect on the surface figure of the mirror (Figures 5 and 6).

The enhanced gold coating process contains a dielectric layer which adds compressive stresses to the surface of the mirror. After coating, the surface figure went from approximately 0.6 fringe concave to 1.25 fringes convex due to these compressive stresses. The irregularity of the mirror increased to approximately 1.2 fringes (Figure 7).

ELECTROLESS NICKEL PLATING FOR ENHANCED GOLD COATING: A LESSON IN BIMETALICS

Steven Scott
Member, Group Technical Staff
Texas Instruments Incorporated
Dallas, Texas

Abstract

A single-point diamond machining process has been developed to obtain optical quality surface characteristics at room temperature using a lightweight aluminum mirror plated with electroless nickel. The nickel is required for adhesion of an enhanced (greater than 99-percent average reflectance from 7.6 to 11.9 μm at 12- and 45-degree angles of incidence) gold reflective coating for infrared applications. This paper describes the geometry and optical specifications of the aluminum mirror, the process used to obtain a stable mirror (at room temperature), the optical figure changes caused by the enhanced gold coating, and the effects of temperature variations on the optical figure of the finished mirror.

BACKGROUND

Requirements for optical coatings on front surface reflective mirrors often include adhesion, hardness, humidity, and salt fog testing in addition to the minimum reflectivity requirement. Evaporated gold coating gives greater than 99-percent average reflectivity over the 7.6- to 11.9-μm wavelengths at 12- and 45-degree angles of incidence. This coating does not usually perform well when tested for hardness, adhesion, and environmental effects. An electroless nickel plating was applied to an aluminum substrate to improve the environmental performance of the enhanced gold coating. Electroless nickel plating was chosen because of its uniform thickness and relative ease of application, and because it contains fewer inherent flaws than electrolytic nickel.[1]

The differing thermal coefficients of the aluminum substrate and the electroless nickel plating (13.1E−06 in./in./°F versus 7.2 to 8.0E−06 in./in./°F, respectively)[2] cause stress-related problems during the nickel plating process[3] which require subsequent stress relieving steps in the fabrication process. Also, to minimize bimetallic effects of temperature variations after final figuring of the mirror, the entire mirror was electroless nickel plated.

MIRROR GEOMETRY

The mirror for this study was machined from 6061 T6 aluminum alloy. The webbing in the back of the mirror left a nominal 0.120 inch of material for the mirror surface (Figure 1). The final mirror surface was to be flat to less than 4 fringes (2 wavelength of 0.633 μm HeNe laser) spherical power and 1 fringe (0.5-wavelength) irregularity. The surface finish requirement for the mirror was to be less than 2 microinches RMS because of its infrared application.

The aluminas in conjunction with the flocked or felt polishing pads eroded down the sides of the voids and made them flair out like funnels so the amount of surface area affected by the void was 10 to 100 time greater than that present after polishing with the diamond. We surmise that the aluminas polish in a 3 body mode and are not firmly locked into or attached to the fibers of the flocked polishing pad.

Other barriers to a finely polished surface are gross defects, particularly voids that go down to the substrate and are filled with some sort of hard core. This core can be removed by even the softest polishing pad and severely scratch the surface. It is not clear whether it is the hardness of the core or its size that creates the problem, but we have found that almost every large void that goes down to the substrate will produce a single large scratch that originates at the void. The particle generally breaks down rapidly or is wiped off of the lap by the edge of the work and does no further damage but the initial scratch tends to be so large that it becomes the worst (or most easily visible) defect on the surface. It is very difficult to remove this type of defect with out taking so much material off that the overall figure of the work is affected.

Another type of defect that is troublesome is a blister if it is too large. The blister will then lift the lap up off the surface and thus create a local high around the blister even though the very top of the blister is being worked aggressively by the polishing process. There is the likelihood, because a large area defect has been created, that it will affect the figure or longer spatial wavelength errors on the surface.

This gives a few of the initial observations on the polishing of e-nickel and will hopefully be useful to either the opticians responsible for such polishing and/or to the engineers who have to deal with the problem of improving a diamond turned surface until it meets performance requirements. We plan to update the results of this work as we progress with our experiments into the effects of other lap and lubricant materials and lap sizes.

also good at removing the crystalline surface structure that sometimes comes through the e-nickel plating as the result of etching prior to plating. Also, if the substrate is diamond turned before the e-nickel plating as is often desirable to increase the single point diamond tool life, even the best e-nickel plating tends to have microscopic bubbles (or what appear to be bubbles) on the surface. This may be a residual of the actual e-nickel growth process, but for optical applications it tends to give the plated surface a slightly dull or "grey" look that causes wide angle scatter. Again, a light post polish with submicron sized diamond can restore the full brightness of the surface.

On the subject of diamond size, we have found that with the Pellon lap and the loads we are using, that 3 micron diamond, while it makes things happen fast, is too aggressive for use on critical optics. Even 1 micron may be too large because it will leave definite individual scratch marks from the diamond particles that can be easily seen with a 40x Nomarski microscope objective, a sure sign that the surface is not a low scatter one. For the smoothest surfaces, it is necessary to use sub-micron diamond but of course the removal of surface defects is much slower.

If the surface has voids, there may be no choice but to use the sub-micron diamond for the whole job because if the larger diamond gets caught in pits on the surface and then not flushed out during cleaning, traces of the larger diamond will remain after going to the finer diamond. If the surface is free of all but superficial voids, then polishing can begin with 1 micron diamond and a switch made to submicron after a thorough cleaning of the surface, and edges of the part. Of course, a new lap will be needed for the finer diamond.

Another observation has been that the fine alumina polishing compounds do not work well, at least when used with flocked polishing pads. We attempted to 'brighten' up surfaces polished with both 1 micron and 1/4 micron diamond by using both Linde A (0.1 micron nominal particle size) and Linde B (0.03 microns). In both cases, just a few minutes polishing made both surfaces drastically worse. Most obvious were voids that the alumina compounds both deepened and widened to the point that they were easily visible to the unaided eye. These were voids that were 10 to 20 microns in diameter that the diamond had not polished to the bottom of but that still had clean sides that were perpendicular to the polished surface.

length of travel of a diamond on a polishing pad used to remove the diamond turning marks is on the same order as the travel of the tool used to cut the surface.

Using this lap construction, a load of about 100 gm/cm^2 (about 1.4 psi) and a velocity of 0.1 m/sec, we have observed that the diamond acts like a miniature single point tools, that the nickel removal is ductile and only the highest features on the surface are removed. The height discrimination is not a step function, but it is easily shown that 80% of the 1 micron diamonds used would discriminate between closely spaced (100 micron separation) features that differed in height by 0.05 microns. There is also some evidence that only the larger diamond do ductile removal and that some of the smaller diamonds may simply compact the surface. This observation is based on optical microscopy and must be confirmed by some SEM work. If this is the case, it may explain why we can produce surfaces with finishes of 0.2 nm rms using 0.1 or 0.25 micron diamond.

Virtually all the evidence we have to date shows the diamond particles are firmly socketed in the Pellon and do not move when the diamond encounters a void such as a bubble. The clearly defined groove of the diamond including intra groove features due to the multiple facets of the diamond particle are exactly reproduced when the diamond starts cutting again on the other side of the void. There is no evidence of chatter or movement of the diamond. Further, the cut marks on either side of the void are completely clean, no material is pushed into the void or thrown onto the shoulders of the cut on the far side of the void.

This observation is also borne out be an examination of the swarf from the polishing. We have not observed curled chips but rather what looks like particles to the level of resolution of the optical microscope. Even cursory SEM examination of the swarf did not show curled chips but rather particles as though the amorphous electroless nickel was removed as a powder.

Because of the excellent height discrimination of the diamond polishing, many types of surface texture problems can be corrected by diamond post polishing. The technique is obviously well suited to the removal of diamond feed marks left over from diamond turning, whether the substrate was diamond turned before e-nickel plating or after. Post polishing is

Observations on polishing electroless nickel plated surfaces

Robert E. Parks
University of Arizona
Chris J. Evans
National Institute of Standards and Technology

It is the objective of our work to learn how the post polishing of diamond turned surfaces can be most effectively accomplished. In many cases, particularly for 2 axis cuts, post polishing can remove residual, high spatial frequency surface errors without affecting the overall contour or figure of the machined surface. Ideally, one would like only to remove those errors that affect the function of the surface and not degrade the surface in the spatial wavelength regions where there are no significant errors.

This suggests that it would be desirable to establish how well certain polishing lap sizes and constructions affect the removal of errors of particular spatial frequencies. Our goal, in fact, is to determine a "transfer function" for the post polishing process as a function of polishing lap size and hardness. There is already a theoretical basis for this idea of a transfer function associated with the polishing lap and it is becoming common to specify sophisticated optical systems in terms of a power spectral density of surface errors.

We are at the very beginning of this work but have already made some significant observations about the polishing process. It is these preliminary observations that we wish to convey in the paper. Because these are preliminary observations, it is not yet clear which aspects of post polishing are most important, so we more or less just list these observations. The ordering here does not infer significance. We will start however, by giving the parameters of the polishing to date because that carries through all the work presented here.

Largely because we have found it works well, we have so far limited our polishing laps to medium hardness (Gogalz 73) pitch covered with a single layer of self adhesive Pellon, a nonwoven fabric used as a stiffener in clothes making but adapted as a polishing media. We have used paste diamond compound in a medium concentration and used the "extender" supplied with the diamond as the lubricant. The extender slightly dissolves the pitch but the Pellon appears to be impervious to the extender so this is not much of a problem. The diamond paste is used very sparingly because it seems to keep on cutting well without the addition of more paste. The

Distribution:

American Society for Precision Engineering

Erika Deutsch-Layne

Oak Ridge Y-12 Plant

H. L. Gerth
J. E. Keyes (2)
R. D. Mikkola (2)
R. C. Waldrop
Y-12 Central Files (RC)

The procedure to gold plate onto the aluminum substrates includes the following steps;

* Clean
    * non-etch caustic cleaner
* Deoxidize:
    * 66 vol% nitric acid (63 wt%) + 2 vol% hydrofluoric acid (48 wt %)
* Zincate:
    * 13 oz/gal zinc oxide, 70 oz/gal sodium hydroxide, 13 oz/gal ferric chloride, + 1.3 oz/gal Rochelle salt
* Copper Cyanide Strike
    * deposit approximately 0.1-0.2 mil
* Gold Plate:
    * approximately 20 mils thick

The use of hardened gold allowed conventional machining parameters to be used. Parameters very close to the ones used for machining aluminum were found to be acceptable. The tool rake angle was increased to -1 ° as is conventionally used with other materials (Figure 2). Several plated gold mirrors having a 0.3 meter (12 in.) diameter were machined. Results were good when the hardness of the gold deposit was above 100 Knoop. Virtually no tool wear was experienced when the harder gold was machined. In fact the same tool edge was used for all the roughing as was used for the finish passes.

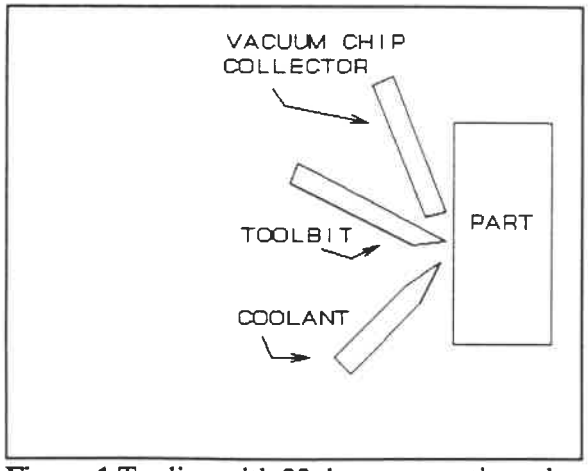

Figure 1.Tooling with 33 degree negative rake.

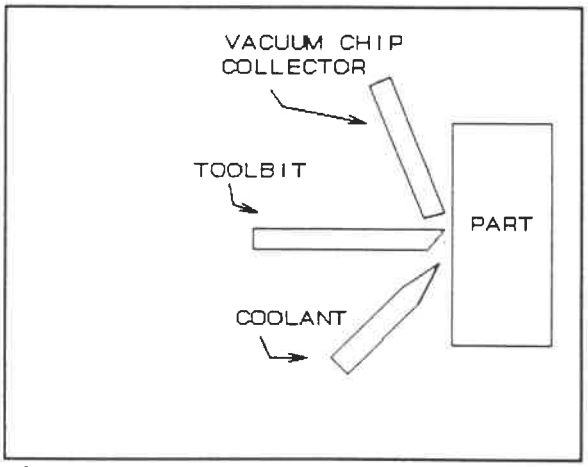

Figure 2.Tooling with 1 degree negative rake.

Inspection of all machined surfaces was accomplished by using a Tinsley unequal path interferometer operating at a wavelength of 6328 Å. All inspections were done on an 8.6 meter (28-ft) vibration-isolated inspection table. The machining process produced mirrors with a total contour error of approximately 1.3μm peak-to-valley.

and temperature while raising the current density will produce deposits of greater hardness. These efforts did indicate an increase in the deposit hardness but not sufficient to produce the required results. Experimentation with a cobalt additive developed at Y-12 eventually led to gold deposits of sufficient hardness that produced a high quality diamond machined part. Table 1 lists the effects of the cobalt additive on the deposit hardness.

TABLE 1. ADDITIVE EFFECTS ON DEPOSIT HARDNESS

Co IN BATH	Co IN DEPOSIT	HARDNESS
NONE	NONE	45-50 KNOOP
160 PPM	NONE	80-100 KNOOP
200 PPM	NONE	80-100 KNOOP
400 PPM	20-35 PPM	90-125 KNOOP

Table 2 lists the makeup for the gold plating bath for depositing gold of approximately 100 Knoop hardness, which is sufficient to permit diamond machining of optical quality on large substrates.

TABLE 2. GOLD BATH MAKEUP

	CONCENTRATION
GOLD (AS METAL)	0.5-0.7 TR OZ/GAL
PHOSPHONIC ACID	200 GRAMS/GAL
POTASSIUM HYDROXIDE	0.25 GM/GM PHOSPHONIC ACID
COBALT ADDITIVE	400 PPM Co
TEMPERATURE	140 DEG F
Ph	3.7 OPTIMUM
CURRENT DENSITY	3 AMPS/FT^2

THICK GOLD PLATING FOR OPTICAL SURFACES

R. D. Mikkola, R. C. Waldrop, H. L. Gerth

Oak Ridge Y-12 Plant*
Martin Marietta Energy Systems, Inc.
Oak Ridge, Tennessee, 37831

The Oak Ridge Y-12 Plant has developed capabilities for machining electroplated surfaces of sufficient quality to serve as optical reflectors in the as-machined condition. This quality of machined surface is obtained by using special, high precision machine tools and tool bits that are ground from single crystal diamond. This diamond machining procedure is applicable to most materials having face-centered cubic grain structure (Al, Ag, Cu, Au, etc). The process becomes very economical when large sizes are required or when aspheric surfaces are required.

This procedure was recently used to manufacture high precision reflective mirrors approaching 3.6-m (4-ft) in diameter. The machined surface was to be of electroplated gold having a finished thickness of 250 μm (0.010-in) on a 6061-T6 aluminum alloy substrate. During the preproduction test machining of 30.5-cm (12-in) diameter parts, considerable wear of the diamond tool was experienced. Wearing of the tool began to degrade the surface finish after about 260-cm^2 (40-in^2) was machined. A search of applicable literature and conversations with experts in the field revealed that virtually all experience with this material had been with samples of 50-cm^2 (8-in^2) or less. As a result, the tool wear associated with this material was undiscovered.

Initial efforts to solve the tool wear problems involved the search for machining parameters that would reduce or eliminate the wear. It was quickly discovered that tool wear was not affected by the tool feedrate, tool radius, or the surface feet per minute. Numerous coolants were evaluated without any improvement. Several tests were conducted to optimize the configurations for applying the coolant and removing chips. The only noticeable improvement occurred when a high negative rake was used with a large stream of coolant and vacuum chip collection from above the tool. A 400-500 percent reduction in tool wear was accomplished with a rake of -33° (Figure 1). This was not enough improvement to make the required high quality machined parts. Observations of the machining process and chip formation indicated that the chips were extremely ductile and were hanging or welding onto the edge of the tool. Once there, the chip would scratch the newly machined surface. This indicated that it was not feasible to use a soft gold (45-50 knoop) for this application.

Development studies involving methods to increase the hardness of the gold electrodeposit included adjusting the plating parameters; pH, current density, and temperature. Generally, lowering the pH

*Managed for the U.S. Department of Energy by Martin Marietta Energy Systems, Inc. Under Contract DE-AC05-84OR21400.

OPTICS FOR SYNCHROTRON RADIATION: A USER'S PERSPECTIVE*

Wayne R. McKinney
Accelerator and Fusion Research Division
Lawrence Berkeley Laboratory
Berkeley, CA 94720

The nature and differences between the three types of synchrotron radiation source were discussed. Bending magnet sources have a broad continuous spectrum. Wiggler and undulator sources have narrower bandwidth radiation, and have less angular extent. They differ in the strength of their magnetic field, and the coherence of the emitted radiation. The physical plant of the Advanced Light Source was shown, and photographs were presented showing the present state of construction of the magnetic structures and vacuum vessel.

An optical diagram showed the design of the LBL 55 meter spherical grating monochromator at Stanford Synchrotron Radiation Laboratory. This monochromator serves as the prototype of the two monochromators that will be built as part of the two proposed project beamlines. The salient features of this design were presented by discussion and photographs, including the water cooled grating carriage. Next a 15 inch long water cooled mirror for the ALS was shown. This mirror is a brazed assembly of Glidcop, an alumina dispersion strengthened OFHC copper alloy.

This technology, together with electroless nickel as the polishable layer was chosen because finite element calculations showed that side cooling of regular glass optics would not maintain the necessary optical figure tolerances for the Advanced Light Source. The required optical specifications were reviewed, and typical data were presented both from older optics that did not meet specification, and prototypes from the ALS optical component development program.

This data showed the acute need for precise optical metrology at all spatial wavelengths of surface shape. Our program uses a microprofiler (WYKO or equivalent) to measure spatial wavelengths of 5 mm or less, and an improved model of the long trace profiler of Peter Takacs at Brookhaven National Laboratory to measure the longer spatial wavelengths from 5 mm up to the length of the optic. We have constructed two of these instruments and have installed one of them at Tucson Optical Research Corp. so that the optical finisher can have direct feedback about the efficacy of the polishing methods during fabrication. This feedback is essential for the fabrication of the mirrors and grating substrates for the Advanced Light Source.

* This work was supported by the Director, Office of Energy Research, Office of Basic Energy Sciences, Materials Sciences Division of the U.S. Department of Energy, under Contract No. DE-AC03-76SF00098.

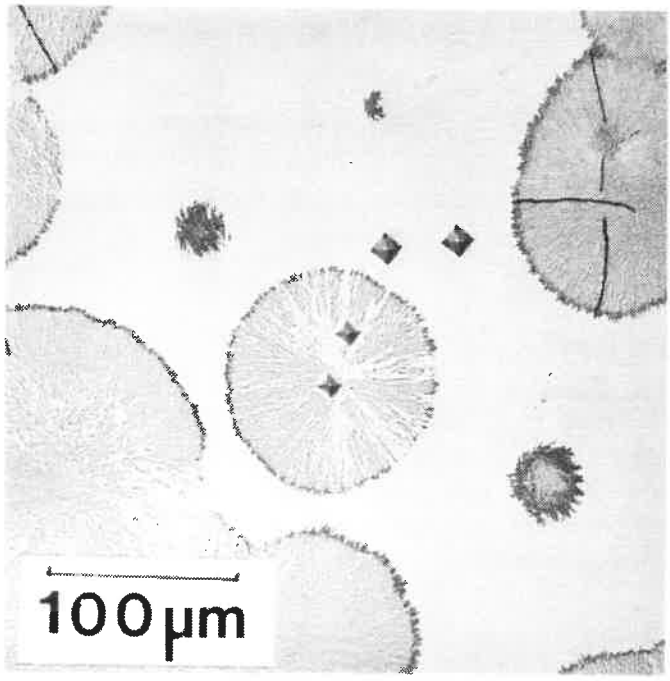

Fig. 4 Rosettes formed by partial crystallization of amorphous NiP when heated to 265°C for 2 h.

Fig. 5 Micrograph of surface of diamond-turned aluminum deposited at 1 A/dm^2 with a 10 percent duty cycle. Plating thickness before machining was 75 µm.

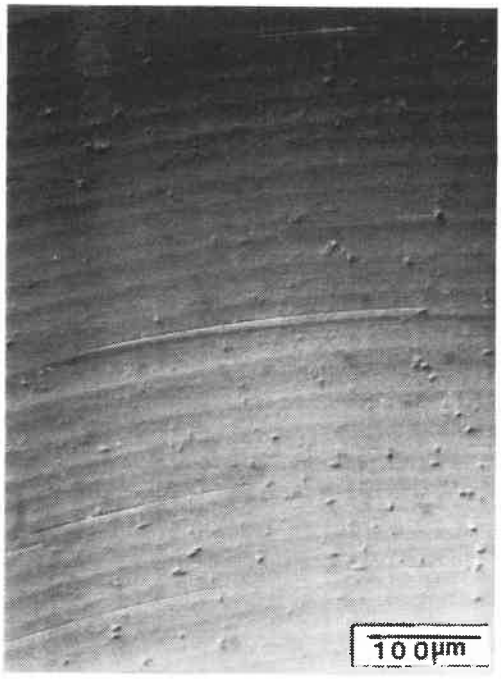

Fig. 6 Micrograph of surface of diamond-turned commercial-grade aluminum. Pits are probably result of removal of inclusions in aluminum alloy.

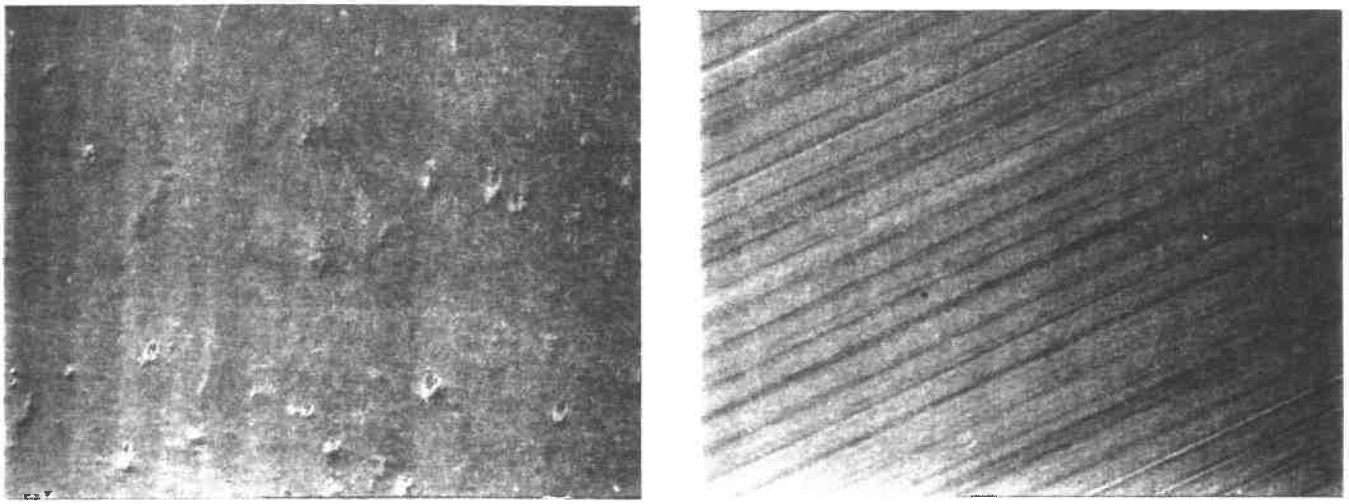

E11105002

Figure 2. 6061 Aluminum Versus Electroless Nickel Diamond Machined (Enlarged 200×)

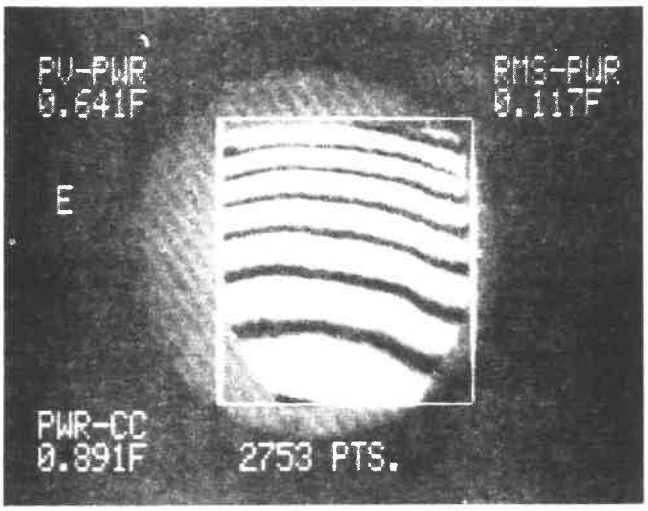

E11105003

Figure 3. Diamond-Machined Mirror

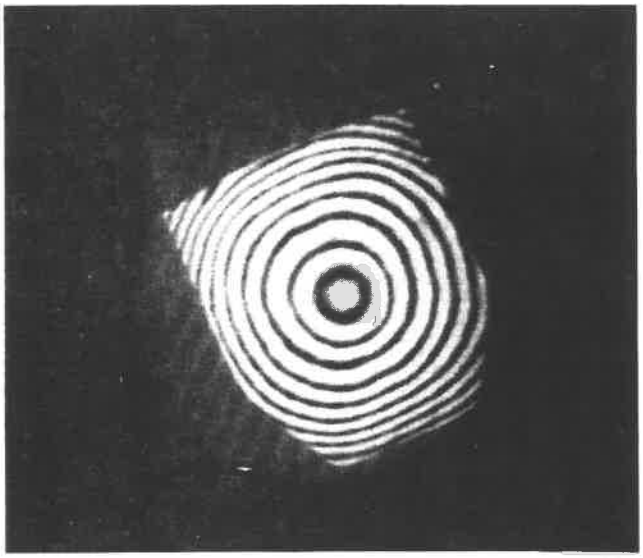

E11105004

Figure 4. Mirror After First Thermal Cycle

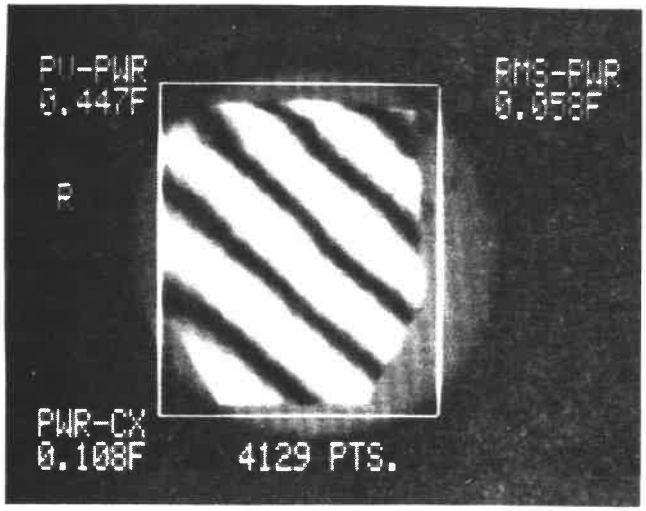

Figure 5. Re-Machined Mirror

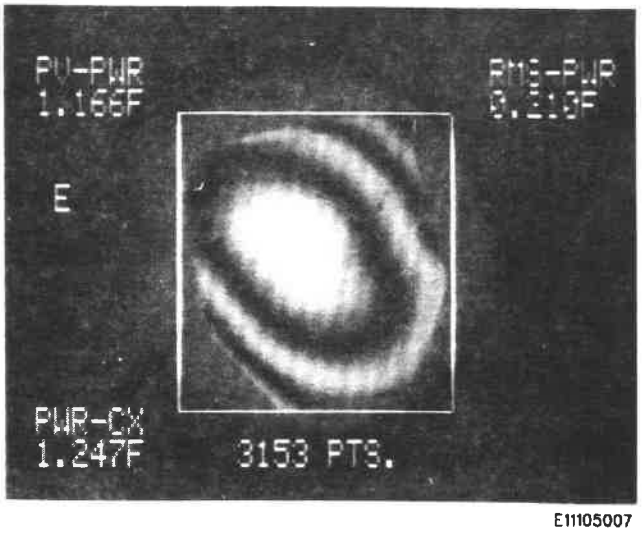

Figure 7. After Enhanced Gold Coating

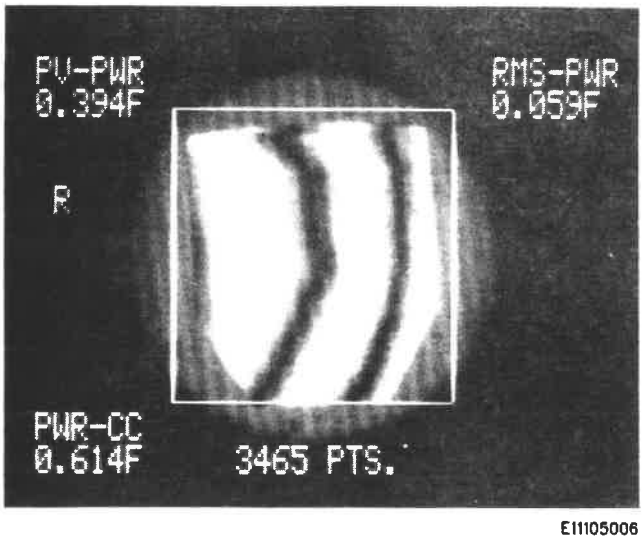

Figure 6. After Re-Thermal Cycling

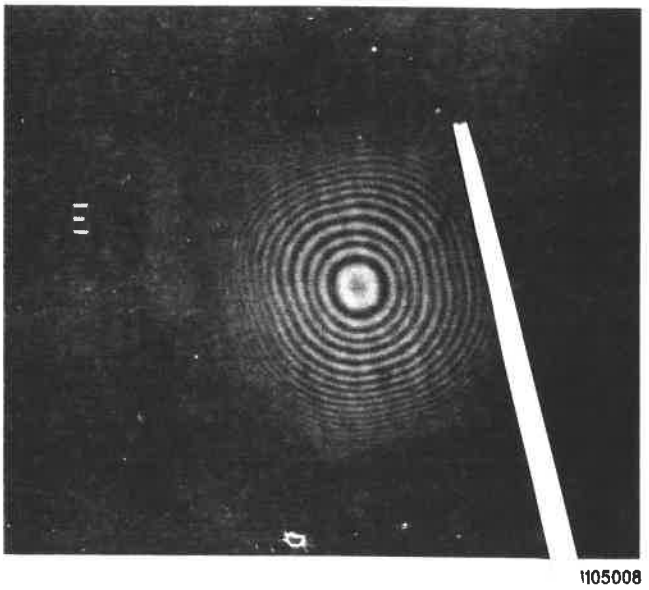

Figure 8. At Approximately 200°F

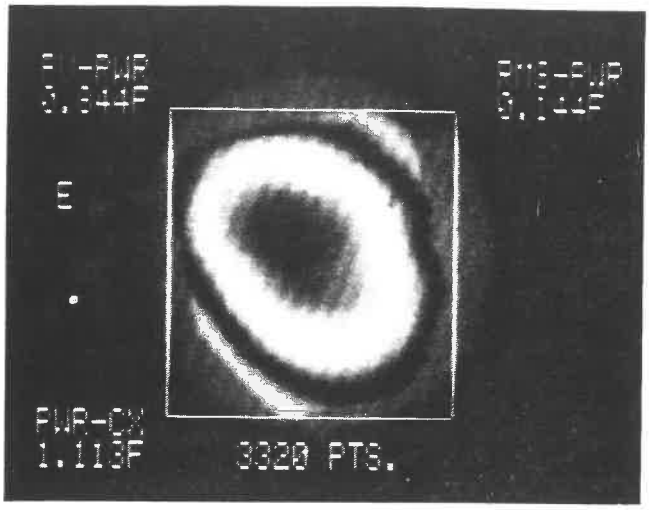

E11105009

Figure 9. At Room Temperature

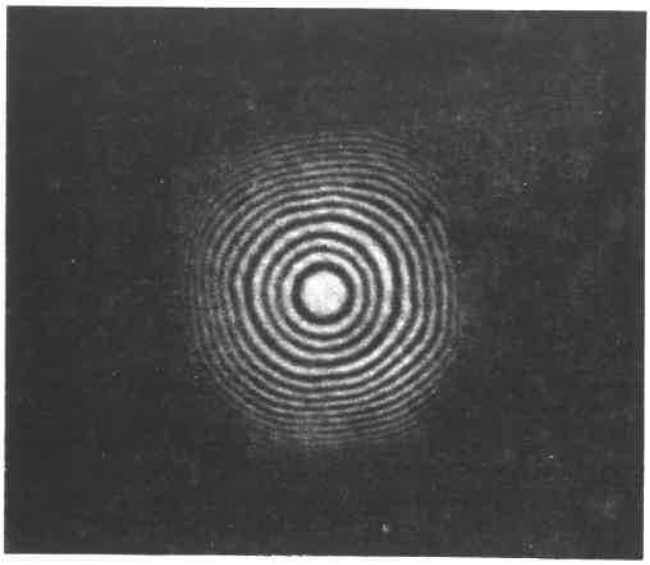

E11105010

Figure 10. At Approximately 5°F

DESIGN OF ARTICLES TO BE ELECTROPLATED AND ELECTROFORMED

R. Schneck and J. Margolin
Metal Surfaces, Inc.
Bell Gardens, CA

The purpose of these guidelines is to assist in understanding the limits of electroplating and electroforming. These limits, if understood and applied, will yield plated products that perform as they are expected to. Often, after a part is plated, someone will ask "what was the plater thinking of when he plated this?".

If discussions between the purchasing agent, the engineer requesting the plating and the plater occur before the work is started, the parts will look and perform as they were designed. This is also the time to consider the limitations of the particular plating process and limit the effect to the end product. Occasionally, you will even prevent parts from being designed and manufactured that can't be plated at all.

Design Considerations

When an article is electroplated, it is processed through a series of tanks containing cleaners to remove soils and oils. Then various acids are used to remove oxides on the metal surfaces, leaving the metal ready to accept the deposit. The part is then placed in the proper plating tank and the electro chemical process of plating begins.

As the direct current is applied electrically, flux fields are set up in the plating tank. Because the current tends to follow the path of least resistance, the edges and ends of a part will receive the greatest deposit thickness. Recesses, inside corners and holes will be thinner. On outside diameter threads, the major diameter receives the thickest deposit and the minor diameter the thinnest, while the pitch diameter will receive the average.

When a flat or cylindrical part is plated, the thinnest deposit will be in the center and, as a rule, will require one and a half the calculated time to plate (amp/minute).

With a part that has a sharp 90 degree angle, or flange, two times the plating time (amp/minute) will get the minimum thickness in the corner. This is only true when the corner has a radius equal to or greater than the plating thickness.

Deep holes and recesses create the biggest challenge to a plater. As the edges build up, the hole or recess closes and becomes even more inefficent. This means three to four

times the plating time (amp/minute) is required to get the minimum deposit thickness. Often a machine operation is required to reopen the recess, hole or groove. A second plating operation is used to achieve the required deposit thickness.

Because sharp edges draw current and build up extra thickness, this robs the metal from adjoining areas. Acute angles, tubular parts and blind holes present the same problem and, in some cases, little or no coverage is possible. Countersinks, or a radius, can lessen the effect in the case of a hole.

Point Of Measure For Plating Thickness

Measurement points need to be determined with the function of the coating in mind. If the minimum thickness is required anywhere on the part, the cost can escalate. When plating precious metals, this quickly becomes obvious. Consider the above rules for plating thickness when estimating gold useage and you can see that two or three times the required gold could be needed to cover the part. However, if the functional thickness is near the outside edges, gold useage and price can be reduced.

Threaded Parts

A threaded part being plated to a thread gage requires special thickness adjustments due to the angles. Generally, 0.0001 inch of plating thickness will change the pitch diameter 0.0004 inch when measured with a thread gage.

Dissimilar Metals

Dissimilar metals in the item being plated often create assemblies that will not allow proper activation, causing adhesion failures.

Electrical Connection Points

In order to plate, electricity must pass from the power source to the part. This contact point will often make extremely thin marks or bare areas.

Solution Traps

Blind holes, rolled edges, bolted assemblies, seams, porous welds and other crevices will trap solution. This causes processing solutions to bleed out during or after plating. Bleed out poisons the plating or causes stains.

Large Heavy Parts

Large mass parts are hard to handle, displace process solutions, and rob heat from processing solutions. This cooling can cause rejects.

Liability

When a plater accepts a $100,000.00 part and charges you $300.00 to plate, it is not reasonable to expect him to accept liability for $100,000.00 if something goes wrong. The time to negotiate the liability is before you start the job. Liability is normally considered to be three times the cost of processing or the cost of the part, whichever is greater. On precious metal plated parts, the liability is somewhat less as the cost of metal is normally deducted prior to calculating any liability.

Selecting a Plating Source

When looking for a qualified plating source, many things come to mind. The first, and most important, is to ascertain that the plater has the equipment to do the job properly. In order to do that, it is imperative for your source man to visit the facility. That may sound like a very basic premise, but you would be amazed at how many hi-rel companies have never been inside their plater's facility. Visit, look carefully, ask for his QC manual, talk to the technical people, and make sure that the equipment is maintained and kept up-to-date. If someone tells you their shop is proprietary, chances are they are ashamed of it. In today's marketplace, few items are so unique that seeing them would enable you to pass vital information on to the competition. An area, maybe, the whole shop.....go somewhere else!

Okay, now you have gone and visited a number of shops and have qualified three sources for plating. Your purchasing agent has the information and is ready to place orders. Whom should he use?

It's easy now to look at pricing as the determining factor and, of course, while pricing is important, there are many other factors. How much extra does it cost if it doesn't get there on time? What if it isn't done right? Quality and service must be weighed into the equation. It is part of the cost of doing business. While this again appears basic, too often it is ignored.

Communication is the key. There must be trust and a mutual understanding between customer and vendor. If your company has plating requirements for many part numbers, chances are there will be differences in pricing between your vendors. If you always go to the low bidder, something has to give. Your perception as a major customer may suffer, and that could hurt when you are in a hurry or need something special. Keep your sources honest by being price conscious and aware of what is going on in your industry. Look at the company that is willing to go the extra mile, rushes your parts when you need them, gives advice on how to do it better, and has an open door policy. It will make your job a lot easier.

Again, we cannot emphasize enough how important it is to meet with the plater during the design stage.

Hopefully, the above information can help you get started in reaching a good working relationship with your plating sources. The image of our industry has not been the best at times, but most of us are working hard to change that. The demands of modern industry and a growing understanding of SPC requirements are causing many small shops to fail. Look for a smaller, more efficient group of survivors in the future.

Paper presented at: ASPE Spring Topical Meeting "Metal Platings for Precision Finishing Operations", 15-18 April 1991, Tucson, AZ

Figure and Finish Characterization of High Performance Metal Mirrors

Peter Z. Takacs
Brookhaven National Laboratory

Eugene L. Church
USA ARDEC

Most metal mirrors currently used in synchrotron radiation (SR) beam lines to reflect soft x-rays are made of electroless nickel plate on an aluminum substrate. This material combination has allowed optical designers to incorporate exotic cylindrical aspheres into grazing incidence x-ray beam-handling systems by taking advantage of single-point diamond machining techniques. But the promise of high-quality electroless nickel surfaces has generally exceeded the performance. We will examine the evolution of electroless nickel surfaces through a study of the quality of mirrors delivered for use at the National Synchrotron Light Source over the past 7 years. We have developed techniques to assess surface quality based on the measurement of surface roughness and figure errors with optical profiling instruments. It is instructive to see how the quality of the surface is related to the complexity of the machine operations required to produce it.

SURFACE ROUGHNESS

Surface roughness is of supreme importance to users of SR beamlines - roughness levels above 10 Angstroms scatter excessive amounts of x-rays incident at grazing incidence. A revolution in roughness measurement instrumentation occurred early in the 1980's with the application of phase-measuring interferometry to microroughness measurement by non-contact optical methods. The microinterferometer quickly became the instrument of choice to characterize large aspheric SR mirrors. These mirrors are often in the shape of segments of cylinders up to 1 meter in length with minor radii in the order of several centimeters, bent slightly in the longitudinal direction into toroidal shapes with major radii in the range of hundreds of meters to several kilometers. It is extremely difficult to measure the surface quality of such large mirrors with stylus instruments, but it is very easy with optical interferometers. We began making measurements in 1984 on a variety of mirror shapes, sizes and substrate materials. It quickly became apparent to us that there was a distinct difference between the quality of electroless nickel surfaces and glass/ceramic/fused silica surfaces. A summary of the roughness measurements on flat mirrors is presented in the first two figures[1]. One can see that most of the roughness values for the glass mirrors lie below the 10Å level, while most of the values for the ENP material lie above the 10Å level. This same pattern holds for roughness measurements made on aspheric mirrors - cylinders and paraboloids, for example. The ultimate smoothness of the surface microroughness is not related to the overall figure of the mirror. The reasons for this pattern are not clear. One can speculate on a number of possible explanations - the ENP material is softer than glass/ceramics, improper polishing compound chemistry, non-optimized grain structure in the ENP material, etc. - but a definitive answer has yet to be proffered.

Microinterferometry is also useful as a diagnostic tool to evaluate the performance of precision machining operations. Figure 3 shows a surface profile measurement from an off-axis paraboloid (P1) that has been precision machined with a diamond tool in electroless nickel on an aluminum substrate. One can easily see large amplitude, periodic errors in the surface profile

caused by insufficient control of the machine parameters. Contrast this to the profile in Figure 4 of a similar paraboloid (P2) made on the same machine at a different time - the large periodic fluctuations are not in evidence and the surface structure looks more random. More quantitative information about the surface structure can be obtained by computing the power spectrum of the surface roughness[2,3]. The power spectral density (PSD) curves for the two ENP paraboloids are shown in Figures 5 and 6. Both spectra are averages computed from profile measurements made over several regions of each surface. One can immediately see the spectral line in the P1 paraboloid corresponding to the distinct sinusoidal pattern evident in the profile. Also apparent are several higher frequency components, a broad base surrounding the fundamental spectral line, and a general power-law decrease at higher spatial frequencies. The spectrum of the P2 paraboloid does not show a distinct spectral line feature at low frequency but exhibits a power-law spectrum over more than two decades in spatial frequency with a characteristic -3/2 power slope. By integrating the area under each spectrum, one is able to compute the root mean square roughness over any desired spatial frequency bandwidth. The average roughness computed for the P1 paraboloid is about 310 Ångstroms, while the roughness of the P2 paraboloid is 91 Ångstroms. Analysis of PSD curves provides a wealth of information about surface quality and machine performance.

SURFACE FIGURE

Measurement of the "figure" of large grazing incidence mirrors is a particularly difficult task, since conventional interferometric measurement techniques are usually impossible to employ. We have developed a non-contact scanning profiling instrument, the Long Trace Profiler (LTP), which is optimized for measuring the quality of large cylindrical aspheres with sub-arc-second precision and accuracy[4]. The LTP uses a pencil-beam interferometer technique[5] to measure the local slope of the surface with 1mm sampling increments along the length. The LTP measurements overlap the long spatial period region of the microroughness measurement, providing a continuous spectrum of the roughness from micron spatial periods up to the 1 meter range. Roughness in the centimeter and meter spatial period range is traditionally called "figure error", but the distinction between the two concepts is merely an artifact of the traditional, mutually-exclusive measurement techniques previously used to make each measurement.

The same analysis techniques can be used to analyze LTP scans that are used to analyze microroughness measurements, i.e., the power spectrum of the "roughness". Figure 7 is an example of a composite spectrum of the departure from the ideal shape of a 700mm long cylinder mirror diamond-machined and then post-polished from a single-crystal silicon substrate. The right-hand curve segment was made with a WYKO NCP-1000 optical profiler with a 2.5X objective and covers the spatial period range from 5mm down to about 10 microns. The left-hand curve segment was made with the LTP and covers the spatial period range from 500mm down to 4mm. One can see how well the surface fits a power-law spectral model over 4 decades in spatial frequency. The large amplitude increase in the lowest spatial frequencies is caused by a height discontinuity of about 0.5 microns in the middle of the mirror, while the sharp spectral line at 20mm spatial period is caused by a sinusoidal error which has an RMS amplitude of about 23 Ångstroms with an equivalent maximum slope error of 1 arc second. Spectral analysis of the LTP data reveals a great deal about the nature of the machining and polishing processes and indicates ways that they could be improved.

Examples of LTP measurements on electroless nickel mirrors are shown in Figures 8 and 9. The first is a measurement of the surface of an off-axis paraboloid similar in construction to P1 and P2 but 3 times the length. One can see the large amplitude fluctuations in the central region of the mirror indicating a severe departure from the ideal shape. Also evident is the edge roll-off at the extreme ends and the trough and hill immediately preceding the edge roll-off. This signature is

common in most of the ENP mirrors that are post-polished after the precision machining step. The mirror in Figure 9 is an off-axis ellipsoid of more recent vintage with smaller amplitude errors in the central region. The RMS slope error for this mirror is about 3 arc seconds. This mirror is one of the early ellipsoids made by Carl Zeiss in Oberkochen for the SX-700 monochromator at BESSY in Berlin. More recent ellipsoids produced by Zeiss have RMS slope errors below 1 arc second, which has improved the performance of the monochromator significantly.

SUMMARY

High-performance mirrors made in the shape of segments of ellipsoids or paraboloids are extremely difficult to produce by conventional means. Only since the advent of precision diamond-turning machines has serious thought been given to such surfaces in optical systems, especially those designed for grazing incidence x-ray reflection. The new manufacturing techniques have required the development of new materials compatible with the diamond turning process. Electroless nickel has emerged as the leading candidate for precision optical surfaces, computer disks and other high technology items. It has been an often painful process to fabricate SR mirrors with the required accuracy using the new technologies. The development of metrology instrumentation that can make relevant measurements of surface finish and figure has enabled manufacturers to improve their processes and produce a much better electroless nickel product than possible a decade ago. The future should bring even more breakthroughs in the surface quality of electroless nickel parts.

REFERENCES

(1) P.Z. Takacs "Understanding the Performance of X-ray Mirrors" in Synchtotron Radiation in Structural Biology," R.Sweet and A. Woodhead eds. pp.303-316,Plenum (1989)

(2) E.L. Church and P.Z. Takacs "Use of an Optical Profiling Instrument for the Measurement of the Figure and Finish of Optical-quality Surfaces", Wear, vol. 109, 241-257 (1986)

(3) E.L. Church "Fractal Surface Finish", Applied Optics vol. 27, 1518-1526 (1988).

(4) P.Z. Takacs, K. Furenlid, R. DeBiasse, and E.L. Church, "Surface topography measurements over the 1 meter to 10 micrometer spatial period bandwidth", Proc. SPIE vol. 1164, "Surface Characterization and Testing II", J.E. Grievenkamp and M. Young, eds., p.203-211 (1989)

(5) K. von Bieren "Interferometry of wavefronts reflected off conical surfaces" Applied Optics vol. 22, 2109 (1983).

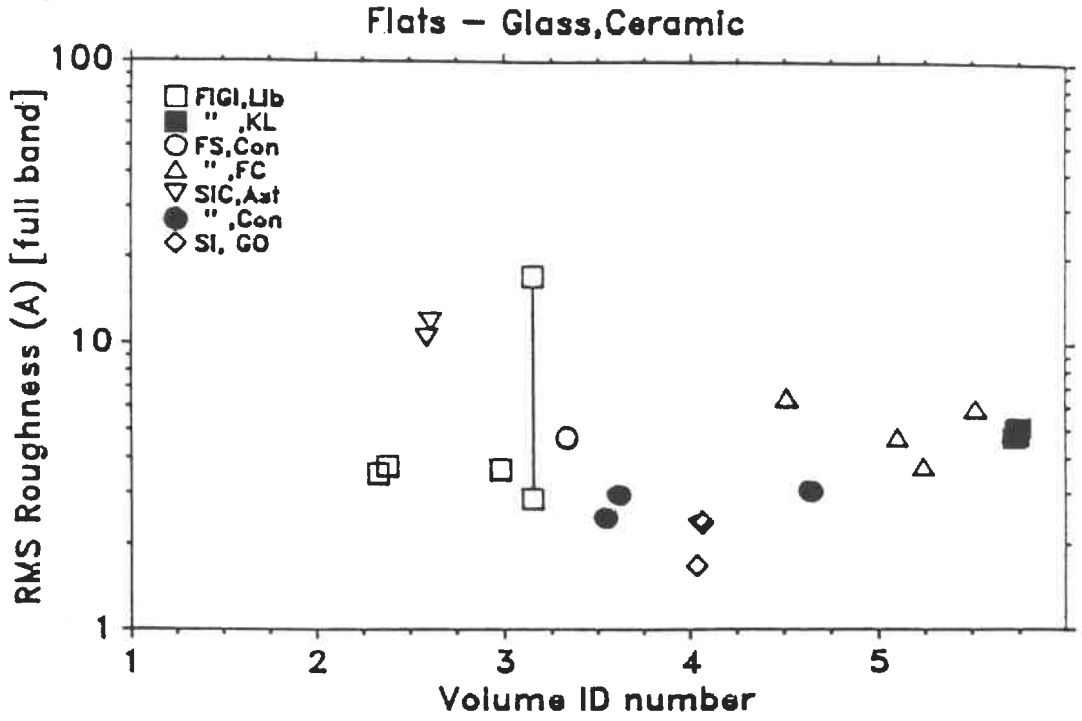

Figure 1 - Summary of surface roughness measurements made on glass, fused silica and ceramic flat mirrors with a WYKO NCP-1000 optical profiler with a 2.5X objective. The abscissa is roughly a time sequence starting in 1984 and ending in 1988. Most measurement values lie below the 10Å level for these materials.

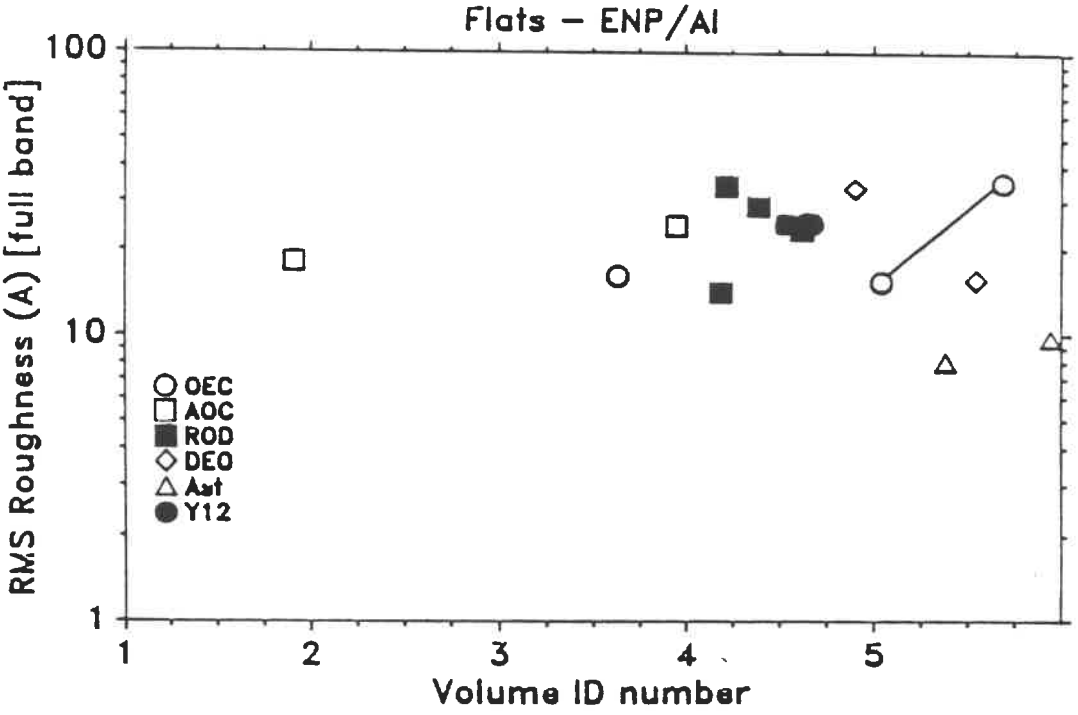

Figure 2 - Summary of surface roughness measurements as in Figure 1, but for electroless nickel coated flat mirrors, usually on an aluminum substrate. Notice that most of the measurements lie above the 10Å roughness level, in contrast to the glass results.

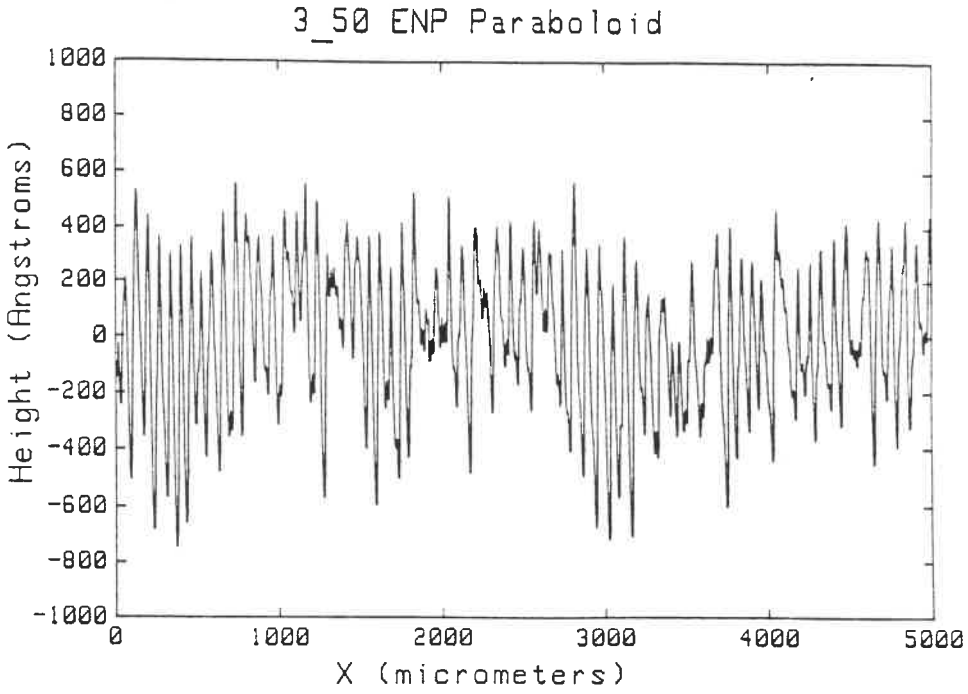

Figure 3 - Surface roughness measurement on an electroless nickel-plated paraboloid (P1) that was diamond machined in 1981. The large amplitude sinusoidal pattern indicates insufficient control of all the machine parameters during this run. It was not possible to remove the residual surface roughness by post polishing this surface.

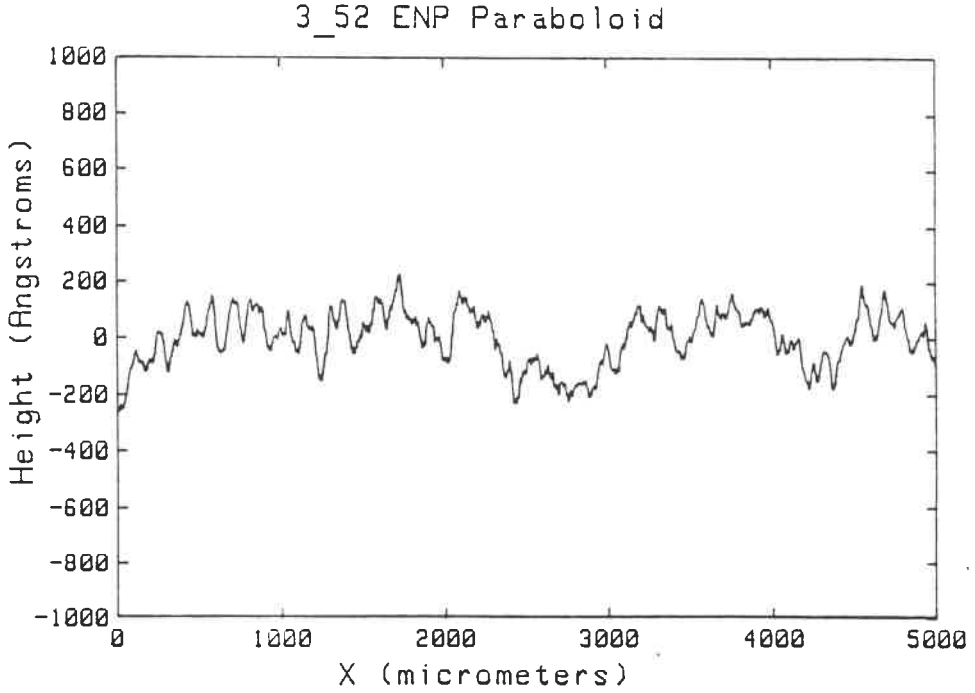

Figure 4 - Surface roughness measurement on a paraboloid (P2) with slightly different shape parameters from that in Figure 3, which was machined on a different day under different set-up conditions. The residual surface roughness is more random with a much lower amplitude.

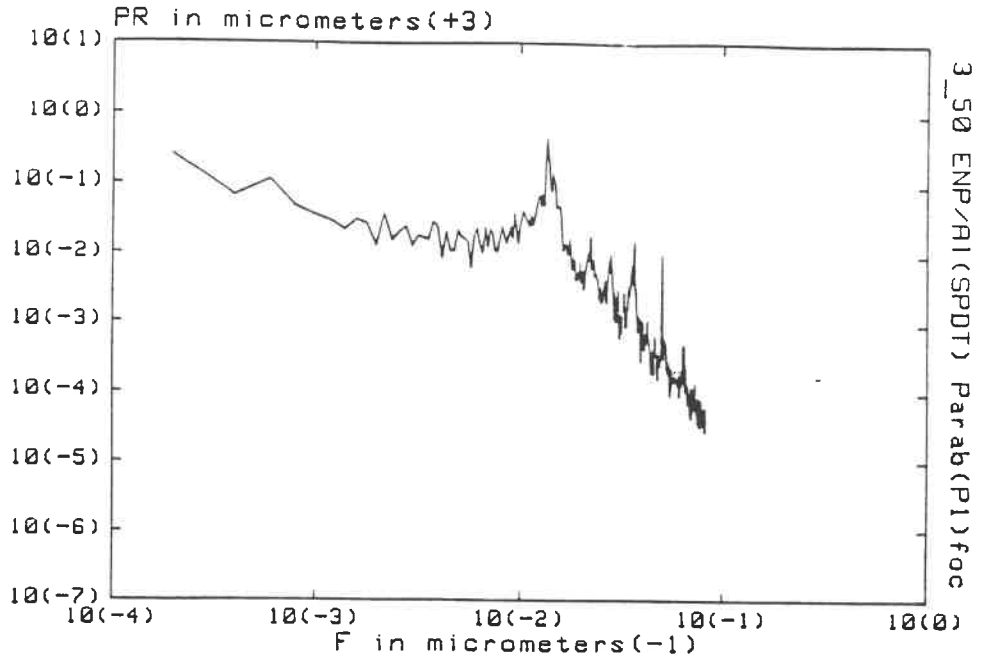

Figure 5 - The average power spectrum of the P1 surface in Fig. 3 showing a distinct peak at the spatial frequency corresponding to the sinusoidal period in the profile. This curve is an average over several locations on the surface. The RMS roughness for this surface computed from the area under this curve is about 310 Ångstroms. Peaks at frequencies higher than the fundamental provide useful information about machine performance during the diamond turning process.

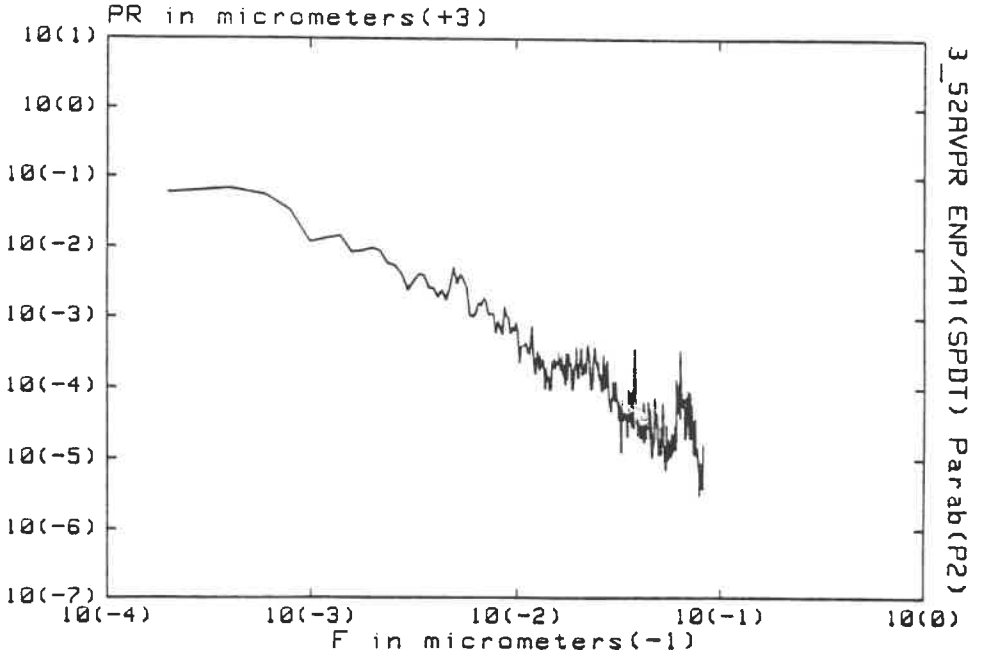

Figure 6 - The average power spectrum of the smoother P2 surface, showing an inverse power-law spectral shape characteristic of fractal-type surfaces. No distinct spectral features are apparent, in contrast to the P1 spectrum. The average roughness for this surface is about 91Å RMS

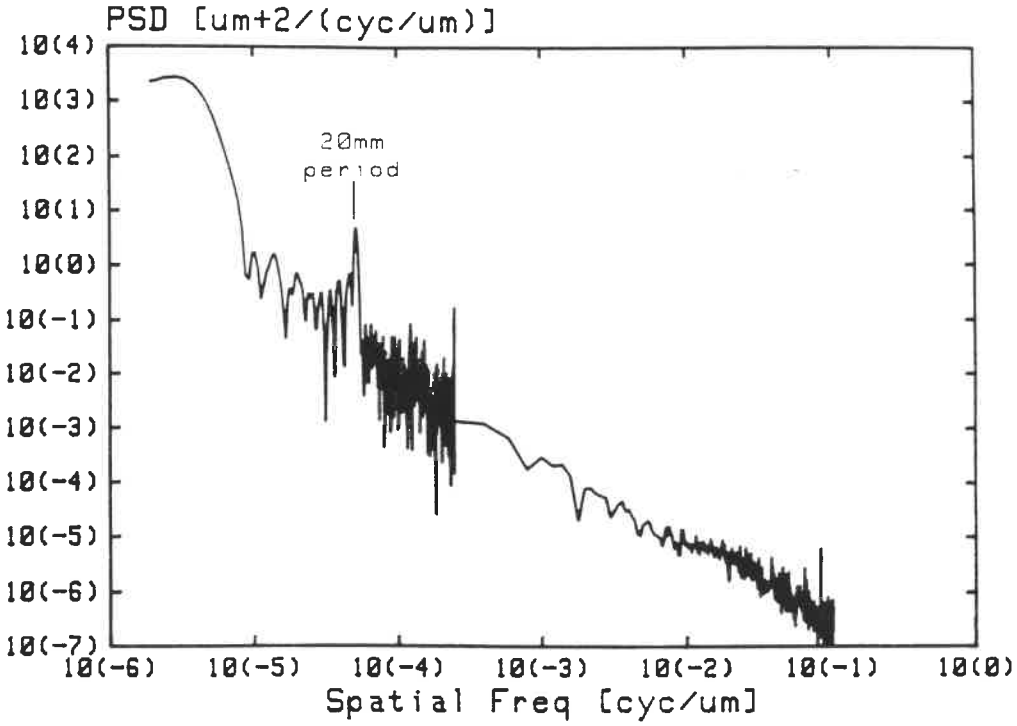

Figure 7 - Combined LTP and WYKO power spectra for a polished single-crystal silicon cylinder mirror 700mm in length. The LTP spectrum covers the 500mm to 4mm spatial period range, or equivalently the $2x10^{-6}\mu m^{-1}$ to $2.5x10^{-4}\mu m^{-1}$ spatial frequency range, and the WYKO covers the spatial period range from 5mm down to 10μm. The inverse power law description of the surface roughness holds over 4 decades in spatial frequency for this surface. The spectral feature at 20mm period corresponds to a sinusoidal polishing defect with a 23Å RMS amplitude and a maximum slope error of 1 arc second. The increase in amplitude at the lowest spatial frequencies corresponds to a residual step height of about 0.5 microns in the surface which could not be removed during the polishing process.

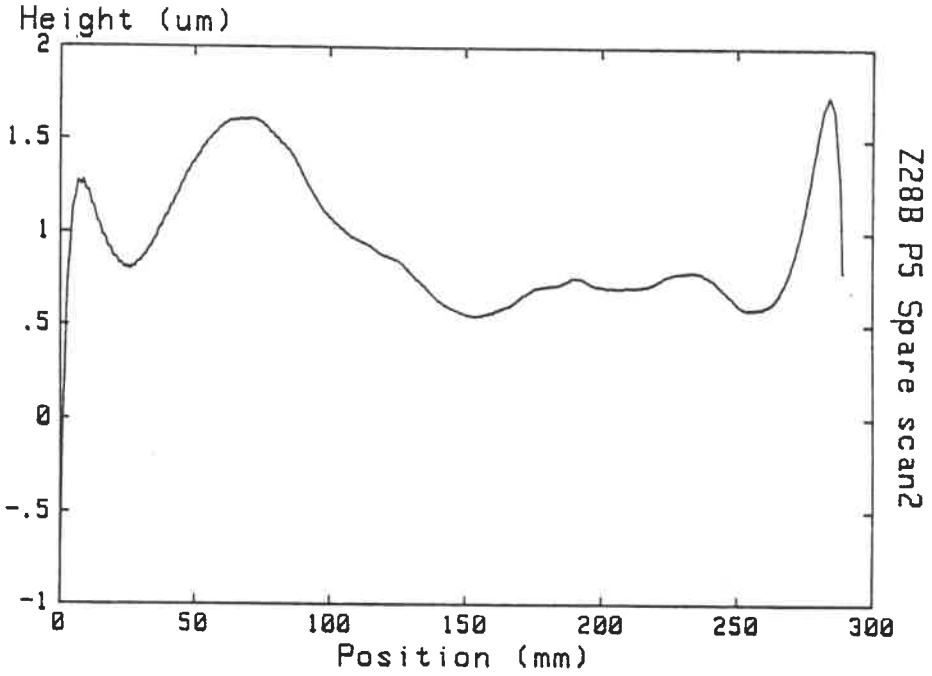

Figure 8 - LTP measurement of the shape of an electroless nickel paraboloid 300mm long manufactured in 1981. The edge roll-off and the trough region just inside the edge are typical defects found on polished metal aspheric optics.

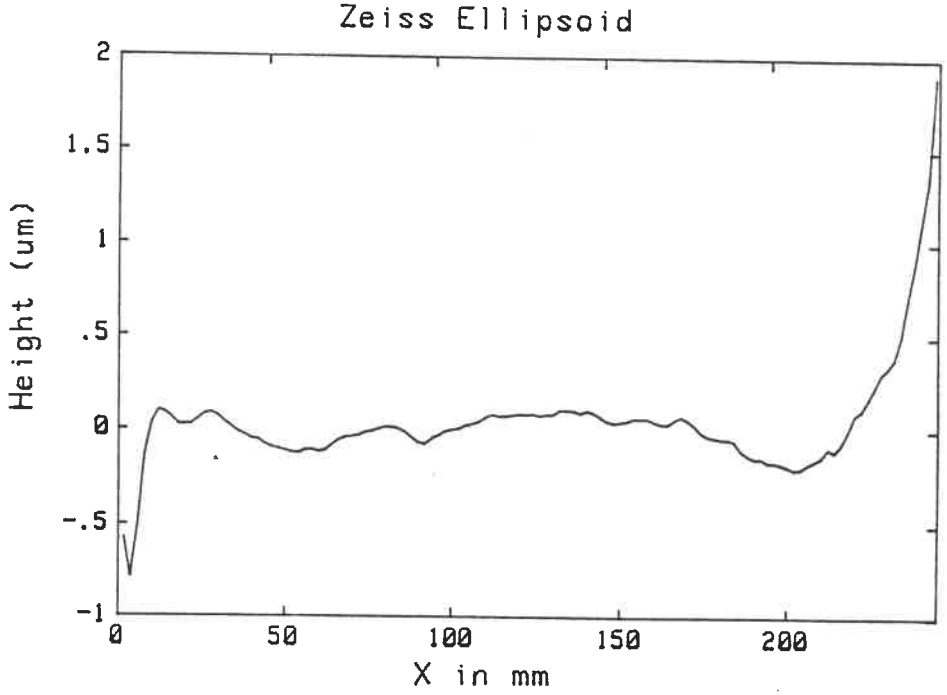

Figure 9 - LTP measurements on an ENP ellipsoid manufactured by Carl Zeiss in Germany during the mid 1980's. The residual surface error is on the order of 3 arc seconds RMS. Current technology is capable of producing surfaces on ENP mirrors with less than 1 arc second slope error on flats, spheres and aspheres.

Fabrication of a Metal-Plated Mirror, Beginning from a Performance Requirement

John S. Taylor
Lawrence Livermore National Laboratory

Chris J. Evans
National Institute of Standards and Technology

The principal steps in manufacturing a metal-plated mirror are substrate fabrication, plating, and final surface finishing. The intermediate specifications for these operations, as well as the final specification, are ideally developed during an iterative planning process that includes the optical designer, the project engineer, a metrologist, and manufacturing engineers; this latter group includes a diverse set of disciplines spanning substrate preparation, metallurgy, plating, and surface finishing. Each of these specialists identifies problems and offers solutions that might not be considered without them. The outcome of this process is a plan for meeting the customer's specifications that balances cost, schedule, and technical risk.

In practice, however, a lack of expert input to the planning process often arises because of limited funding or personnel and/or simply from a management structure that hinders information exchange. This can lead to unreasonable intermediate specifications and/or incompatibilities among manufacturing steps such as:

- arbitrary optical design of the mirror calling for the clear aperture to extend fully to the edge: input from the surface finisher would have recommended a roll-off tolerance if polishing was necessary

- assignment of a final surface finish specification without regard to how it would be measured or over what spatial wavelengths it should apply: input from the metrologist would have recommended couching the specification with respect to specific instruments (all have a finite bandwidth) or in terms of power spectral density.

- choice of a polishing fluid without regard to cleanability or it's influence on the coating process; input from a coater might have advised against using a fluid such as silicone oil (this point is subject to controversy)

The goal of this discussion is to describe issues that affect the ability of the surface finisher to meet his specifications. Some of these issues are inherent to the finishing process, while others are due to incompatibilities with other manufacturing steps. The finisher may have

the final manufacturing responsibility for meeting performance specifications and must contend with problems and deficiencies accumulated throughout the manufacturing process.

Since plating immediately precedes final finishing and it's "quality" significantly affects the ability of the finisher to meet his specifications, we will focus on the finisher/plater relationship and pertinent plating issues. However, the ability of the finisher to meet his specifications is not uniquely determined by plating quality: both the plater and the finisher are dependent upon decisions regarding other manufacturing steps, such as substrate material preparation, substrate finishing, and material selection/specification. Ultimately, the need to resolve these compatibility issues among the different manufacturing steps underscores the importance of good planning early in the fabrication project.

Before discussing in detail the concerns of the finisher, we will briefly describe how, ideally, manufacturing tolerances evolve from overall performance specifications. We will also consider the roles played by the other members of the manufacturing team in determining the quality of the plated surface. Throughout this discussion we will refer to plated mirrors, although the same concerns generally apply to precision finished plated mechanical components.

The Project Team

Fig. 1 shows the many roles involved in producing a metal-plated mirror [this is intended only for illustration, not as a rigorous design methodology]. For some projects, one person may assume multiple roles, although in one form or another, decisions are made in each of these areas.

The Customer is concerned about meeting the Performance Specifications for a particular application, and staying within budget and schedule; his input is in terms of Optical Requirements and Mission Requirements such as wavefront distortion, weight, and fixturability. The Project Engineer translates the Performance Specifications into engineering quantities, such as substrate geometry, material properties, and surface requirements. These are then distributed to various Manufacturing Engineers for evaluation of potential materials, manufacturing methods, appropriate tolerances, and metrology. Specifically, these include the Materials Engineer, Substrate Material Supplier, Substrate Finisher, Plater, Plating Finisher, Metrologist [his tasks include both overall QA and verification of intermediate specifications], and if necessary, a Coating Engineer.

Ideally, as decisions are made about materials and manufacturing methods, there should be a mechanism for feedback among the Project and Manufacturing Engineers. Iteration among team members may result in a modified mirror geometry, different materials, or revised intermediate specifications, all leading to an optimization of performance and manufacturability.

In the next sections, the Performance and Engineering Specifications are briefly described to show the driving influences in setting manufacturing tolerances.

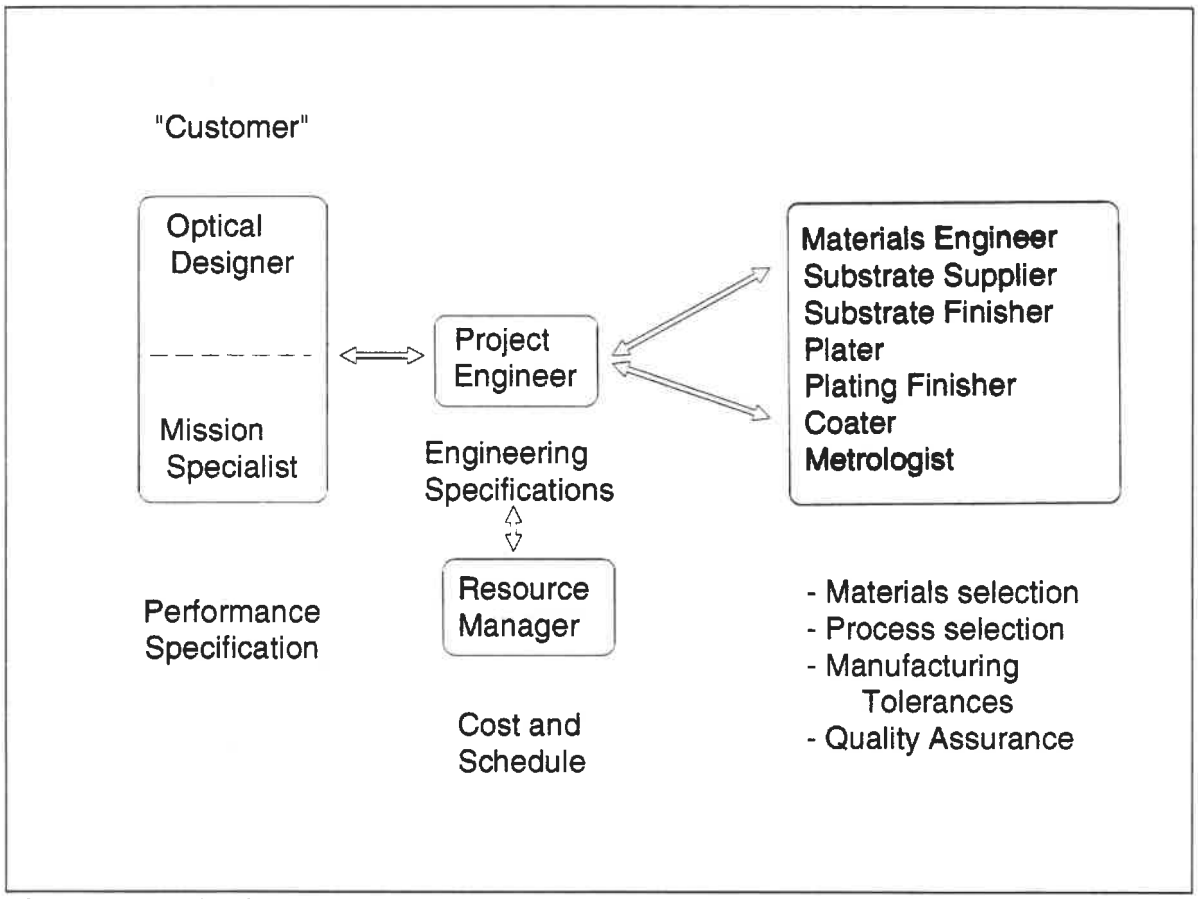

Figure 1. Fabricating a metal-plated mirror involves contributions from an interdisciplinary project team.

Performance Specification

The starting point in our discussion is the customer's requirement, the Performance Specification, which is the ultimate yardstick for determining the success of the project; these typically comprise both Optical and Mission Requirements as listed in Table 1. The Optical Requirements specify the quality and quantity of light reflected from the mirror, as represented by tolerances for wavefront distortion, resolution, scattering, and throughput. Wavefront errors[1] result in image distortions and are caused by geometrical shape errors in the mirror surface. Although the theoretical resolution (of an imaging system) is determined by aperture size, surface-induced wavefront distortions often limit the effective resolution. Light scattering from the mirror surface limits performance for two reasons: light scattered into the field of view degrades contrast at the detector by adding noise; and scattering out of the field of view simply

[1] This discussion emphasizes wavefront errors due to fabrication, however some aberrations may be intrinsic to the optical design.

reduces the total light available for detection. Collection area and surface reflectivity also determine throughput from the mirror.

The Mission Requirements listed in Table 1 are the other requirements necessary for utilizing the mirror. These include any size, weight, and geometry requirements for the mirror to be compatible with its housing. Similarly, the mirror must be fixturable in a way that minimizes distortions of the reflecting surface from induced stresses but allows precise mechanical alignment. Some level of structural integrity is necessary to prevent damaging the mirror during transportation (e.g. launching) or handling[2]. The service lifetime of the mirror is the total timeframe over which the mirror must meet it's Optical Requirements and need to withstand or perform satisfactorily over a range of conditions, such as varying temperature, drives a stability requirement. Cleanability and abrasion resistance protect against intentional and unintentional contact with the reflective surface. High energy laser or synchrotron applications impose special damage resistance requirements. Finally, the technical options available for fabricating the mirror are typically limited or optimized by cost and schedule concerns.

Table 1: Performance specifications for metal plated mirrors represent the customer's requirements

Optical Requirements	Mission Requirements
- *wavefront distortion*	- *size*
- *scattering (s/n)*	- *weight*
- *resolution*	- *structural integrity*
- *through-put*	- *fixturability*
scatter	- *service lifetime*
aperture	- *stability*
reflectance	- *abrasion resistance*
	- *radiation damage resistance*
	- *cost*
	- *schedule*

Engineering Specifications

The role of the Project Engineer is to generate specifications (Table 2) in terms of engineering variables that are relevant to manufacturing engineers, yet fully comprehensive and consistent with the Performance Specifications. In some cases, the Performance Specification is directly transferrable to fabrication, while in other cases, the connection to actual hardware is somewhat vague or abstract and thus requires a conversion to measurable and controllable

[2] Specific stiffness requirements to prevent excessive distortions due to gravity sag, vibrations, etc. are developed under Engineering Specifications based on the Performance Requirement for wavefront distortion.

parameters. For example, a Performance Specification for wavefront distortion is often given in terms of "waves of distortion" for different types of optical aberrations, e.g. Zernike polynomials or Seidel aberrations (coma, astigmatism, etc.). Although computerized interferometers and polishing machines are attempting to respond directly to this terminology, it may be more useful to the fabrication engineer if they were presented in terms of peak-to-valley deviations, rms errors, or in terms of spatial wavelength and power spectral density. The conversion to spatial wavelength is useful because the fabrication engineer can associate different fabrication methods and measurement techniques directly with their "smoothing" ability as a function of spatial wavelength and in-process metrology with the bandwidth of the instrument used.

Table 2: Engineering specifications are based on a compromise between performance requirements, available manufacturing technology, and cost/schedule limitations.

Engineering Specifications

Surface finish	*Metallurgy*
- rms, power spectral density	*- dimensional*
- discrete scatters	*- chemical*
Contour accuracy	*Reflectance*
- dimensional, rms, p-v	
- power spectral density	*Geometry*
- aberrations (coma, spherical etc)	*- stiffness, lightweighting*
	- sharp edges,
Thermo-mechanical properties	*- roll off tolerance*
- CTE	
- density	*Datum surfaces*
- Young's modulus	*Cost/schedule*
- conductivity	
- hardness	

Surface errors with short spatial wavelengths, i.e. roughness or surface finish, degrade performance by light scattering. Surface finish is typically discussed in terms of rms or peak-to-valley error, but again, the power spectral density is useful for distinguishing important ranges of spatial wavelength. Scattering is also caused by discrete surface artifacts not conveniently described by rms or power spectral density. For example, pinholes, bubbles, or surface inclusions in the final surface scatter light and might be specified in terms of allowable areal defect density (e.g. discrete artifacts to account for < 1% of the surface). Larger discrete artifacts are typically covered in a scratch/dig specification.

Acceptable ranges for thermo-mechanical properties and substrate geometry are determined from several of the Optical and Mission Requirements. A requirement for low

distortion due to thermal variations usually implies low coefficients of thermal expansion (CTE), similar values of CTE for the substrate and the plating, and high thermal conductivity. Low distortion due to mechanical loading implies a high stiffness and thus a high Young's modulus and moment of inertia. Weight and size restrictions may impose limits on the density (primarily on the substrate) and substrate thickness. Abrasion resistance and cleanability imply a plating material with a high hardness. Radiation damage resistance might also imply low CTE, high thermal conductivity, and high heat capacity.

One of the most important material parameters is the reflectivity of the plating at the design wavelength(s). If the plating material is not sufficiently reflective, then a coating, e.g. gold, may be specified; in this case, coating issues such as chemical compatibility, cleanability, and metallurgical stability become important.

Metallurgical requirements include both dimensional and chemical stability. Microstructural changes in any of the mirror materials may result in stresses that distort the shape of the mirror or cause increased roughness (scattering), e.g. due to grain growth. Chemical reactions at the mirror surface with either the environment or cleaning solvents may lead to either degraded performance (reflectivity) or a shortened service lifetime. Plating stresses may also represent future adhesion problems and result in surface cracks.

Fixturability of the mirror typically requires datum surfaces for mating or aligning with other elements in the system. These may include kinematic mounting pads and/or toroidal centering surfaces that have a precise relationship to the mirror surface. The dimensional specifications for these surfaces may be as stringent as for the optical surface.

Manufacturing Process Specifications

From the Engineering Specifications, the manufacturing engineers select materials, processing methods, and working tolerances consistent with available equipment, procedures, and measuring instruments (metrology). As already mentioned, this is the principal time in the planning process where conceptual design and "top-down" specifications are confronted with the limitations of current technology. If a specification is tighter than can be realized by available technology, or if cost, schedule, and technical risk exceed acceptable limits, then a reassessment of the engineering and/or performance specifications is necessary.

The technologists that establish the manufacturability of the mirror are the materials engineer (metallurgist), the substrate material supplier, the substrate finisher, the plater, the plating finisher, the metrologist, and perhaps the coater. Although, it is outside the scope of this paper to give detailed discussions about each of these areas, they all play a role in determining the task of the plating finisher. In particular, the specifications for the plating and the ability of the plater to meet these specifications have a strong influence on finisher's task of meeting the final manufacturing specifications (excluding coating). In the next section, the task of the finisher is described, with a particular emphasis on plating.

Surface Finishing

The principal responsibility of the plating finisher is to achieve the final surface finish and contour (figure) accuracy specified by the Project Engineer. However, the initial task, in conjunction with the Metrologist, is to further translate the finish and figure specifications into tolerances compatible with available measurement instruments; some examples are given in Table 3. Since all profile measuring instruments are bandlimited, it is important for the instruments to be sensitive over the same spatial frequencies that are important for mirror performance[3].

Table 3: Examples of manufacturing tolerances based on engineering specifications.

1. *Surface finish measured at XX places with XYZ instrument (XX mag.) to be <1.5 nm rms*

2. *Peak-to-valley surface trace over full aperture is:*
   < 125 nm 1/2 - 1 cycles/F.A.
   < 75 nm 1 - 3 cycles/F.A.
   < 25 nm > 3 cycles/F.A.

3. *Total discrete defect density on surface to total <1% total area*

4. *No pinholes in clear aperture*

Surface finish and contour accuracy are typically evaluated by either interferometry or traces by either a stylus or a non-contact optical probe; readings at several locations are usually necessary to estimate statistical and systematic variations over the surface. However, two measures of surface finish are not easily measured with standard surface profiling instruments: scratch/dig and other discrete defects. Scratch/dig typically refers to cosmetically visible defects such as scratches and gouges as might arise from handling damage or deficiencies in final finishing. Other discrete defects not typically covered in scratch/dig terminology are plating inclusions, imbedded polishing grit, pinholes, and plating bubbles. Scratches, digs, and other discrete defects are usually found by visual inspection by eye (with high a intensity lamp) or microscopic inspection.[4]

[3] A bandlimited profiling instrument is one that is sensitive or accurate only over a limited range of spatial frequencies. The measured rms roughness will in general be lower for narrower bandwidths. If there are spatial frequencies that cannot be effectively measured (at least during fabrication), then the Project Engineer must decide on an acceptable level of technical risk based on available measurements and assumptions about the finishing methods.

[4] Automated methods for finding discrete defects can be envisioned that optically scan the surface and trigger on atypical levels of scattered light.

Given manufacturing tolerances, the finisher assembles a set of operations designed to transform the mirror from the as-plated condition to the final specifications, e.g. several passes of diamond turning, followed by polishing. This series of processes is derived by considering the effectiveness of each of the candidate operations in removing errors in relevant ranges of spatial frequencies. For a successful sequence, the net reduction (improvement minus degradation) in surface errors for all spatial frequencies of interest must be sufficient to meet overall tolerances.

Two basic sequences are typically employed for the final finishing of metal-plated mirrors. The first involves a relatively thin plating (< 25 micrometers) on a precision diamond turned substrate; in this case, the plating is directly polished to the final surface finish and figure accuracy without first being diamond turned. If the machined substrate is sufficiently accurate and the plating is sufficiently uniform, then the role of polishing is to simply maintain figure accuracy while converging on final surface finish. The other scenario involves a relatively thick coating (typically 75 micrometers) on a substrate that might be held to somewhat looser figure tolerances than in the thin coating case. The plating is then diamond turned to high figure accuracy, and if necessary, polished to improve the surface finish.

Table 4: Factors influencing the ability of the finisher to meet final specifications

Part geometry
- *datum surfaces, fixturability*
- *sharp edges, roll off tolerance*
- *stiffness*

Material type (eg %P, heat treatment)
- *diamond tool wear*
- *polishability*
- *thermal distortion*

Initial surface roughness
- *substrate etching*
- *print through of substrate features*

Plating uniformity
- *figure accuracy*
- *risk of breakthrough*

Masking accuracy/integrity
- *preservation of datum surfaces*

Plating defects
- *voids, bubbles, pinholes*
- *inclusions*

Plating adhesion

Finishing Issues

A number of the important issues affecting the finisher's ability to meet his specification are listed in Table 4. In this section, several of these issues are discussed in detail.

Material Type

The choice of material has a strong bearing on the finishing process. Although, the global material selection, such as electroless nickel on aluminum, may be dictated by performance requirements, specific choices for the phosphorus content and heat treatment play an important role.

Diamond turning tests performed on a variety of electroless nickel compositions and heat treatments revealed that surface finish was optimized for a high phosphorus content and moderate heat treatment temperature: 13% P, 200 deg. C [1]. For this preparation, the plating was determined to be amorphous and to have a minimum hardness. The low values of surface roughness that were measured are attributed to low rates of tool wear.

Because tool wear is a major cause of surface finish degradation during diamond turning, an extended cutting distance machining study was performed with the optimum electroless nickel preparation [2]. However, even for this material, the measured surface finish degraded from < 10 Å rms to over 80 Å rms in a moderate cutting distance of 14 miles. The wear mechanism is attributed mainly to chemical wear between the diamond and the nickel, with some evidence of microfracture[5]. Ultimately, this type of experiment suggests that a material can only be considered "diamond turnable" if the surface finish does not exceed it's specification over the entire length of the cut. Thus, the size of the part must be considered when assessing diamond turnability.

Polishing behavior typically improves with harder work materials. Therefore an optimum preparation of electroless nickel for polishing might have a phosphorus content of 7-8 percent, which is considerably lower than for optimal diamond turning. Polishing softer materials results in a greater tendency for deep sleeking (scratching) or for the polishing abrasive to imbed itself into the surface. When both polishing and diamond turning are necessary for a surface, a compromise plating might be selected, depending on the size of the part and the specification.

Another materials issue is the thermal deformation of the workpiece due to dissimilar values of the CTE for the plating and the substrate. This is an issue if the workpiece temperature is different during plating, finishing, measurement, or application. Note that the "zero stress state" during plating may occur at significantly elevated temperatures. Thermal deformation may also result in significant stress levels at the plating/substrate interface, posing adhesion or cracking problems. Calculated deformation levels (Fig 2.) are substantial for one-sided coatings [3], but may also occur for fully coated parts that are non-symmetric or have a non-uniform front-to-back coating thickness. Even in the case of similar ambient temperatures for the different processes, adequate thermal equilibration times are necessary to avoid deformation.

---

[5] High phosphorus electroplated nickels are available (see presentation by Lashmore in this volume) and have been diamond turned (see Mayer et al and Dini, this volume) with excellent results.

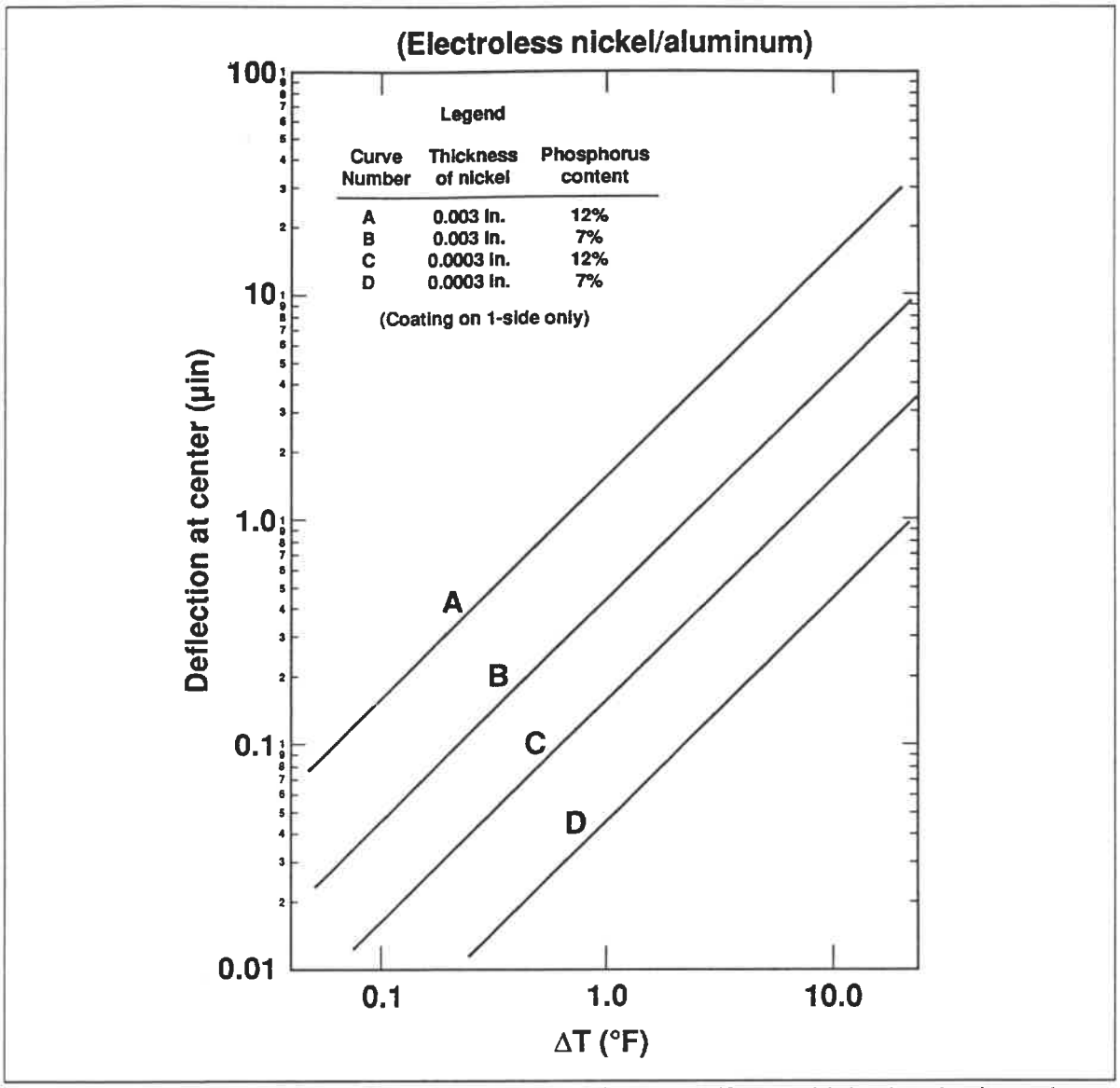

Figure 2. Center deflection (sag) of a 300 mm diameter, 50 mm thick plated mirror due to a uniform temperature rise [B. Kornblum, LLNL]

Plating Inclusions

Inclusions are any discrete solid phase particles characterized by different material properties than the bulk plating. Of interest here are particles that are harder than the bulk plating such as alumina. As already mentioned, if these are exposed to the surface, they will scatter light and will affect the performance of the mirror. Our interest in this section is their effect on fabrication.

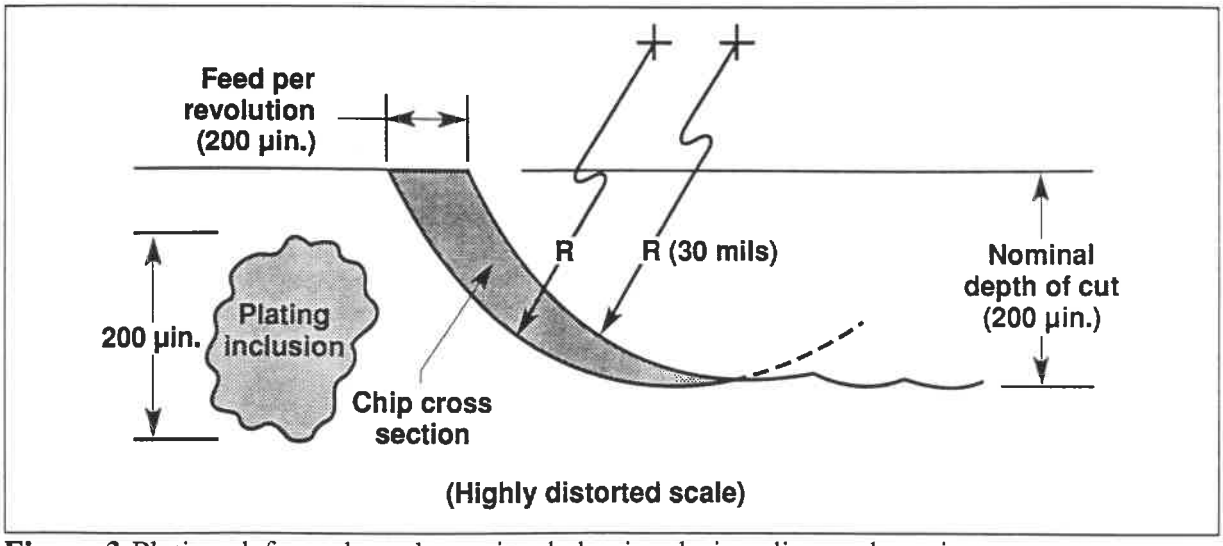

Figure 3 Plating defects degrade cutting behavior during diamond turning

During the diamond turning of a plating, the polished edge of a single crystal diamond tool cuts through the material and leaves its geometrical imprint on the surface. The nominal depth of cut is the penetration of the tool normal to the surface and may be as low as 0.1 µm. for some finishing cuts, and as high as 50 µm in roughing. However, in either a turning or a fly-cutting operation, the tool sweeps out a crescent-shaped chip of material where the maximum thickness at the top of the shoulder is an order of magnitude less than the nominal depth of cut. It is only at the thin bottom region of the crescent that adjoins the final machined surface, because the rest of the shoulder is removed by the next revolution of the tool. The significance of this is that depth of cut in the zone of importance is of order 0.01 µm, while the size of plating inclusions may be >> 1 µm (Fig.3). Therefore, the inclusion will not be simply swept away by the tool, but may nick and gouge the fragile tip of the tool during a number of revolutions.

Previous work on the diamond turnability of electroless nickel demonstrates the influence of tool wear on the final surface finish [2]. Stylus probe traces of diamond turning feedmarks taken at different cutting distances for the same tool show significant evolutional changes in feedmark geometry. Although chemical wear may be the dominant mechanism in degrading this tool, the dramatic changes in feedmark geometry suggest microfracture of the tool tip, which may be linked to plating inclusions. Other work [4] suggests that a fine dispersion of hard second phase material in a chemically reactive matrix may lead to a combination of chemical and fatigue wear mechanisms. Inclusions may also be dragged through the finished surface, degrading surface finish, or be pushed into the part, springing back after the tool has passed to cause "orange peel".

The polishing of platings with hard inclusions also results in tool degradation. Metal platings are often polished with diamond (0.25-2.0 µm) on pitch. The procedure usually begins by pressing the pitch on the optical surface to obtain an intimate fit between the lap and the part.

Any space that remains may result in either non-uniform polishing rates under the lap or pockets where diamond can come out of the pitch matrix and roll on the part, causing scratching[6].

In one polishing geometry, the lap is stroked in the y-direction while the part slowly translates back-and-forth in the x-direction; thus the lap takes a sinusoidal path over the part. The rate of material removal is proportional to lap pressure and relative velocity. [An exact retracing of the lap's motion over the part is usually avoided to prevent observable lay patterns from developing in the surface finish.]

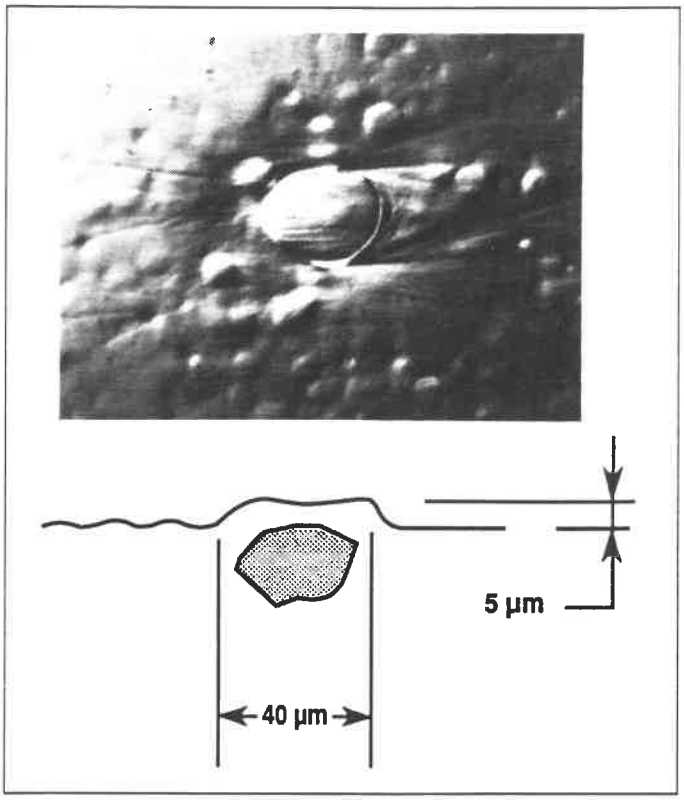

Figure 4. Hard plating inclusions which can destroy a lap

If a plating inclusion is present on the surface, it will not be abraded away at the same rate as the bulk plating. [Because of the hardness difference, it may not diminish at all.] This will leave a point (e.g. 5 µm) defect protruding above the surface that will serve to disrupt the pitch and the diamond in the lap (Fig. 4). Since the pitch is a soft visco-elastic material that is easily removed, this eventually leaves a channel cut into the pitch that is the width of the lap's stroking motion (Fig. 5). This channel destroys the close fit originally obtained during pressing.

Degraded areas in the pitch result in non-uniform polishing that leaves bands on the surface with different roughness values. In addition, material removal is impeded in these regions, and thus the figure accuracy also degrades as bands of higher material are left. The band cut in the pitch also leaves room for the diamond abrasives to roll around and cause scratching[7].

Summarizing, plating inclusions impede or prevent the finisher from meeting the figure and finish requirements for the mirror. Both of these issues tie directly back to the light scattering and wavefront distortion specifications outlined in the Performance Specifications.

---

[6] The discussion here focusses on pitch polishing. The effect of inclusions may be different on, for example, fabric faced laps.

[7] We have seen a striking rainbow of colors in these bands due to light diffraction from the roughness patterns.

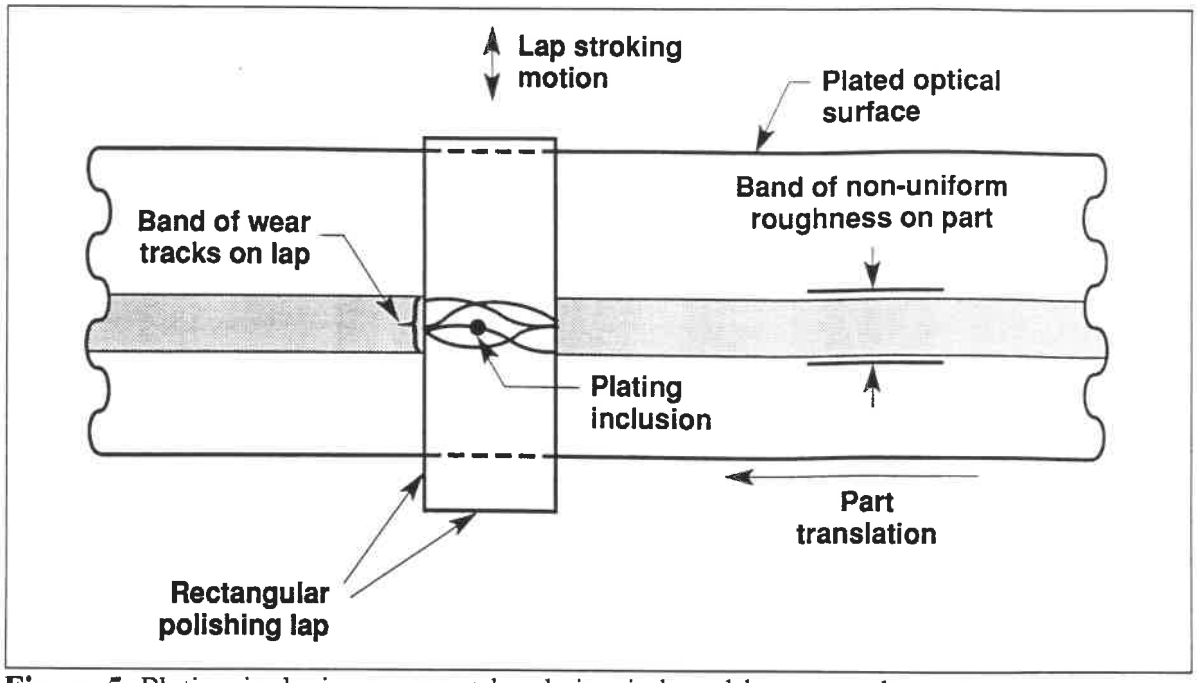

Figure 5. Plating inclusions can cut bands in pitch and hence on the part

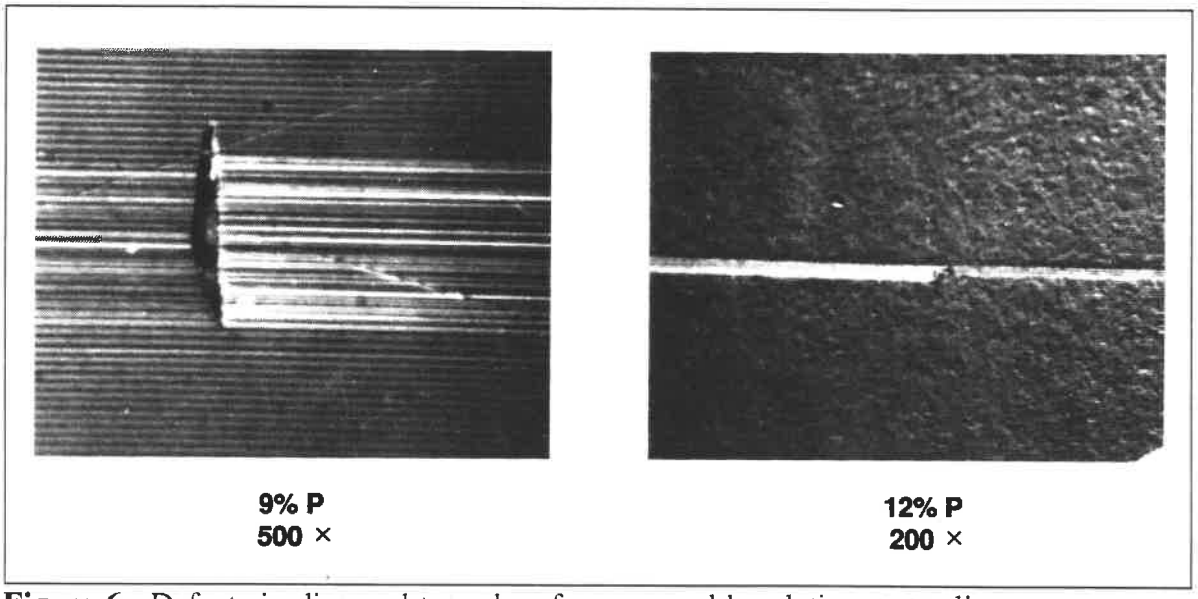

Figure 6. Defects in diamond turned surfaces caused by plating anomalies

Plating Pinholes and Bubbles

Pinholes and bubbles in the plating are a somewhat less disastrous problem for the finisher than are inclusions. In diamond turning, the presence of a small hole in the material may cause the tool to plunge into the material a short distance causing a comet shaped divot to be removed on the exit side of the hole. The abrupt change in cutting conditions at the hole may

change the tool's cutting behavior, such as by picking up a piece of contamination. Nomarski micrographs of these surfaces show examples of irregular feedmarks passing through voids in an electroless nickel plating. Some of the feedmarks leaving these holes have the appearance of scratches, suggesting that either the cut depth changed or that a piece of contamination was dragged along by the tool (Fig. 6).

Voids have a similar effect on polishing in that some of the pitch and diamond may be pulled out of the matrix near the hole. This may also cause the hole to enlarge by forming sloped edges. Certainly, if the disruption of the lap is significant, then a general degradation of the finish may occur as with inclusions.

This enlargement is not observed when a fabric faced lap is used to polish pitted platings[8]. Difficulties are encountered, however, in removing diamond from these pits, which can act as a reservoir of larger diamond after a change in nominal abrasive size.

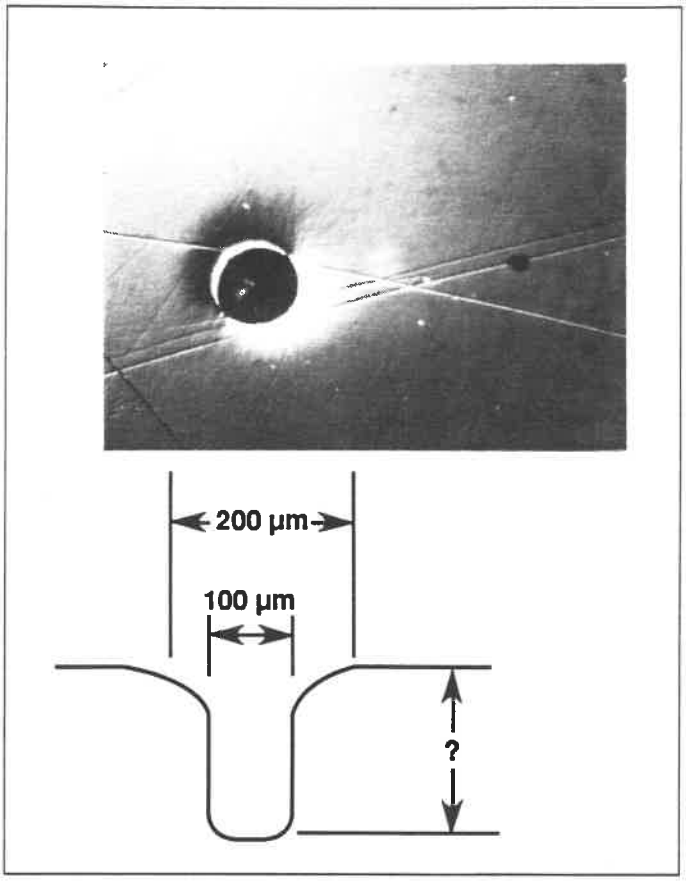

Figure 7. Polishing can form sloped regions around plating holes

Plating Roughness

The initial roughness of the plating influences the convergence to the surface finish specification for both diamond turning and polishing.

Diamond turning experiments performed on electroless nickel plated copper disks have shown a tendency to replicate feedmarks generated during the machining of the substrate [1]. Surface profiles of the diamond turned plated surface showed a dominant periodic contribution corresponding to the substrate feedrate that persisted after 6 finishing passes. For these tests, both the substrate and the plating were machined on-center; thus, the final turning was performed "parallel" to the substrate feedmarks. One explanation for this phenomena, referred to as "print-through", is the elastic deformation in the machine tool structural loop due to the increased cutting force along the feedmarks. This observation has resulted in a greater concern for substrate machining specifications. Proper stress relief between substrate machining and plating is essential; otherwise print through of the substrate machining feed rate may be seen later in either the manufacturing cycle or, implicitly, during the final product's life cycle.

[8] See paper by Parks and Evans elsewhere in this volume

Although not documented, print-through of other low frequency errors in the substrate, such as due to figure errors, may also occur.

A major concern in polishing is the initial roughness level. The rate of smoothing during pitch polishing is determined by the pressure differential between the high spots and the low spots [5]. For high spatial frequencies, the polishing lap bridges over the low spots, resulting in a high smoothing rate, while for lower spatial frequencies the lap contacts the valleys, resulting in a low smoothing rate. The attenuation of the roughness amplitude is an exponential function of the amount of material removed. High initial roughness values might be caused by excessive etching during the plating process or from poor substrate preparation. For either case, more material must be removed to achieve a given roughness specification. Typically, figure distortions, edge roll-off, and the risk of breaking through the plating increase with the amount of material removed.

Synthesis

The occurrence of plating defects that hinder the task of the surface finisher is a symptom of poor communication, particularly in establishing plating specifications that are sensitive to the finishing concerns. An approach to mitigate this deficiency is for platers to be aware of the unique problems encountered in finishing precision surfaces, and for finishers to be knowledgeable of potential plating problems and the latitude available to the plater to prevent them. These issues are vitally important to the customer and the project engineer, in that they impact the likelihood of fabricating an acceptable mirror, on time and within budget. Ultimately, project management will face these issues at the outset during interdisciplinary planning meetings.

Acknowledgements

The authors would like to acknowledge contributions from Norm Brown, Ben Fuchs, and Bob Parks for insights into polishing, and from Barb Kornblum and Stan Bumpas for performing the thermal distortion analysis.

Auspices

This work was performed under the auspices of the U.S. Department of Energy by Lawrence Livermore National Laboratory under Contract No. W-7405-ENG-48.

Notes

1. Taylor, J. S., Syn, C. K., Saito, T. T., and Donaldson, R. R., "Surface finish measurements of diamond-turned electroless-nickel-plated mirrors", Opt. Eng. 25(9), 1013-1020 (1986).

2. Syn, C. K., Taylor, J. S., and Donaldson, R. R., "Diamond tool wear vs. cutting distance on electroless nickel mirrors", Proc SPIE

3. Deformation levels calculated by B. Kornblum and S. Bumpas, LLNL, using the circular-plate solution given in Formulas for Stress and Strain, 5th ed., R. J. Roark and W. C. Young, McGraw-Hill (1982).

4. Evans C. "Cryogenic diamond turning of stainless steel" CIRP Annals Vol 43 (1991)

5. Brown, N. J., Baker, P. C, and Parks, R. E., " Polishing-to-figuring transition in turned optics", Proc. SPIE 306, 58-65 (1981).

ELECTROFORMED ASTRONOMICAL X-RAY OPTICS

By Melville P. Ulmer
Physics and Astronomy Department
Northwestern University
2131 Sheridan Road
Evanston, Illinois 60208

and

Rudy Haidle and Robert Altkorn
Basic Industry Research Laboratory
Northwestern University
1801 Maple Avenue
Evanston, Illinois 60201

INTRODUCTION

The fabrication of astronomical x-ray optics represents a significant challenge. Such optics must be exceptionally smooth and precisely figured. Their shapes are unusual by optical standards, generally neither flat nor spherical. They must be light and rugged enough for rocket flights, and often thin enough to allow nesting. As with all other products, it is desirable to keep their cost within reason. In this paper, we describe the electroforming of Wolter I grazing-incidence x-ray mirrors on lacquer "polished" metal mandrels. These mirrors are designed to focus 2 - 10 keV (wavelength 6 - 1.2 Å) x rays. We discuss surface quality and compare it to that of metal-overcoated, lacquer-polished test flats.

MIRROR FABRICATION

Figure 1 is a diagram of a Wolter I mirror. The design was first suggested in 1952[1] to eliminate many of the aberrations associated with simpler mirrors. It consists of two sections: the larger is a paraboloid of revolution and the smaller is hyperbolic. X rays striking each surface once at grazing incidence are focused. Our mirrors are gold-lined electroformed nickel shells. We fabricate mirrors of six different sizes to allow nesting and increase collection area. To get an idea of scale, one of the middle mirrors has an entrance aperture of 11.43 cm, an exit aperture of 10.26 cm, and a length of 40.8 cm. The focal plane of each mirror is located 2.0118 meters behind the plane separating the parabolic and hyperbolic sections of the mirror. The mirrors are fabricated from mandrels such as those shown in Fig 2.

The mandrels are fabricated to our specifications by Research Optics and Development (Newton, MA). Each mandrel is fabricated as follows. A cylinder of 6061-T6 aluminum is rough and diamond turned to the required shape with intermediate heat treatment, coated with a 65 μm thick layer of electroless nickel, conventionally polished and then superpolished with a slurry of colloidal carbon in ammonia. At this point we receive the mandrel, which has a high-frequency surface roughness of about 25 Å.

To further reduce roughness and protect the mandrel through multiple replication processes, each mandrel is lacquer "polished" prior to use. This process consists of coating the mandrel with a thin, uniform lacquer layer which is drawn into a smooth shape by surface tension. Although introduced only recently, lacquer polishing is now widely used in the fabrication of various types of x-ray optics[2-25]. Our lacquer-polishing apparatus has been described in detail previously[24]. Approximately 100 L of lacquer, consisting of a 30% solution of acrylic polymer (Rohm & Haas B-82 Acryloid) in 2-butanone, is stored in a stainless-steel reservoir tank. It is recirculated and filtered regularly to remove concentration gradients and particulates. The mandrel is loaded into a coating tank, which is subsequently filled to a desired height with lacquer. A 3 μm filter in the filling line removes solid contaminants. The lacquer surface is cleaned by skimming at various stages of the filling process. The lacquer is allowed to stand in the coating tank until all bubbles have dissipated. It is then pumped out at the rate of about 1 vertical cm/min, leaving a uniform layer approximately 3 μm in thickness on the mandrel. The coating tank is located on vibration-isolating pads, and efforts are made during the coating process to limit vibration due to walking, etc. The coated mandrel is transferred to an oven, heated until it reaches a uniform temperature of 60° C, and baked at this temperature for 2 hr to drive off solvent and further smooth the lacquer by raising it above its glass-transition temperature. This step is somewhat delicate, as a bake that is too long or too hot can damage the lacquer, while insufficient baking leaves the lacquer tacky.

After it has cooled, the lacquer-coated mandrel is transferred to a vacuum chamber and evaporatively coated with about 1000 Å of gold. Gold is an excellent x-ray reflector and also serves as a conductive layer onto which nickel can be electroformed. To prevent thermal damage to the lacquer, the tungsten boats from which the gold is evaporated are positioned at least 50 cm below the mandrel, and the mandrel is rotated about its axis at approximately 30 rpm. A deposition mask is used to limit the angles at which the gold atoms strike the mandrel to near normal incidence.

After gold coating, the mandrel is removed from the vacuum chamber and prepared for plating. All masking operations are done in a laminar flow workstation. Cavities and screw holes are covered with tape and/or stop-off lacquer to exclude plating solution, and both ends of the mandrel are taped to ease mirror removal.

At this point the mandrel is plated. Our electroforming system consists, in part, of a 380-L polypropylene electroplating tank, a 38-L auxiliary tank used for continuous low voltage electroplating (for purification and stress reduction), and a 420-L tank used for treatment and storage. The tanks are interconnected through transfer pumps and filters. A ~5500 L/hr pump/filter system is used to continuously filter and agitate the bath. A ~4500 L/hr in-tank filtration system is used for skimming, additional agitation and filtration, and occasional activated carbon treatment. The pH

is continuously monitored and automatically controlled to 4.0 ± 0.05. An automatic filling system replaces water lost to evaporation.

The plating tank contains four 120-cm long Ti anode baskets filled with Ni rounds. The auxiliary cell contains two 60 cm by 6½ cm diameter Ti anode baskets and a 30 cm by 60 cm sheet-metal dummy cathode. The dummy cathode is run continuously at 1 V. All anode baskets are in bags.

The electroplating solution contains approximately 300 g/L nickel sulfamate, 9 g/L nickel bromide, and 70 g/L boric acid. Sulfamic acid and surfactant are added as necessary. The bath has been extremely reliable in producing low-stress deposits over long periods of time without the need for stress-modifying agents. Deposits are characterized by a matt finish and high ductility. Plating is done at a current density of 3.4 A/dm^2. The rate of Ni deposition is about 20 μm/hr. Typical plating times are 12-18 hr, depending on mandrel diameter and desired thickness. The mandrel is rotated at 40 rpm. Final mirror wall thickness is near ¾ mm.

Mirror removal is accomplished by differential contraction in liquid nitrogen. After removal from the plating tank, the mirror assembly is drained, rinsed, transferred to an insulated container, and chilled in liquid nitrogen. By turning a threaded shaft (Fig. 2), the mirror is guided away from the lacquered mandrel. (The mirror does not rotate during this process; the shaft also prevents the mirror from scraping against the mandrel.) The mirror and mandrel are rinsed and blown dry. To protect the delicate gold surface, the mirror is coated with a strippable polymer. The mandrel is allowed to reach room temperature, solvent cleaned, and prepared for next use. The mirror is trimmed to its final length by wire EDM. Mirror removal is be accomplished even though the draft angle on the mandrels is only 25 arc min and each mandrel has a short zero draft section at each end.

SURFACE QUALITY

Both optical (WYKO NCP-1000 profiler[26]) and x-ray (X-18 beam line facility at Brookhaven national laboratory) measurements were used for surface characterization. For purposes of comparison, superpolished nickel flats were lacquered, coated with gold or palladium, and evaluated along with Wolter I optics. The surface measurements have been described in considerable detail elsewhere[25], and will only be summarized here:

1. The grazing-incidence x-ray reflectivity (intensity vs. angle) of a gold-coated test flat was evaluated at energies of 8, 16, and 40 keV (wavelength 1.5, 0.77, and .31 Å). The reflectivity profile at 40 keV is shown in Fig. 3. The full width at half maximum is ~10.8 arc sec, demonstrating the feasibility of low-scatter reflectivity at extremely short wavelengths.

2. Optical measurements of the same gold-coated, lacquered flat, as well as a palladium-coated lacquered flat and an uncoated, unlacquered flat, are shown in Table 1. It is seen that the gold-coated flat has the lowest high-frequency (100 - 9.8 μm periods) roughness and that lacquering may slightly increase the mid-frequency (5 - 1 mm periods) ripple.

3. X-ray reflectivity measurements of a Wolter I mirror were made at 5 keV using a beam of dimensions 1 mm x 0.1 mm aligned to reflect once at each section of the mirror. In Fig. 4 we show background-subtracted counts vs. angle and relative reflected intensity vs. beam width. The ~35% power point corresponds to a width of ~100 arc sec.

4. Optical measurements were performed on pieces cut from the zero-draft section of a Wolter I mirror. Although the zero-draft section was not superpolished, the high frequency (1 mm - 9.8 μm periods) roughness was good, ranging from 15 to 22 Å.

A detailed comparison between the optical and x-ray measurements has been given elsewhere[25].

FUTURE WORK

We have described a method of producing electroformed replica x-ray optics and have demonstrated their smoothness by x-ray and optical measurements. The major problem we face in improving the quality of these optics is further reducing surface roughness. Although we have produced extremely smooth flats consisting of superpolished Ni substrates coated with lacquer and evaporated gold or palladium, we have yet to duplicate this surface finish in our Wolter I mirrors. Some of the possible reasons for this discrepancy are the following:

1. The surface of the mandrel is rougher than the surface of the flat prior to electroforming.

2. Some aspect of the electroforming process may introduce roughness. Such roughness may be associated with stress or structure present in the initially deposited nickel film, penetration of the plating bath through pinholes in the gold, etc.

3. Roughness may be introduced in the process of separating the mirror from the mandrel.

We are currently involved in work aimed at elucidating and eliminating this source of roughness.

ACKNOWLEDGEMENTS

This work was supported in part by NASA grant NAG5-181 and by the Basic Industry Research Laboratory at Northwestern University.

REFERENCES

1. H. Wolter, Ann. Phys. vol. 10, p. 294, 1952. See also J.H. Underwood, Am. Sci., vol. 66, p. 476, 1978.
2. P.J. Serlimitsos, X-Ray Astronomy in the 1980's, S.S. Holt, ed., NASA TM 83848, p. 441, 1981.
3. P.J. Serlimitsos, R. Petre, and C. Glasser, IEEE Trans. Nucl. Sci., vol. NS-31, #1, p. 786, Feb. 1984.
4. N.J. Westergaard and P.L. Jensen, Proc. SPIE 597, p. 68, 1985.
5. O. Citterio, G. Conti, E. Mattaini, B. Sacco, and E. Santambrogio, Proc. SPIE 597, p. 102, 1985.
6. L. Jalota and R. Willingdale, RAL Workshop on Advanced Technology Reflectors for Space Instrumentation, M. Grande, Ed., p. 214, June 1986.
7. R.C. Catura, E.G. Joki, D.T. Roethig, and W.J. Brookover, Proc. SPIE 640, p. 140, 1986.

8. R.C. Catura, E.G. Joki, J.R. Viera, and W.J. Brookover, Proc. SPIE 691, pp. 118, 1986.
9. R.C. Catura, E.G. Joki, and W.J. Brookover, Proc. SPIE 733, p. 138, 1986.
10. R.C. Catura, E.G. Joki, D.T. Roethig, and W.J. Brookover, Appl. Opt., vol. 26, p. 1563, 1987.
11. H. Kunieda and P.J. Serlemitsos, Proc. SPIE 830, p. 12, 1987.
12. J.A. Nousek, G.P. Garmire, R.J. Pipetti, D.N. Burrows, W.H.-M. Ku, and K.S.K Lum, Proc. SPIE 830, p. 95, 1987.
13. P.J. Serlimitsos, Proc. SPIE 830, p. 179-192, 1987.
14. L. Jalota and R. Willingdale, Proc. SPIE 830, p. 185, 1987.
15. R.C. Catura, R.A. Stern, W. Cash, D.L. Windt, J.L. Culhane, J. Lappington, and K. Barnsdale, Proc. SPIE 830, p. 204, 1987.
16. G. Bonelli, G. Conti, E. Mattaini, and O. Citterio, Proc. SPIE 830, p. 44, 1987.
17. O. Citterio, G. Bonelli, G. Conti, E. Mattaini, E. Santambrogio, B. Sacco, E. Lanzara, H. Brauninger, and W. Burkert, Appl. Opt., vol. 27, p. 1470, 1988.
18. P.J. Serlimitsos, Appl. Opt., vol. 27, p. 1447, 1988.
19. N.J. Westergaard, B.P. Byrnak, F.E. Christensen, P. Grundsøe, A. Hornstrup, S. Henrichsen, U. Henriksen, E. Jespersen, H.U. Nørgaard-Nielsen, J. Polny, H.W. Schnopper, and P. Ørup, Proc. SPIE 1160, p. 488, 1989.
20. A. Hornstrup, F.E. Christensen, and H.W. Schnopper, Proc. SPIE vol. 1160, pp. 507, 1989.
21. O. Citterio and P. Jensen, Proc. SPIE 1140, p. 337, 1989.
22. G. Conti, G. Bonelli, E. Mattaini, E. Santambrogio, O. Citterio, H. Brauninger, and W. Burkert, Proc. SPIE 1140, p.380, 1989.
23. F.E. Christensen, A. Hornstrup, P. Frederiksen, P. Grundsoe, S. Hendrichsen, E. Jacobsen, P. Jonasson, M.M. Madsen, C. Nillson, H.W. Schnopper, N.J. Westergaard, and P. Orup, J. X-Ray Sci. Tech., vol. 2, p. 81, 1990.
24. M.P. Ulmer, R. Haidle, and R. Altkorn, Plating and Surface Finishing, vol. 77, p. 23-25, 1990.
25. M.P. Ulmer, R. Haidle, R. Altkorn, P. Georgopolous, B. Rodricks, and P.Z. Takacs, submitted to Optical Engineering.
26. E. Church and P.Z. Takacs, Wear, vol. 109, p. 241, 1986.

Table 1. Optically Measured RMS Roughness of Test Flats (Å)

	Spatial Period Range			
	5mm-9.8μm	1mm-9.8μm	100μm-9.8μm	5mm-1mm
Ni flat	7.1	6.4	4.9	3.5
Au/lacquer/Ni flat	7.7	6.2	3.5	5.9
Pd/lacquer/Ni flat	13.1	6.1	3.6	11.8

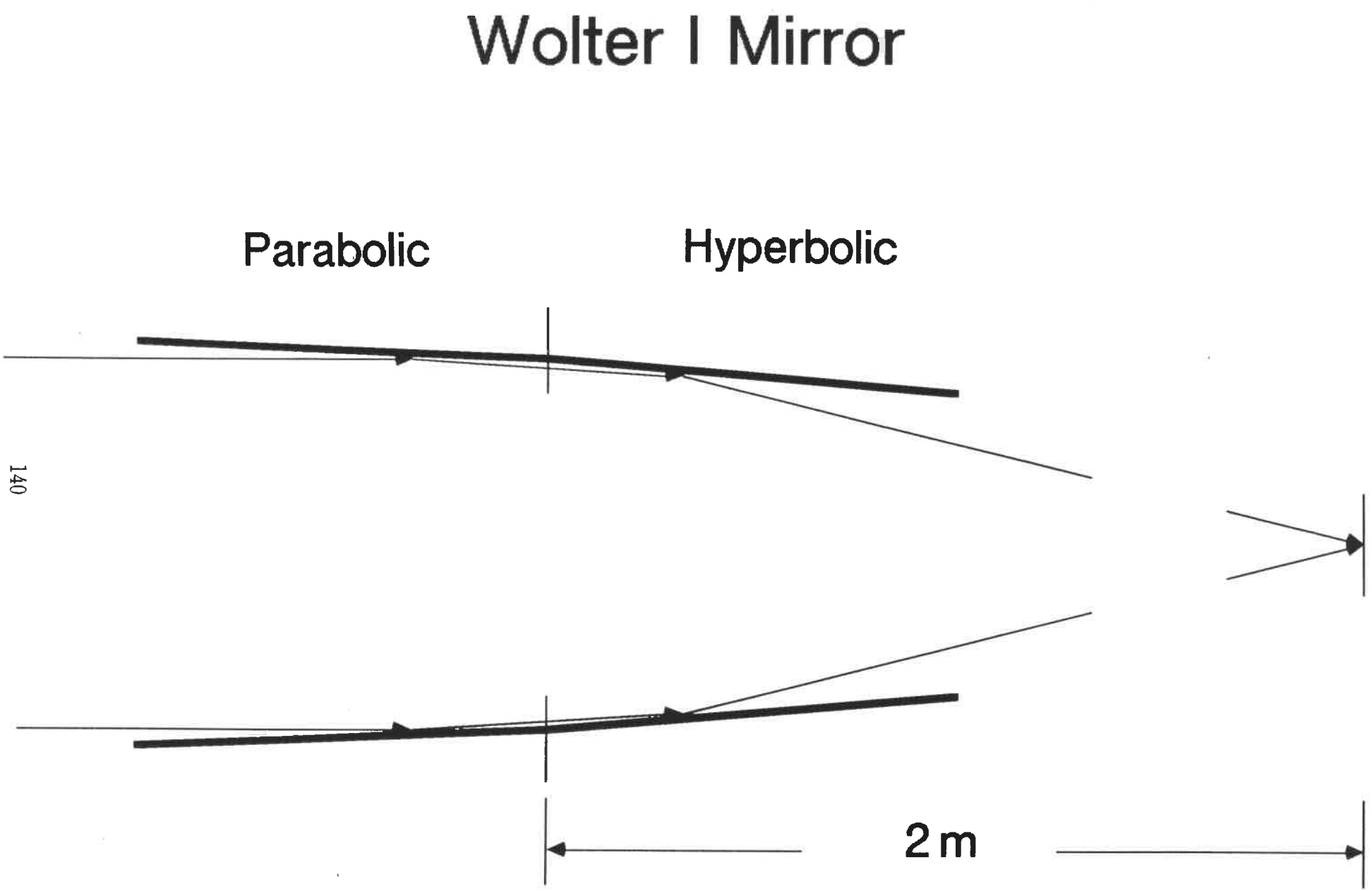

Fig. 1. Drawing of Wolter I mirror showing ray paths (not to scale - length of mirror is 40.8 cm).

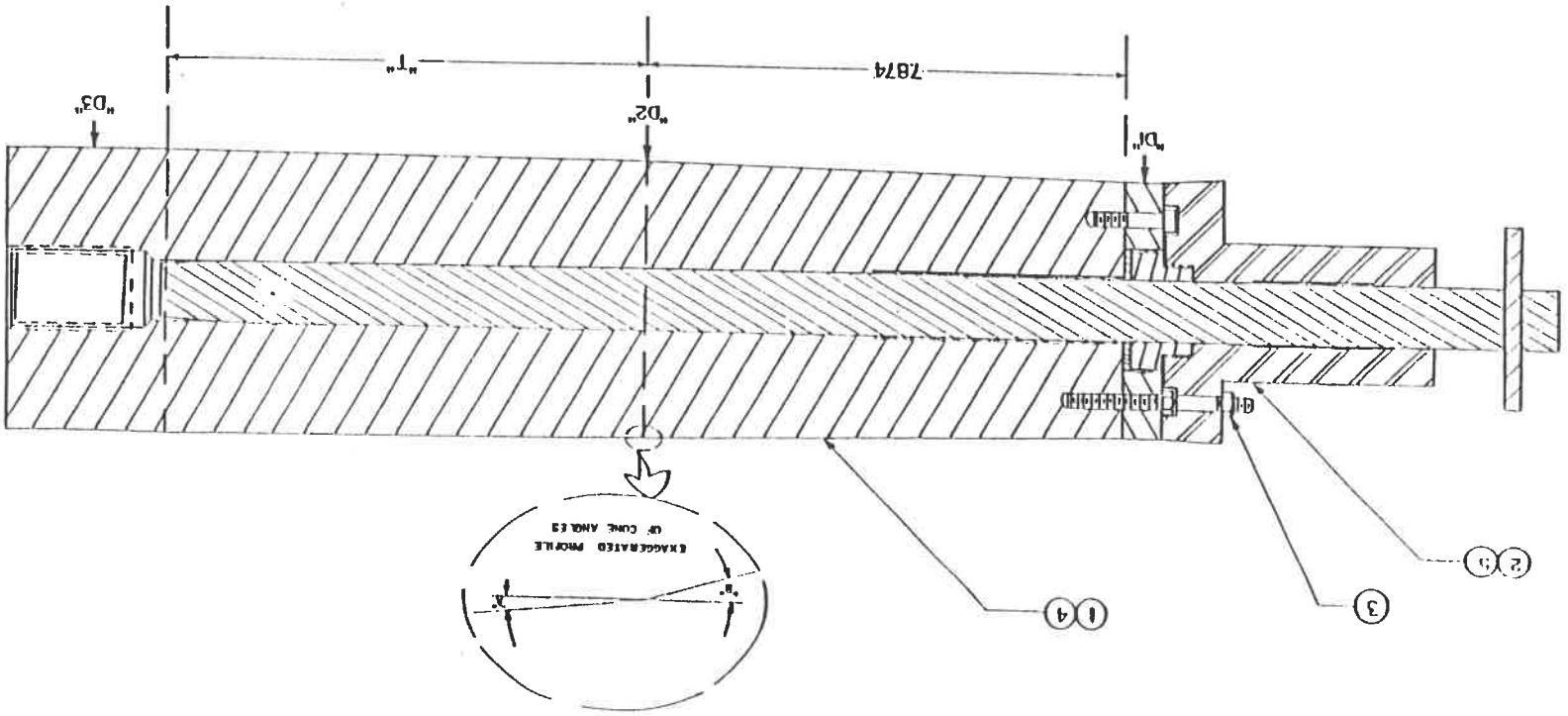

Fig. 2. Schematic of Wolter I mandrel. Zero draft sections are marked D1 and D3.

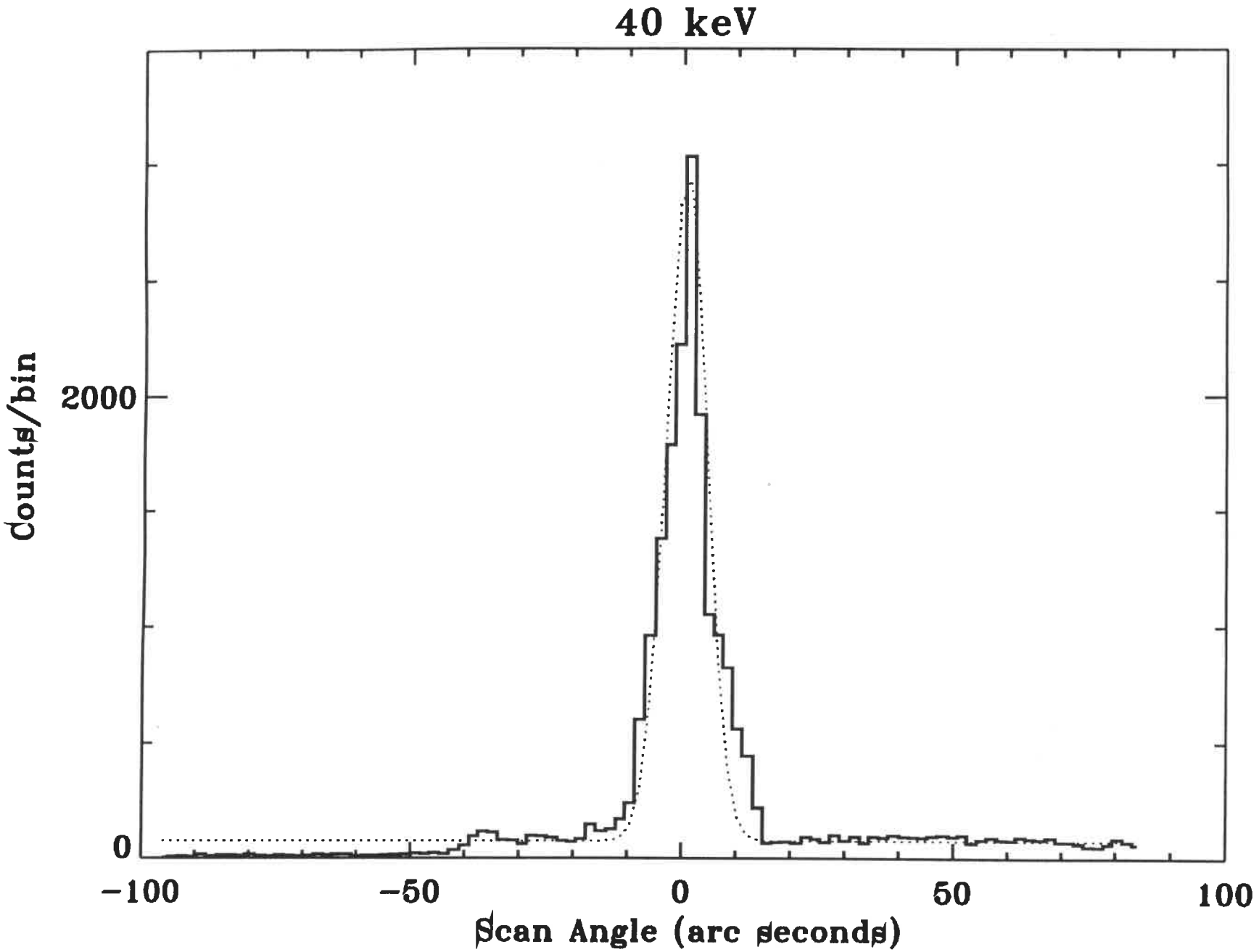

Fig. 3. Scan (intensity vs. angle) of reflected 40 keV (0.3 Å) x-ray beam. Broken line shows gaussian plus horizontal background fit to data.

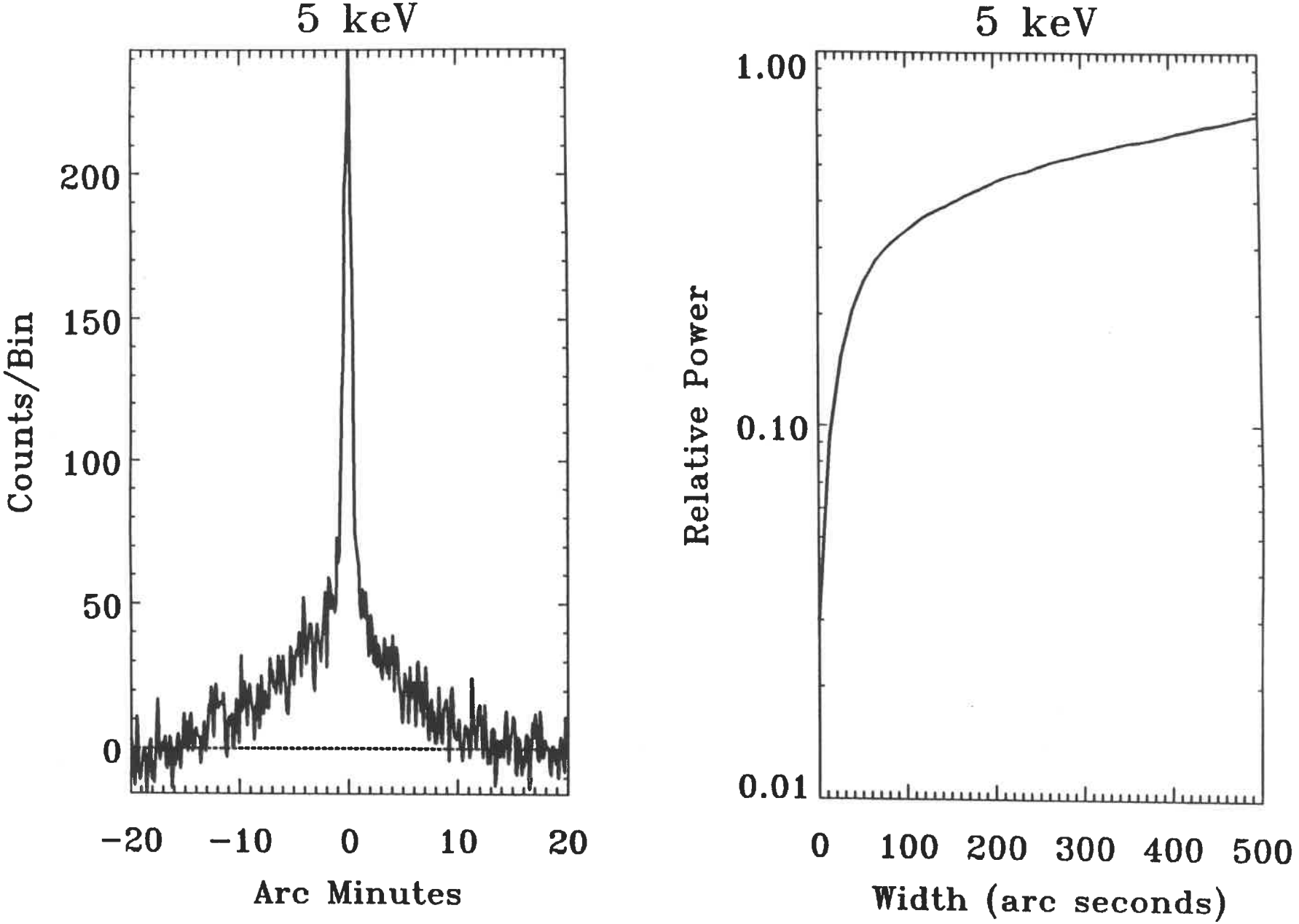

Fig. 4. Left panel shows background subtracted x-ray image from Wolter I mirror. Right panel shows relative power as a function of width of focused x-ray beam.

ON INVESTINGATING MATERIAL PARAMETERS INFLUENCING THE DIAMOND TURNING OF ELECTROLESS NICKEL PLATE

Stanley E. Becker
The University of Tennessee
Knoxville, Tennessee 37996-2210

ABSTRACT

Six specimens of electroless nickel plate on aluminum or copper substrates were diamond turned with varying degrees of success. An examination was made for specimen-to-specimen variation in alloy composition, microhardness, microstructure, and ductility using optical and scanning electron microscopy, X-ray diffractometry, electron probe analysis, microhardness testing, arc spectrometry, and wet chemistry quantitative analysis. Ductility was a determining factor in the ability to machine a mirror finish. Although this work was completed in the late 1970's, it has not been previously reported.

INTRODUCTION

It is generally accepted that a mirror finish may be obtained by turning electroless nickel plate with a single crystal diamond tool. In practice it was found that electroless nickel plate from some suppliers did not yield a mirror finish.

In order to control surface quality, the critical parameters needed to be identified. Some of the properties that might influence machining quality are crystal structure, hardness, ductility, alloy composition, constituent segregation, and thermal history.

PREVIOUS WORK

Others have shown that electroless nickel plate, as plated, consists of laminations of non-crystalline material parallel to the substrate.[1] Upon heating to a relatively low temperature of 200 degrees C (392 F) a crystal lattice is established which causes an increase in hardness. The increase in hardness is an indication of the "establishment of some type of ordered structure".[1] The increased hardness is in the range from 580 to 1000 DHP (54.1 to 69.5 R_c).

RESULTS

Random Samples

Hardness

The microhardness and microstructure of four samples (see Table 1) were examined. It is generally accepted that microhardness is relatively independent of phosphorus content but is a sensitive function of precipitation heat treatment, varying from 550 DPH to 1050 DPH and back to 550 DPH as a function of precipitation temperature.[1,2] Diamond pyramid

microhardness was measured using a Kentron model AK tester. The average values obtained for microhardness are those which would be expected for as-deposited plate or for electroless nickel which has been heat treated at approximately 650-700 degrees C (1200 - 1300 F).

Microstructure

The specimens were mounted, polished and chemically etched. Plating #1 appeared to consist of three distinct layers. The first, next to the substrate, was light in color and probably consisted of an immersion deposit of nickel which is necessary to catalyze the electroless plating reaction. The next layer, wide and dark, had the appearance of a two phase material. The third layer appeared to have an unresolved fine structure that was homogeneous.

In plating #2 three distinct layers were present, (1) a dark galvanic nickel deposit on the copper substrate, (2) a light layer which appeared unetched and (3) a homogeneous layer.

The machined plating on copper substrate (specimens #3 and #4) had a dark catalytic layer of nickel on the substrate. These two specimens differed from the previous ones in that their microstructure was banded. There was a possibility that the difference in microstructure accounted for the difference in machinability.

TABLE 1

Sample	#1	#2	#3	#4
Source	Commercial	Unknown	Y-12	Y-12
Machinability	Good	Good	Poor	Poor
Avg. DPH[+]	609	624	604	534
Microstructure at 500X	Not resolvable	Not resolvanble	Banded	Banded

[+] Diamond Pyramid Hardness parallel to the plate-substrate interface.

Crystallinity

Based on published work investigating the response of electroless nickel plate to heat treatment, one would assume that the banded microstructure observed was crystalline while the other microstructure was not. To verify that assumption, x-ray diffraction examinations were made of banded and unbanded microstructures. The equipment was calibrated using commercial polycrystalline nickel (lattice constant = 3.5238 Angstroms). All of the tests were made using copper K-alpha radiation (wavelength = 1.5413 Angstroms) and a nickel filter with a one degree slit.

Very low intensity, very broad response peaks at a two-theta angle of 45.6 degrees were obtained for both banded and unbanded microstructures. The widths of the broad peaks were used to calculate the size of each specimen's crystallites in the (111) direction. The calculated particle size for both specimens was 0.27 Angstroms (compared to 3.5238

Angstroms for polycrystalline nickel), indicating that both the banded and the unbanded specimen were amorphous.

Controlled Samples

Because of the uncertain history of the first four samples, two new samples with well documented histories were prepared at the Y-12 plant. Both samples were electroless plated onto four inch diameter aluminum substrates that had been flashed with copper. The samples were machined at the Y-12 plant using a single crystal diamond tool and identical speed, feed and depth of cut. Sample #5 exhibited good machinability as measured by surface reflectivity while sample #6 machined poorly.

Microstructure

Sections of both samples were mounted, polished with diamond paste and etched for examination by optical microscopy. Both samples were banded, the banding being faintly visible even in the unetched specimens. Scanning electron microscopy did not resolve any differences in the specimens either when observing the machined surface or the polished, unetched section.

Microhardness

A second set of sections was prepared from samples #5 and #6 for microhardness testing. Microhardness tests were carried out using both a diamond Pyramid (DHP) indenter and a Knoop indenter. The loads used were 75 grams and 100 grams respectively. The results were consistent with those for previous specimens.

Crystallinity

X-ray diffraction showed both samples to be amorphous, particle size being 0.25 to 0.27 Angstroms compared to 3.5 Angstroms for polycrystalline nickel.

Ductility

The substrate of each sample was reduced to 3 mm (0.120") thickness. Thickness of the plating was 0.07 mm (0.003"). Each sample was bent in such a manner as to subject the plating to tensile stress.

Sample #6 exhibited the expected type of glass like fracture associated with a hard (R_c 54) and amorphous material. Scanning electron microscopy showed the smooth, cleavage type fracture associated with materials that are brittle or which have limited ductility.

At low magnification (16X) the fracture pattern consisted of cracks that were straight or that had large radii of curvature. At 160X magnification, the edges of the fractures were vividly smooth. A crack in sample #6 at 400X showed not only a smooth edge but also a cleavage like fracture surface.

Sample #5 exhibited an entirely different type of fracture. Scanning electron microscopy revealed the typical fibrous fracture associated with ductile materials. At low magnification

(40X) scanning microcopy revealed a fracture edge with a sawtooth appearance. At 400X it was evident that the crack had taken a torturous path. The surface of the fracture was rough and fibrous when viewed at 800X and 4000X. By comparing the appearance of the fracture surfaces, the plate of sample #5 was unquestionably much more ductile than the plate of sample #6.

Composition

Chips from the samples were analyzed by arc spectrometry at the Y-12 plant. Wet chemical analysis showed sample #6 to be 6.9 percent phosphorus with less than 0.01 percent copper and sample #5 to be 10.80 percent phosphorus with 0.28 percent copper. Electron probe analysis was also made of each sample.

Segregation

The electron probe was also used to analyze the banded microstructure of sample #6. There appeared to be no significant difference in composition between the light and dark bands.

CONCLUSION

Examination of the limited number of samples indicates ductility to be a significant determining property controlling the machining of a mirror finish on electroless nickel plate.

ACKNOWLEDGEMENTS

The author was assisted by Warren Oliver, student, and Bobby L. McGill, Engineering Technician, who was indispensable for the scanning electron microscopy studies. The author thanks the U. S. Department of Energy for financial support of the investigation under Contract W7405 eng 26, subcontract 3968.

REFERENCES

1. "The heat-treatment of electroless nickel coatings.", K. T. Ziehlke, W. S. Dritt and C. H. Mahoney. Department of Energy Report Number K-1308, Feb. 2, 1959.

2. Metals Handbook, Vol. 5, Surface finishing, Cleaning and Coating, American Society for Metals, 9th Edition, 1982, p. 226-227.

Author Index

Altkorn, Robert 134
Arnold, Jones B. 54
Becker, Stanley E. 144
Blaedel, Kenneth L. 3
Bramlett, R.D. 84
Brown, N.J. ..... *
Bryan, William J. 10
Church, Eugene L. 110
Collins, S.B. ..... *
Crotty, David 14, 15
Day, Robert D. 84
Dini, John W. 17
Dow, Thomas A. 44
Drescher, Joseph D. 44
Egert, Charles M. 54
Engelhaupt, Darell ..... *
Epner, David 66
Evans, Chris J. 3, 95, 118
Fuchs, B.A. ..... *
Gerth, H.L. 91
Graham, Glen H. 70
Haidle, Rudy 134
Krinke, H.L. ..... *
Lashmore, David S. 77
Lunt, David ..... *
Malone, Glenn A. 81
Margolin, Jerry 106
Mayer, Anton 84
McKinney, Wayne R. 90
Mikkola, Robert D. 91
Parks, Robert E. 95
Polvani, Robert S. 84
Rouser, Forrest J. ..... *
Schneck, Rick 106
Scott, Steven 99
Takacs, Peter Z. 110
Taylor, John S. 3, 118
Ulmer, Melville P. 134
Waldrop, R.C. 91

* Paper not available at press time.